Inelastic X-Ray Scattering & Lattice Dynamics

Esen **Ercan** Alp
Advanced Photon Source, Argonne National Laboratory

alp@anl.gov
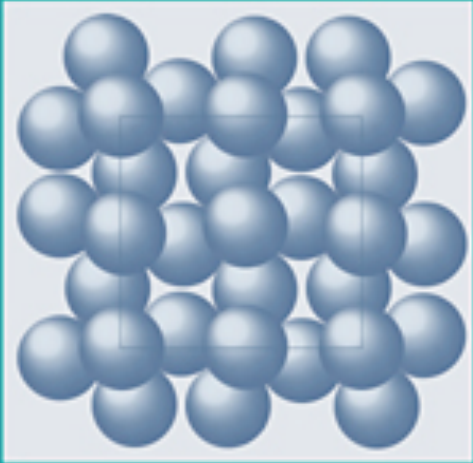
NX School 2018
July 27, 2018, Argonne National Laboratory, Argonne, IL

Lattice dynamics for beginners

Introduction to Lattice Dynamics — MARTIN T. DOVE — Cambridge topics in MINERAL PHYSICS AND CHEMISTRY 4
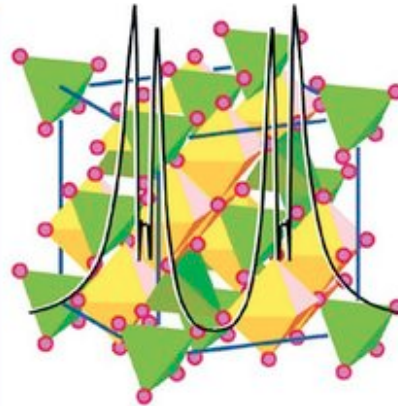
Yi-Long Chen, De-Ping Yang — WILEY-VCH — Mössbauer Effect in Lattice Dynamics — Experimental Techniques and Applications

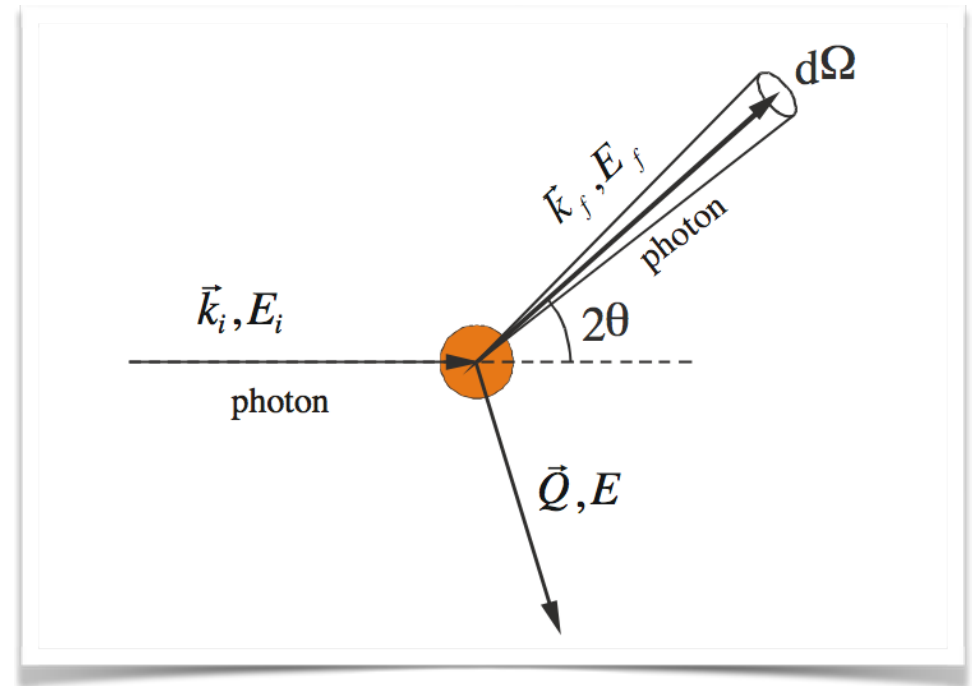THE PHYSICS OF PHONONS — G P SRIVASTAVA
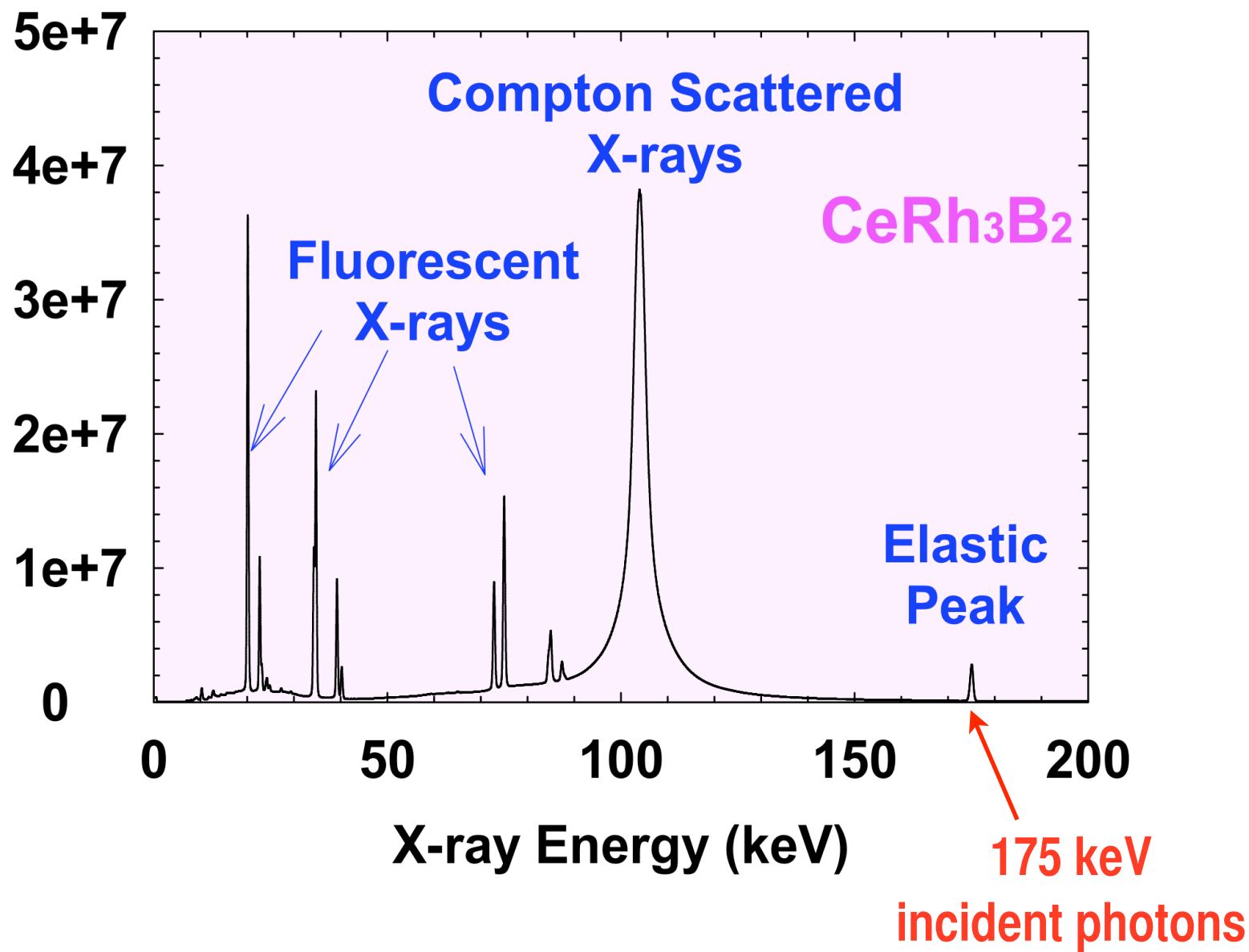
Inelastic X-Ray Scattering & Spectroscopy @ APS

IXS

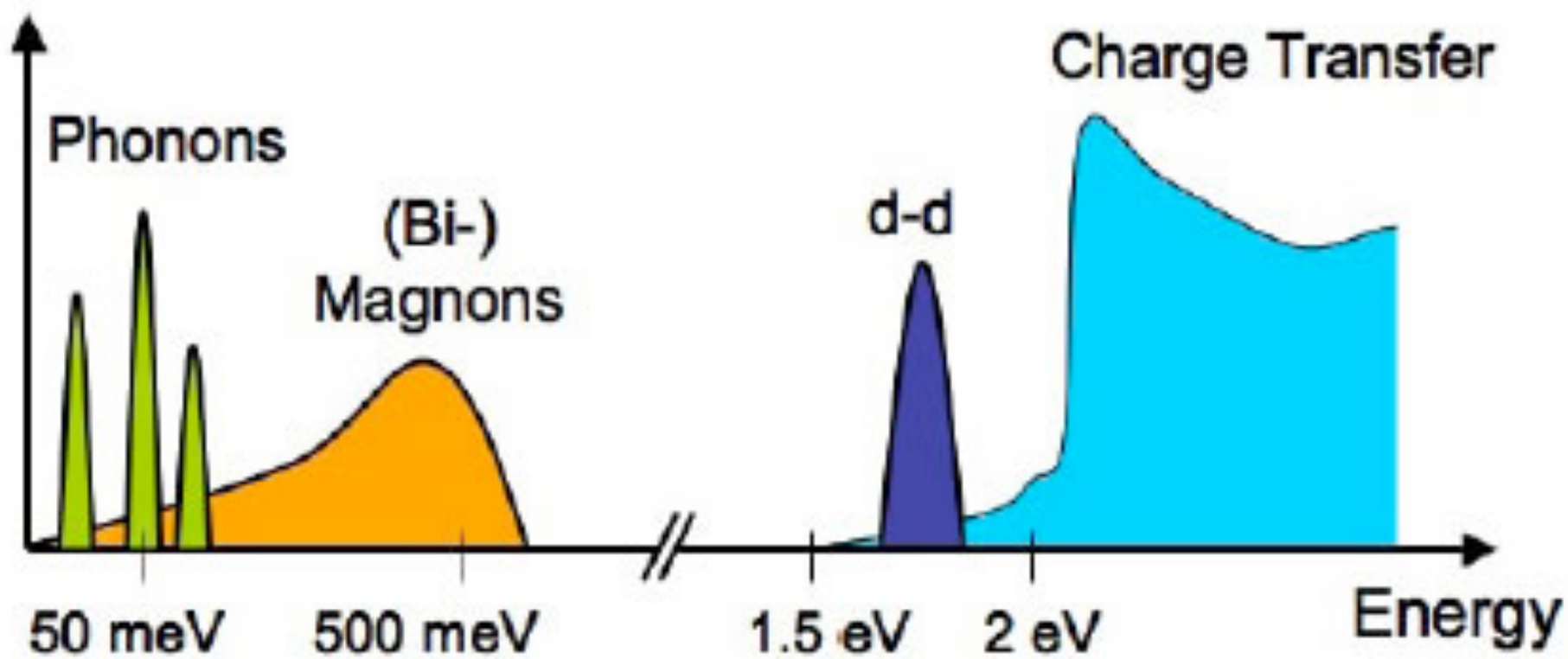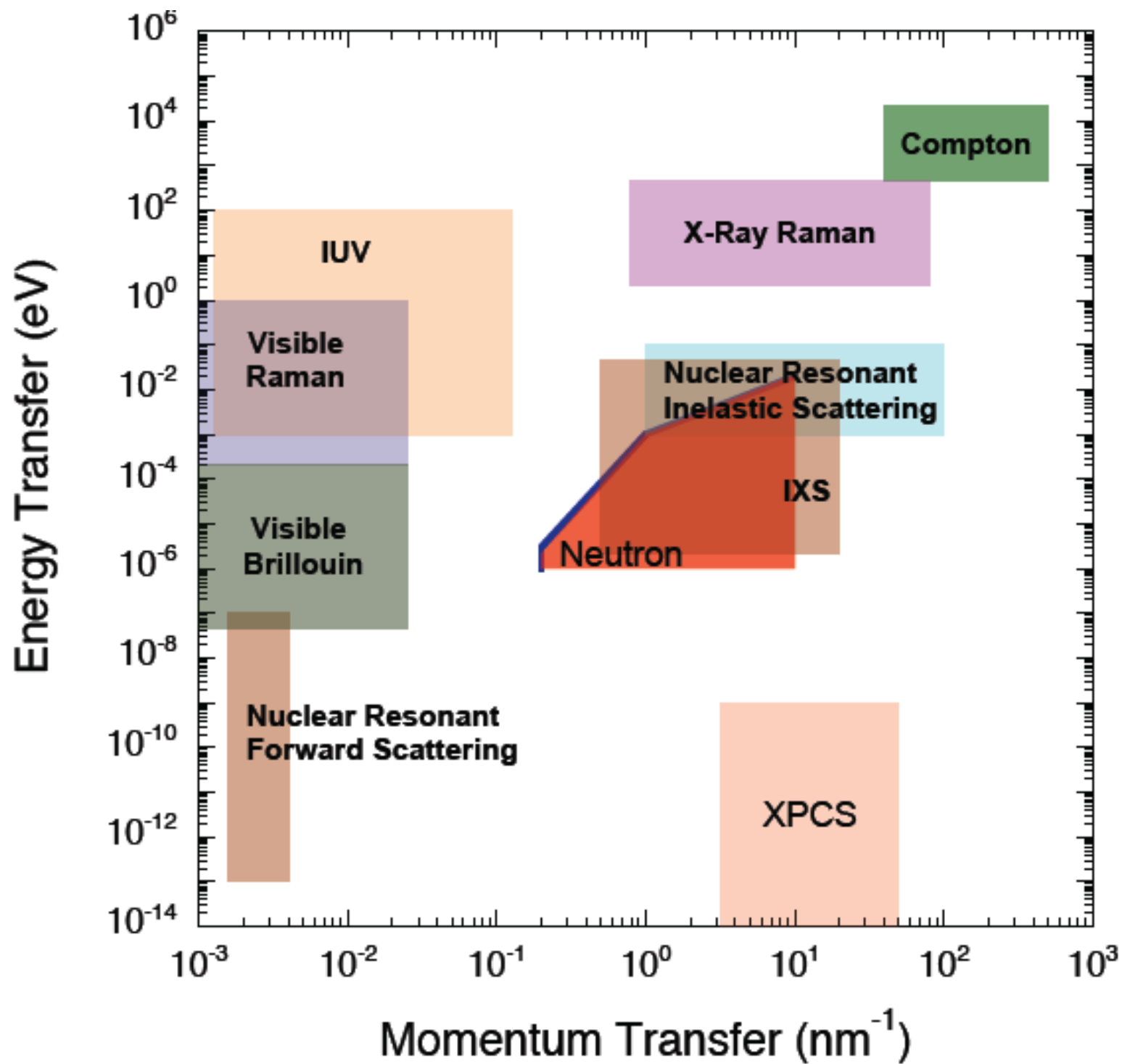**NRIXS** **RIXS** **MCS**

NRIS **XES** **XRS** **Compton**

- **Nuclear Resonant Inelastic X-Ray scattering, NRIXS: Sectors 3, 16, 30**
- **Momentum Resolved High Energy Resolution IXS (HERIX) Sectors 3, 30**
- **Resonant Inelastic X-Ray Scattering, RIXS : Sector 27**
- **X-Ray Raman Scattering, XRS : Sectors 13, 16, 20**
- **X-Ray Emission Spectroscopy, XES: Sectors 6, 13, 16, 17**

Compton Scattered X-rays

CeRh$_3$B$_2$

Fluorescent X-rays

Elastic Peak

175 keV incident photons

X-ray Energy (keV)

4

Incident beam energy

Phonons

(Bi-) Magnons

d-d

Charge Transfer

Energy

50 meV 500 meV 1.5 eV 2 eV
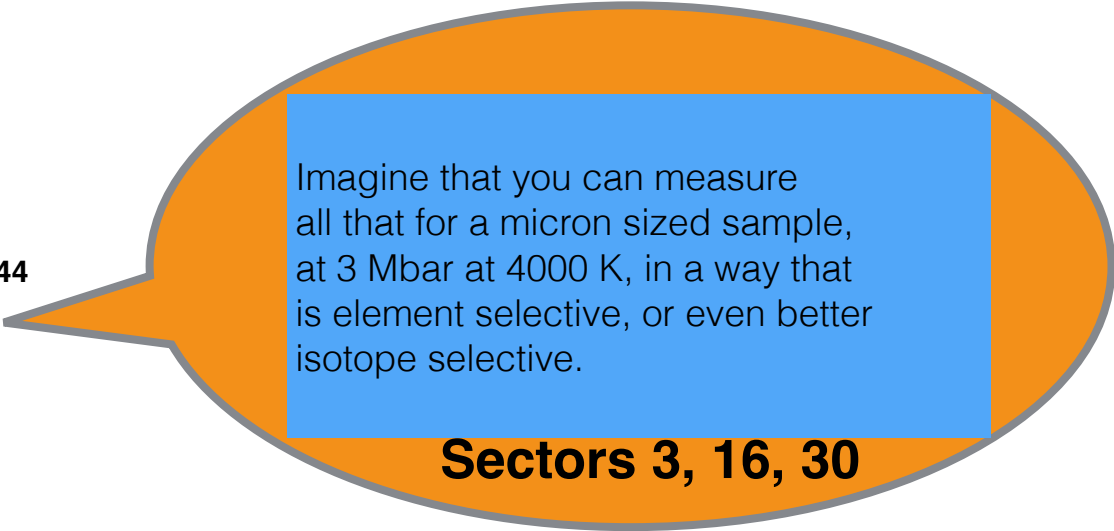
Lattice dynamics for beginners

Lattice dynamics describes vibrations of atoms in condensed matter:

- crystalline solids
- glasses, and
- liquids

However, some of the convenience gained by symmetry or periodic lattice is lost for glasses and liquids. Also, effect of surfaces and defects are glowing short-comings of the classical model.

Lattice dynamics is a reflection of forces acting upon atoms and leads to

- sound velocity: V_s, V_p
- vibrational entropy, S_v
- specific heat, C_p
- force constant, $<F>$
- compression tensor, c_{11}, c_{12}, c_{44}
- Young's modulus, E
- Shear modulus, G
- stiffness and resilience
- Gruneisen constant, γ
- viscosity, ν

Imagine that you can measure all that for a micron sized sample, at 3 Mbar at 4000 K, in a way that is element selective, or even better isotope selective.

Sectors 3, 16, 30

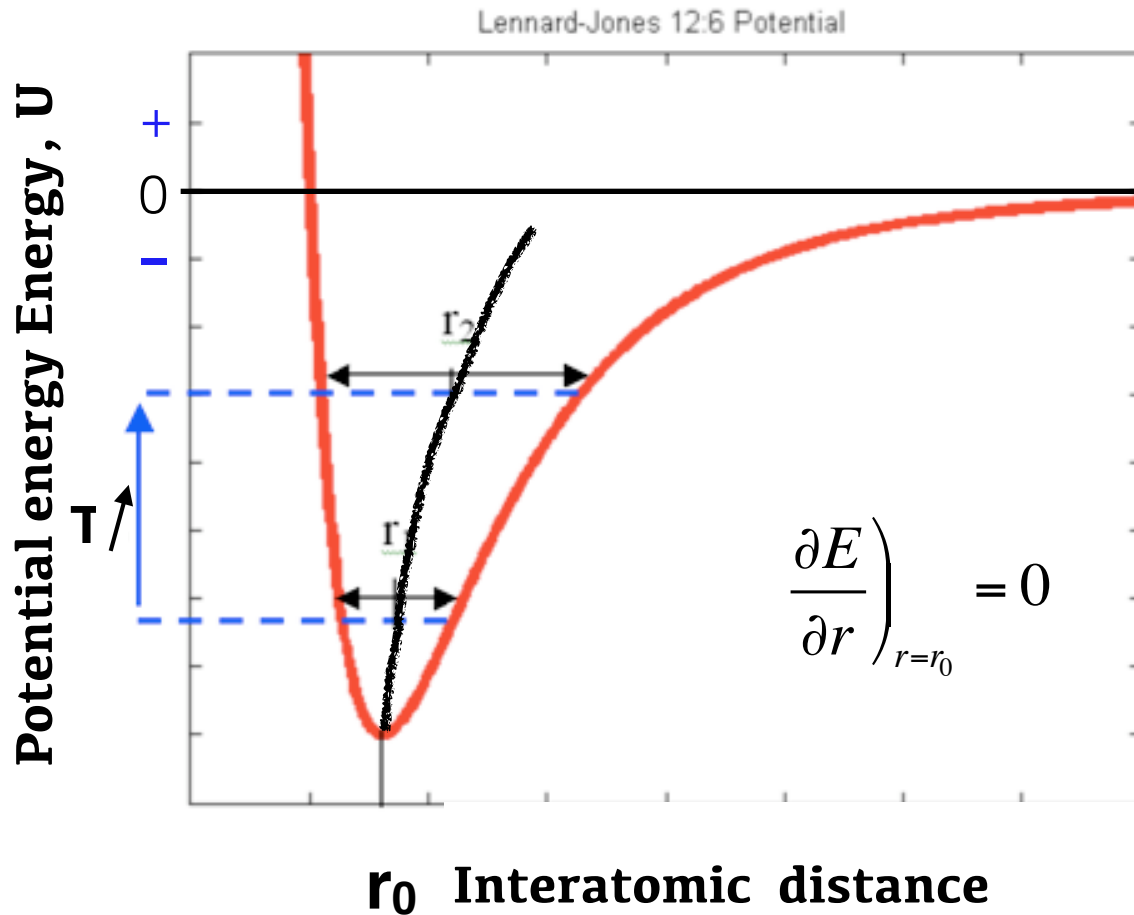**Many experimental techniques exist to study lattice dynamics**

- sound velocity, deformation, thermal expansion, heat capacity….
- spectroscopic methods using light, x-rays and neutrons, and electrons
- point contact spectroscopy

Atomic motions are described as harmonic traveling waves, characterized by

- wavelength, λ
- angular frequency, ω
- momentum vector along the direction of propagation, $\vec{k} = \dfrac{\lambda}{2\pi}$

Two main approximations should be noticed:

- **Born-Oppenheimer (adiabiatic) approximation**

  - Motion of atoms are independent and decoupled from the electrons.
  - All electrons follow the nuclei. This can be justified by considering the time scales involved: 10^{-15} s (femto) for electrons, 10^{-12} s (pico) for nuclei

- **Harmonic approximation**

  - At equilibrium, attractive and repulsive forces are balanced.
  - When atoms move away from the equilibrium positions, they are forced to come back by restoring forces.
  - Magnitude of atomic displacements are small compared to interatomic distance.
  - All atoms in equivalent positions in every unit cell move together.

Lennard-Jones 12:6 Potential

Potential energy Energy, U

r_0 Interatomic distance

$$\left.\frac{\partial E}{\partial r}\right)_{r=r_0} = 0$$

There should be no thermal expansion in the harmonic model.

The fact that there is thermal expansion is an indication that the potential under which the atoms move is not harmonic.

However, harmonic model has so many convenient features that we adopt it to explain many features of atomic vibrations.

$$E(r) = E_0 + \frac{1}{2}\left.\frac{\partial^2 E}{\partial r^2}\right|_{r_0}(r - r_0)^2 + \frac{1}{3!}\left.\frac{\partial^3 E}{\partial r^3}\right|_{r_0}(r - r_0)^3 + \frac{1}{4!}\left.\frac{\partial^4 E}{\partial r^4}\right|_{r_0}(r - r_0)^4 + \cdots$$

ignoring these terms is the harmonic approximation

Diatomic infinite 1-D chain
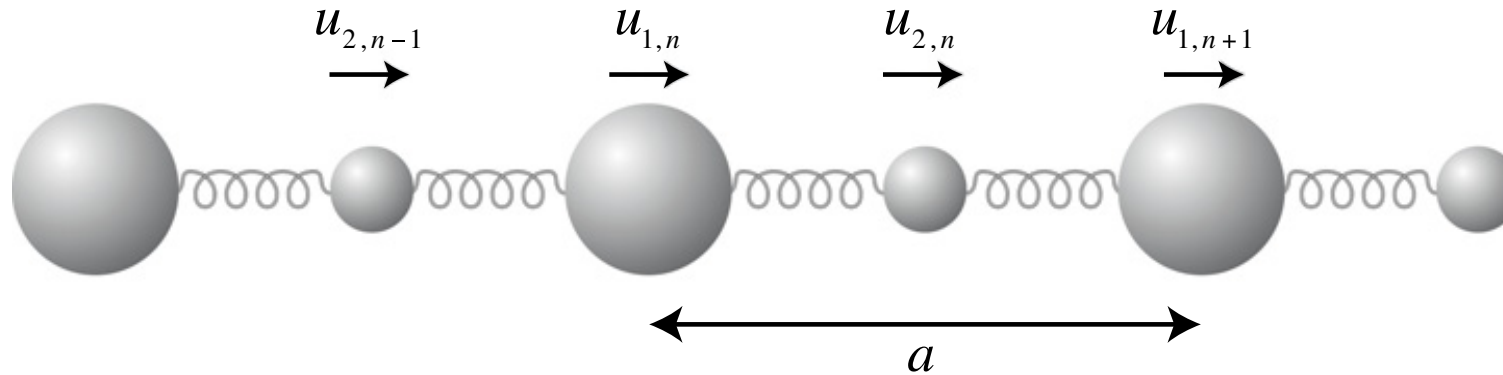
$$E = \frac{1}{2} J \sum_n (u_{1,n} - u_{2,n})^2 + \frac{1}{2} J \sum_n (u_{2,n} - u_{1,n+1})^2$$

$$J = \frac{\partial^2 E}{\partial u_{1,n} \partial u_{2,n}}$$ **Force constant (spring constant)**

$$u_{1,n}(t) = \tilde{u}_1 \exp(i(kna - \omega t))$$

$$u_{2,n}(t) = \tilde{u}_2 \exp(i(kna - \omega t))$$

Time dependent displacement of two atoms in terms of relative displacement of each atom

$$E_{1,n} = \frac{1}{2}J(u_{1,n} - u_{2,n})^2 + \frac{1}{2}J(u_{1,n} - u_{2,n-1})^2$$

$$E_{2,n} = \frac{1}{2}J(u_{2,n} - u_{1,n})^2 + \frac{1}{2}J(u_{2,n} - u_{1,n+1})^2$$

Energy

$$f_{1,n} = -\frac{\partial E_{1,n}}{\partial u_{1,n}} = -J(u_{1,n} - u_{2,n}) - J(u_{1,n} - u_{2,n-1})$$

$$f_{2,n} = -\frac{\partial E_{2,n}}{\partial u_{2,n}} = -J(u_{2,n} - u_{1,n}) - J(u_{2,n} - u_{1,n+1})$$

Force as derivative of energy

$$\ddot{u}_{1,n}(t) = -\omega^2 \tilde{u}_1 \exp i\,(kna - \omega t) = -\omega^2 u_{1,n}(t)$$

$$\ddot{u}_{2,n}(t) = -\omega^2 \tilde{u}_2 \exp i\,(kna - \omega t) = -\omega^2 u_{2,n}(t)$$

Acceleration

$$m_1\ddot{u}_{1,n}(t) = -m_1\omega^2 u_{1,n}(t) = -J(2u_{1,n}(t) - u_{2,n}(t) - u_{2,n-1}(t))$$

$$m_2\ddot{u}_{2,n}(t) = -m_2\omega^2 u_{2,n}(t) = -J(2u_{2,n}(t) - u_{1,n}(t) - u_{1,n+1}(t))$$

Newton's eqⁿ of motion

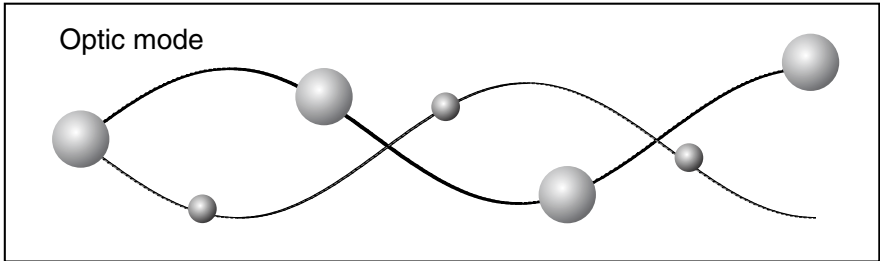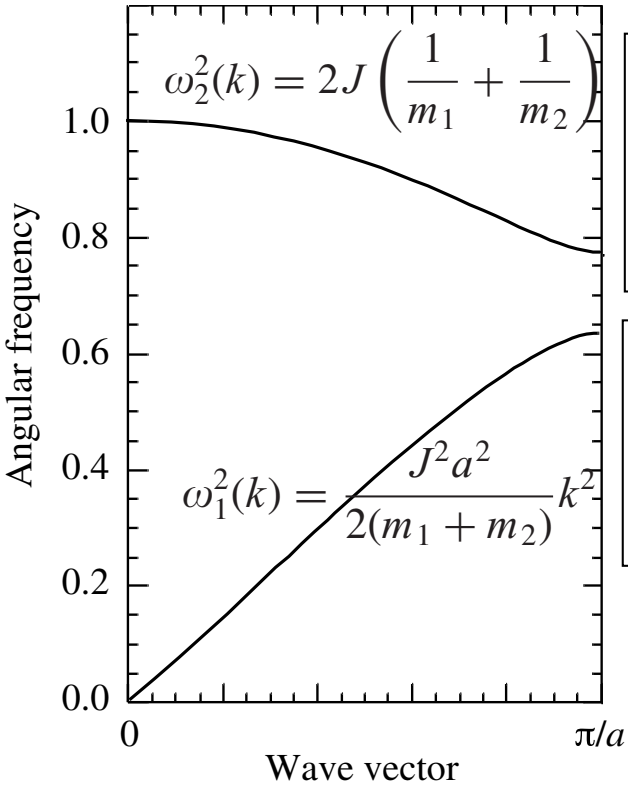$$e_1 = m_1^{1/2}\tilde{u}_1; \quad e_2 = m_2^{1/2}\tilde{u}_2$$

Mass normalized displacements (real)

$$\omega^2 \begin{pmatrix} e_1 \\ e_2 \end{pmatrix} = \mathbf{D}(k) \cdot \begin{pmatrix} e_1 \\ e_2 \end{pmatrix}$$
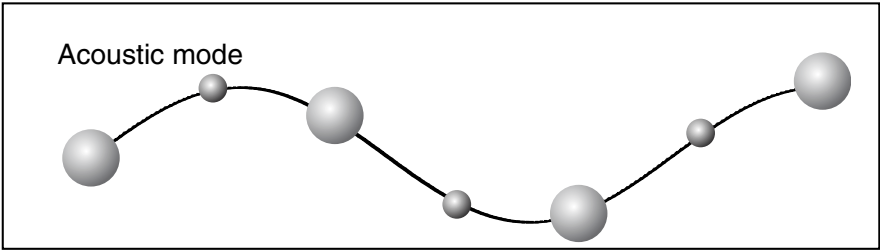
Matrix form of Newton's eqⁿ of motion

$$\mathbf{D}(k) = \begin{pmatrix} 2J/m_1 & -J\left(1 + \exp(-ika)\right)/\sqrt{m_1 m_2} \\ -J\left(1 + \exp(+ika)\right)/\sqrt{m_1 m_2} & 2J/m_2 \end{pmatrix}$$

Eigen solutions

$$\omega_2^2(k) = 2J\left(\frac{1}{m_1} + \frac{1}{m_2}\right)$$

Optic mode

$$\omega_1^2(k) = \frac{J^2 a^2}{2(m_1 + m_2)} k^2$$

Acoustic mode

Angular frequency

1.0
0.8
0.6
0.4
0.2
0.0

0   π/a

Wave vector

out-of-phase
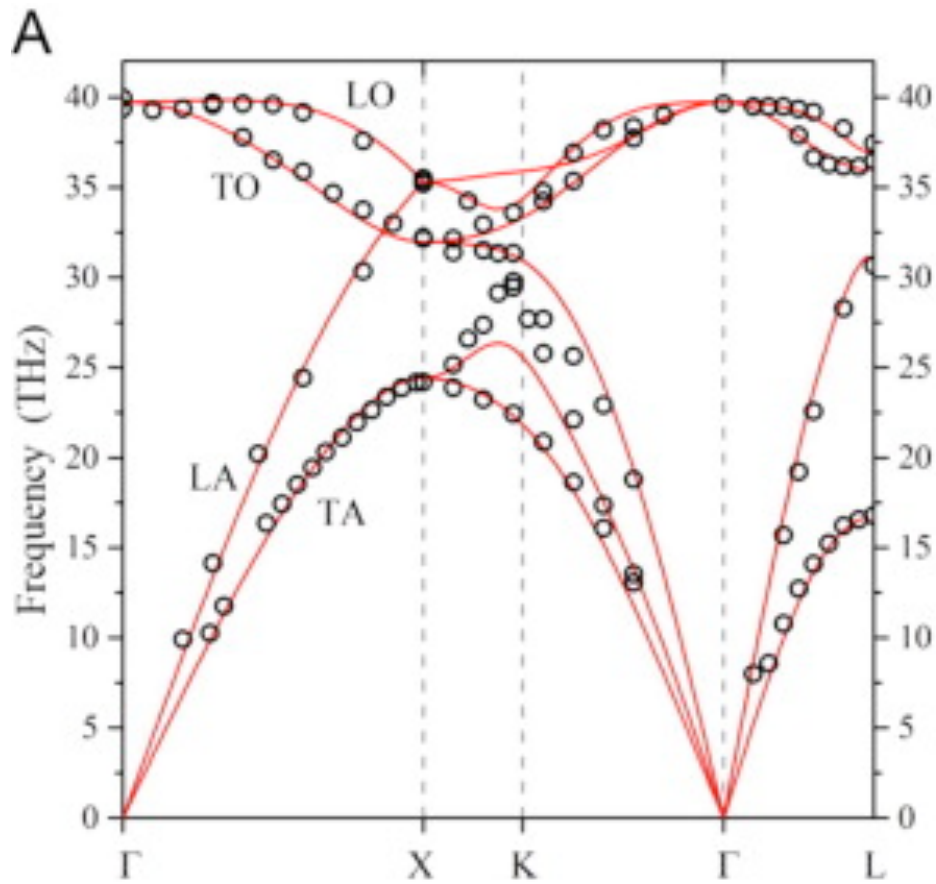
$$m_1^{1/2} e_1 = -m_2^{1/2} e_2$$
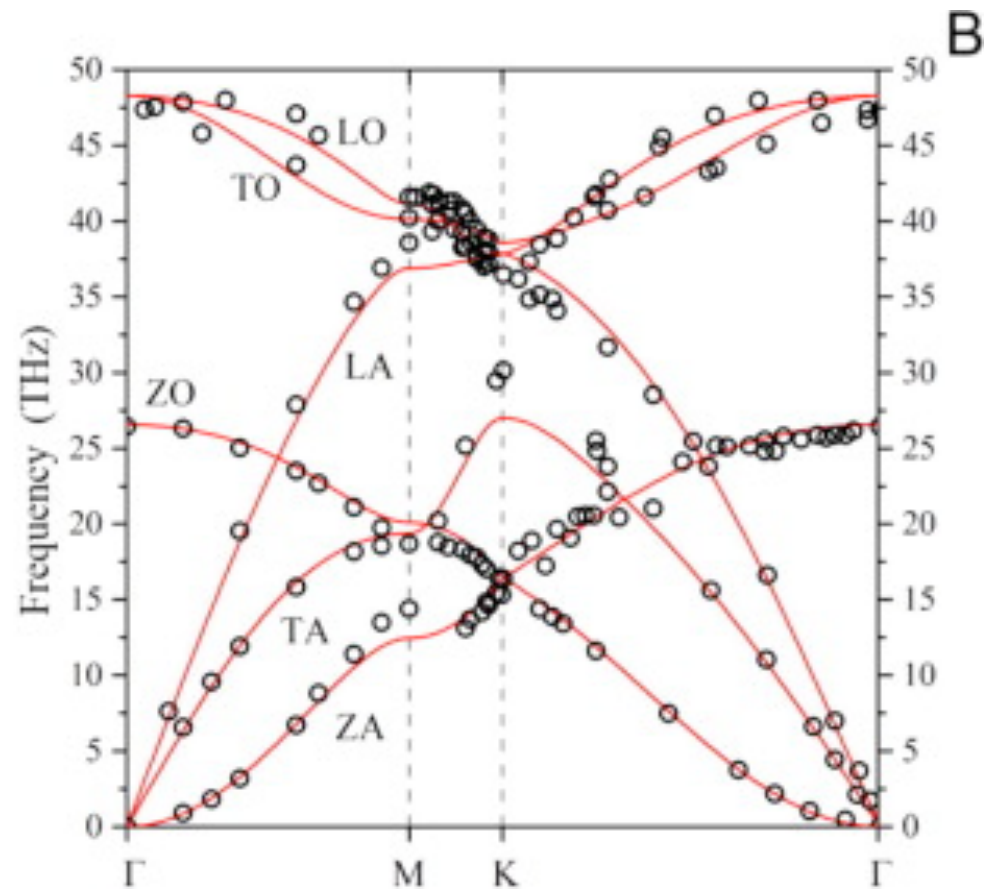
$$m_1^{-1/2} e_1 = m_2^{-1/2} e_2$$

in-phase

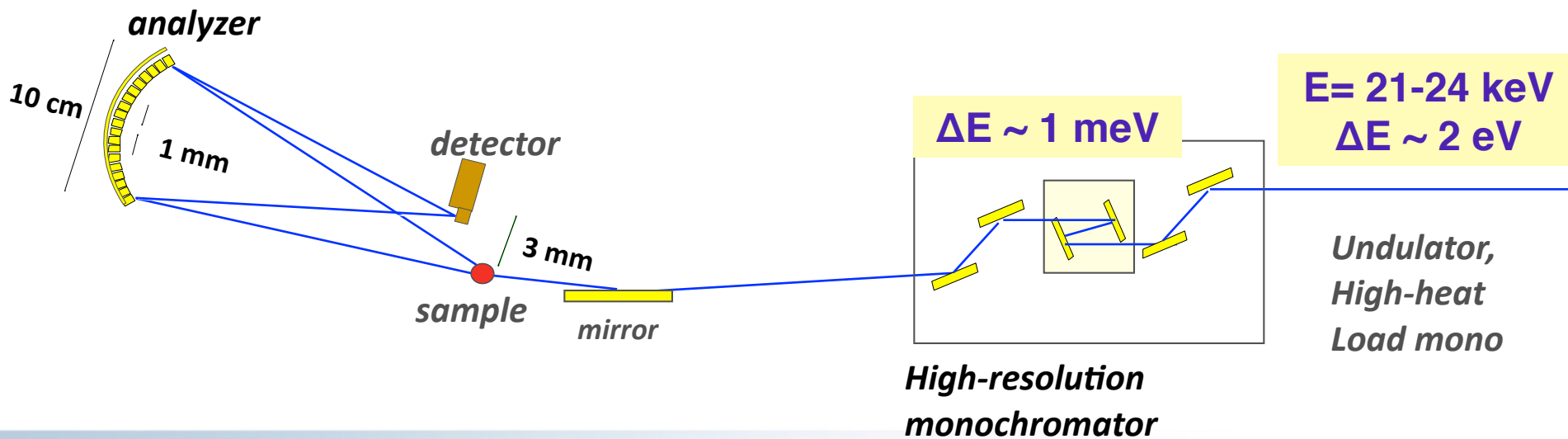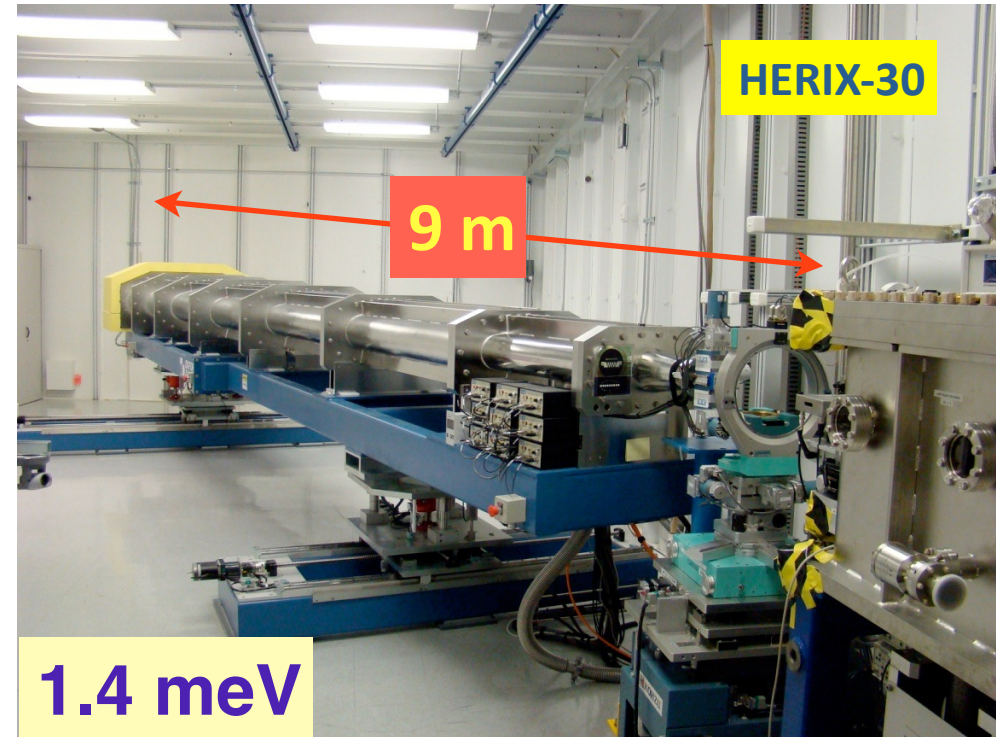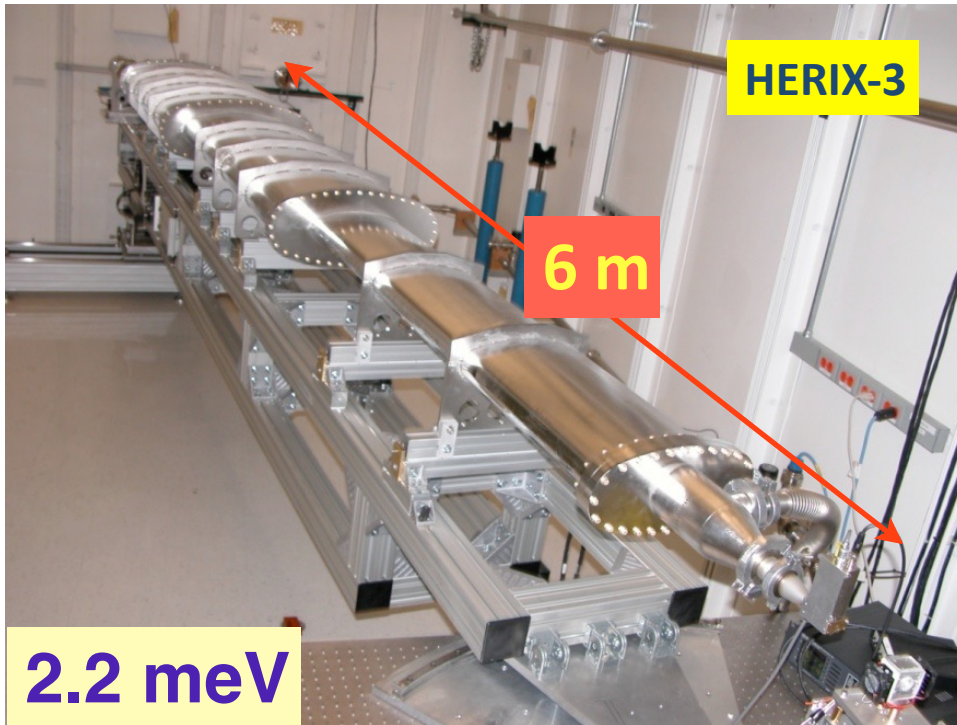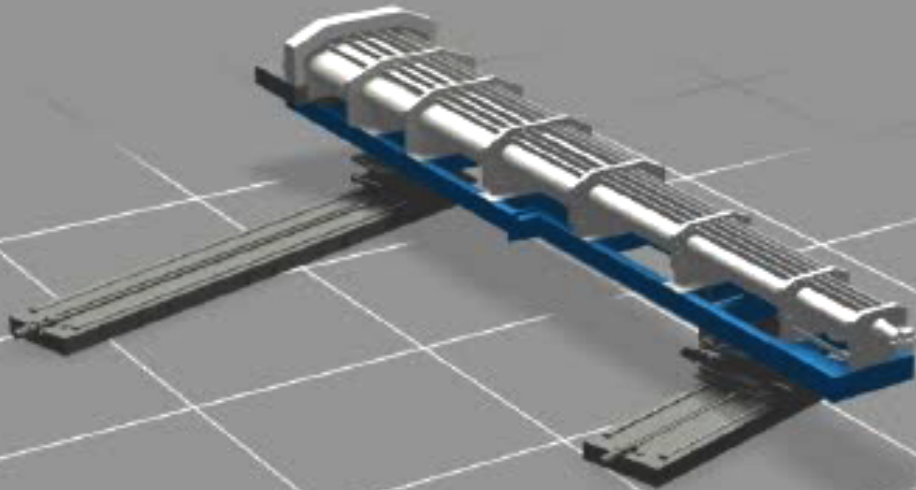# Inelastic X-Ray Scattering: A plethora of different techniques
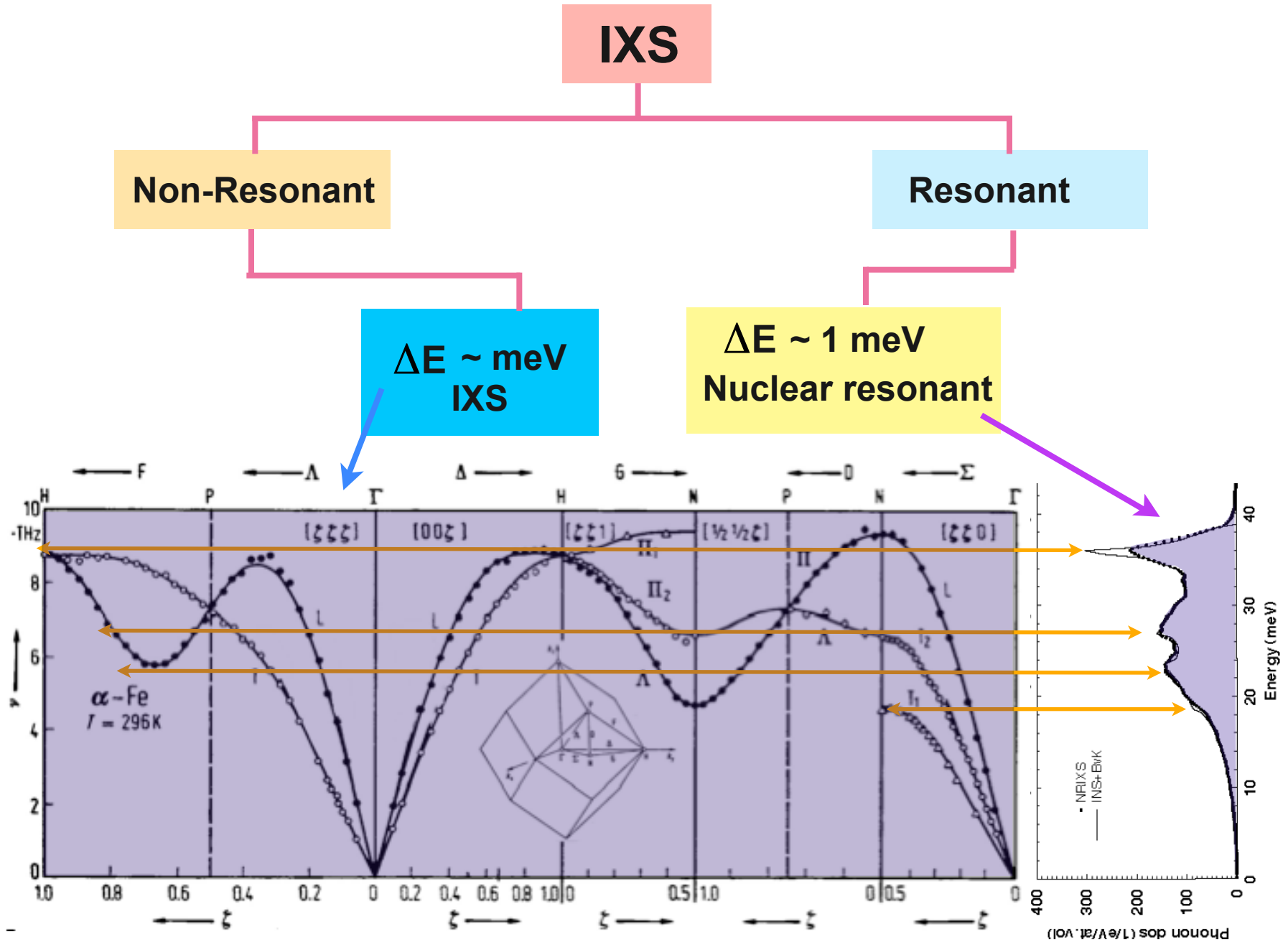
Diamond

**Graphene**

Umberto Monteverde, et al, 2015

HERIX-3 and HERIX-30

HERIX-3

6 m

2.2 meV

HERIX-30

9 m

1.4 meV

analyzer

10 cm

1 mm

detector

3 mm

sample

mirror

ΔE ~ 1 meV

E= 21-24 keV
ΔE ~ 2 eV

Undulator,
High-heat
Load mono

High-resolution
monochromator

CdTe detector

Bimorph focusing mirror
Beam size (VXH)=15X35 μm^2

High-heat-load
monochromator C(111)
$\Delta E\sim1.6$ eV

Si (12 12 12)
Analyzer

High resolution
Monochromator
$\Delta E=1.1$ meV
working at T=123 K

Be compound refractive lens

Choice of energy

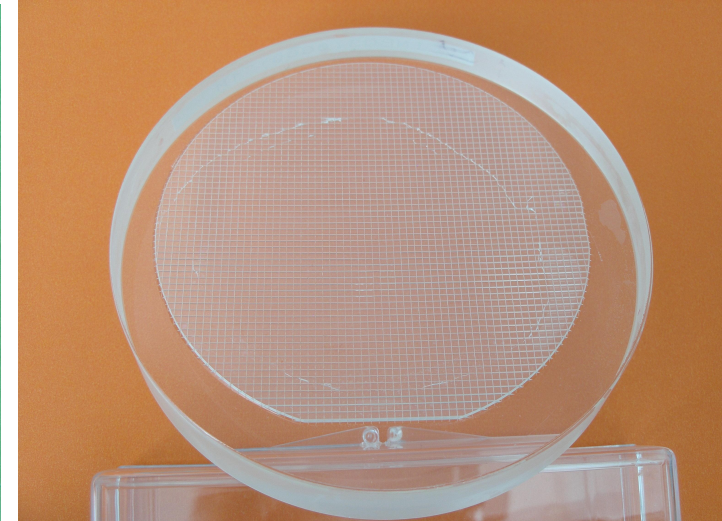| Si Reflection at 90 °	Energy (keV)	Resolution (meV)	Reflectivity (%)
18 6 0	21.657	1.23	78
11 11 11	21.747	0.83	70
13 11 9	21.985	0.81	69
15 11 7	22.685	0.70	68
20 4 0	23.280	0.87	76
12 12 12	23.724	0.80	75
14 14 8	24.374	0.69	74
22 2 0	25.215	0.576	71
13 13 13	25.701	0.37	60

Bent-diced IXS analyzers
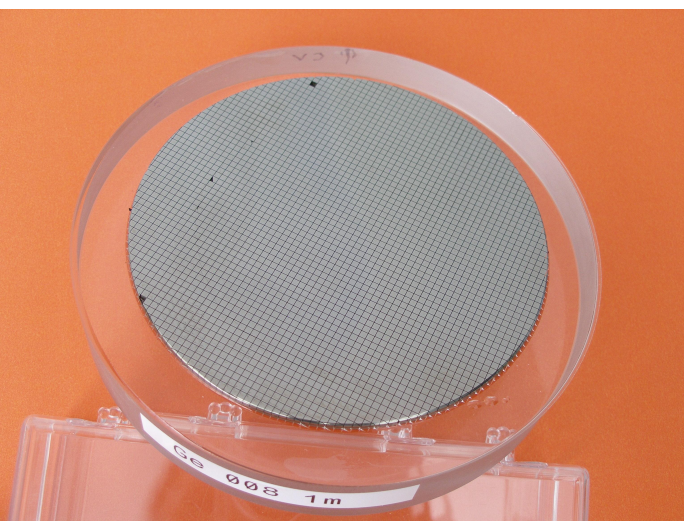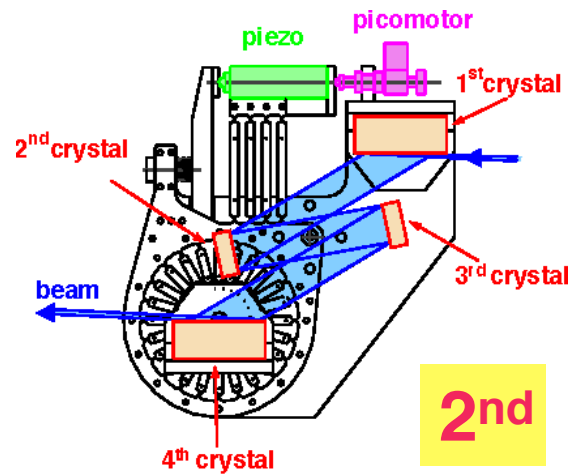

Si
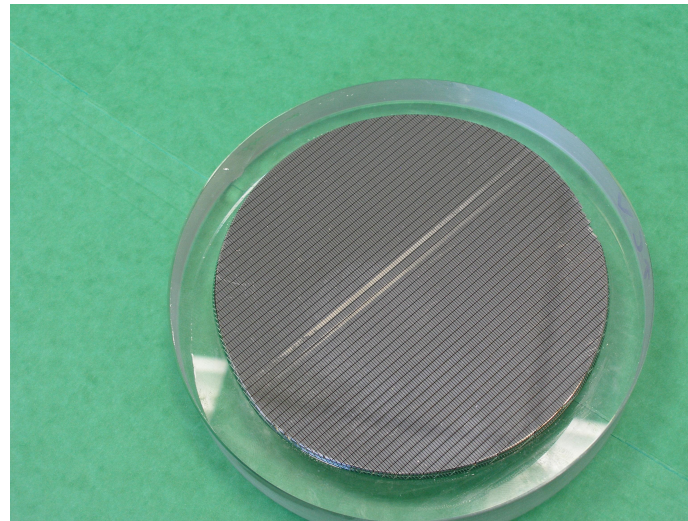
Ge

LiNbO$_3$

Generations of high-resolution monochromators

T. Toellner, D. Shu
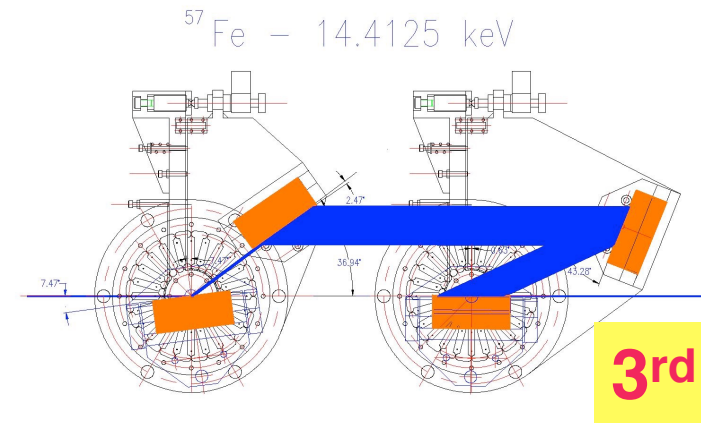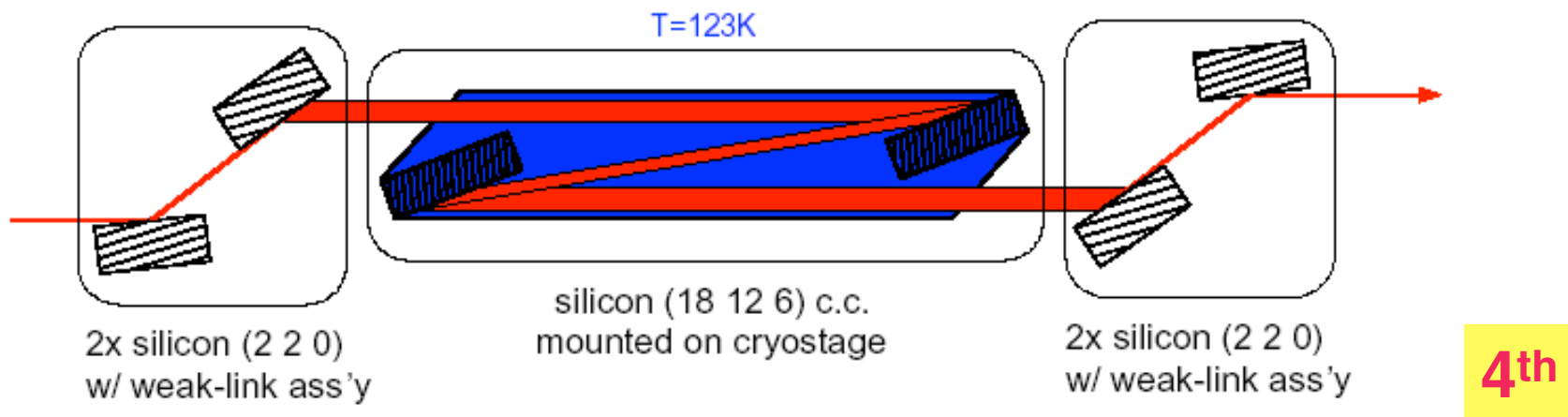
20
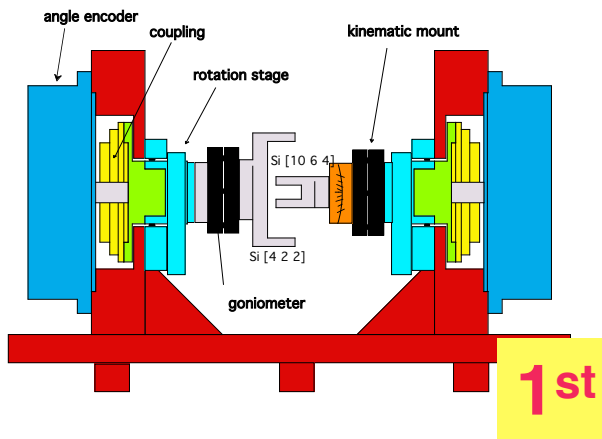
What is being measured ?

$$\frac{d^2\sigma}{d\Omega\, d\omega} = r_0^2 \frac{\omega_f}{\omega_i} |\mathbf{e}_i \cdot \mathbf{e}_f| N \sum_{i,f} \left| \langle i | \sum e^{i\mathbf{Qr_j}} | f \rangle \right|^2 \delta(E_f - E_i - \mathbf{h}\omega)$$

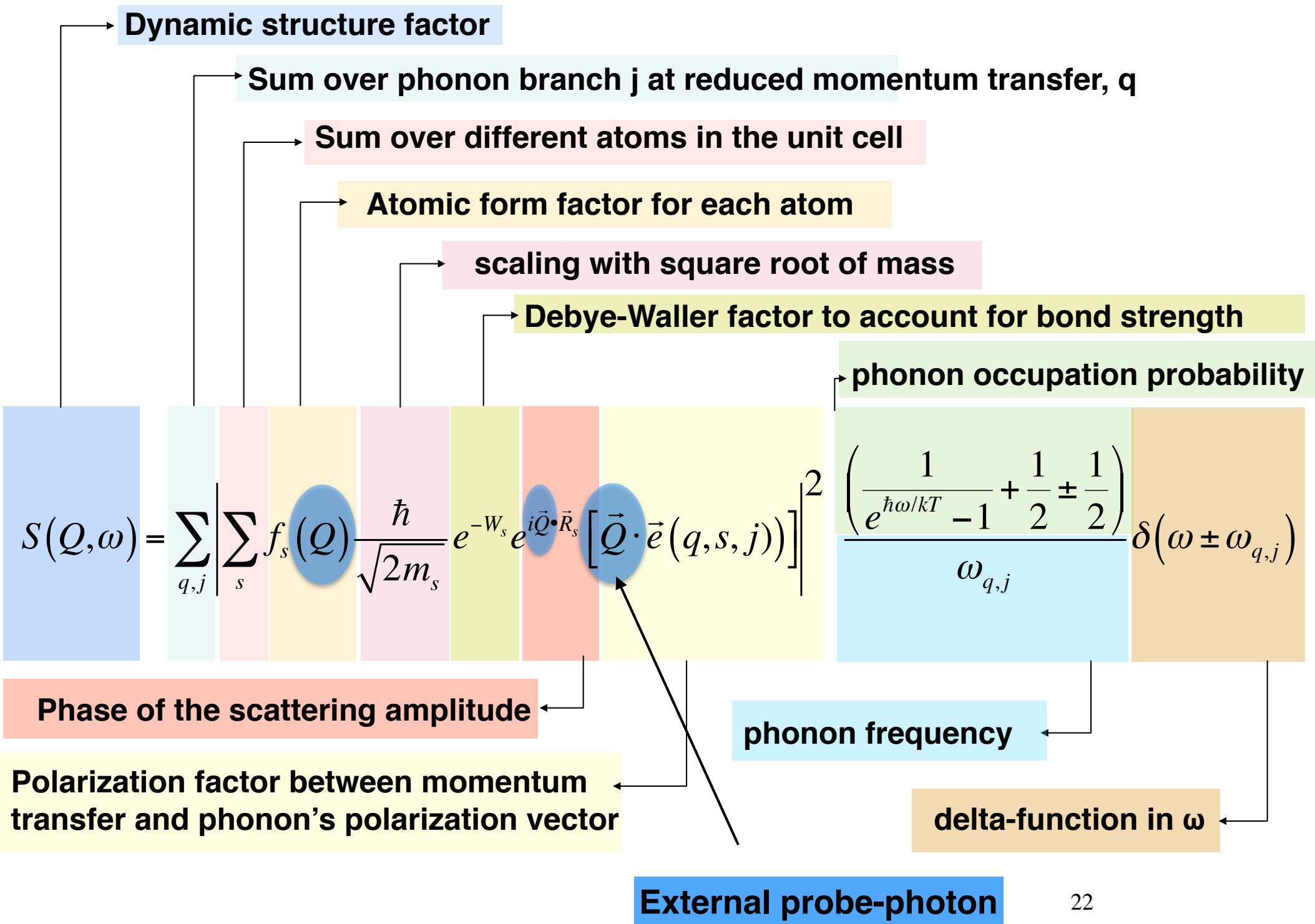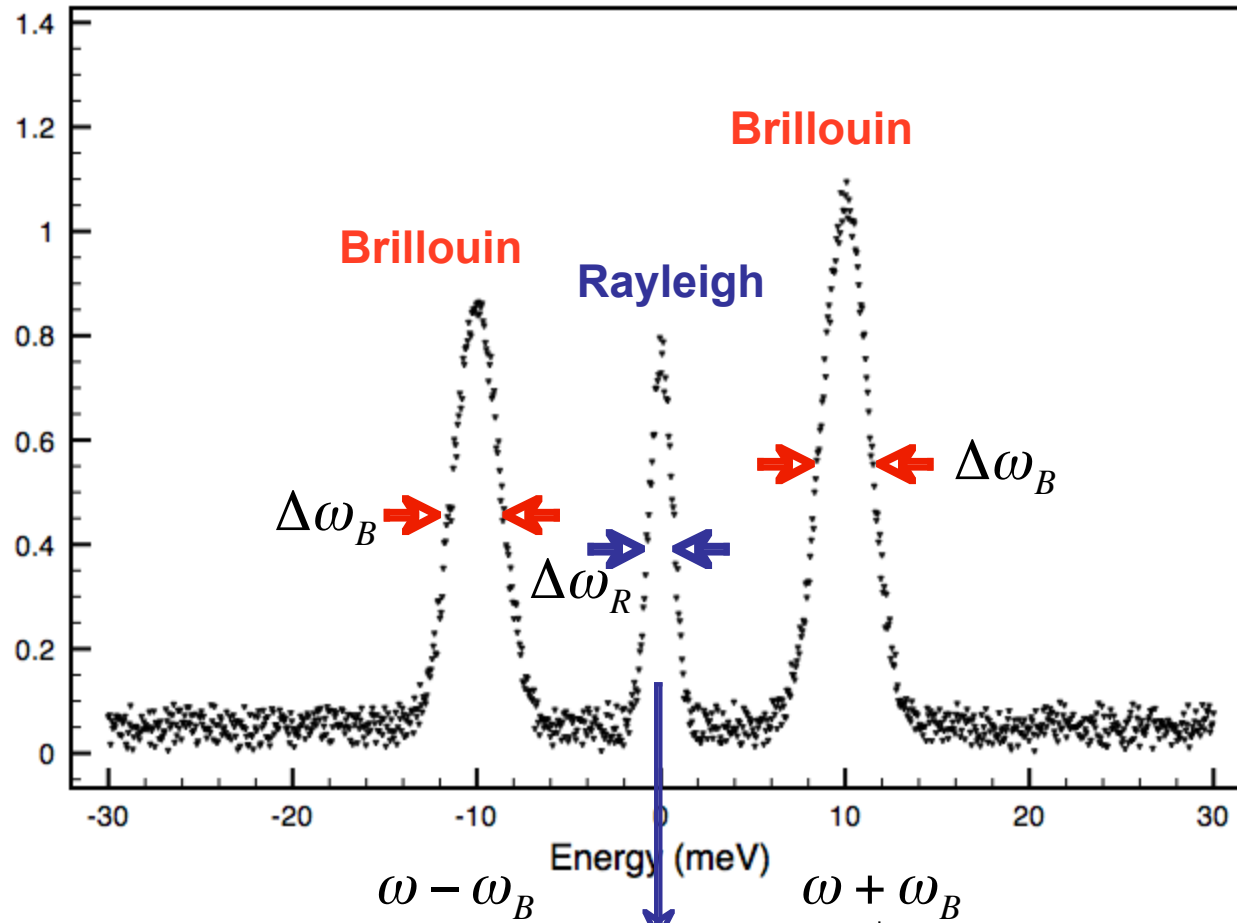**Thomson cross section**   **Dynamical structure factor S(Q,w)**

$$S(\mathbf{Q},\omega) = \frac{1}{2\pi} \int dt\, e^{-i\omega t} \langle \phi_i | \sum_{ll'} f_l(\mathbf{Q}) e^{-i\mathbf{Q}\cdot\mathbf{r}_l(t)} f_{l'}(\mathbf{Q}) e^{i\mathbf{Q}\cdot\mathbf{r}_{l'}(0)} | \phi_i \rangle$$

Density-density correlations

$$f(Q) = f_{ion}(Q) + f_{valence}(Q)$$ **Atomic form factor**

Dynamic structure factor

Sum over phonon branch j at reduced momentum transfer, q

Sum over different atoms in the unit cell

Atomic form factor for each atom

scaling with square root of mass

Debye-Waller factor to account for bond strength

phonon occupation probability

$$S(Q,\omega) = \sum_{q,j} \left| \sum_{s} f_s(Q) \frac{\hbar}{\sqrt{2m_s}} e^{-W_s} e^{i\vec{Q}\cdot\vec{R}_s} \left[\vec{Q} \cdot \vec{e}(q,s,j) \right] \right|^2 \frac{\left(\frac{1}{e^{\hbar\omega/kT}-1} + \frac{1}{2} \pm \frac{1}{2} \right)}{\omega_{q,j}} \delta\left(\omega \pm \omega_{q,j}\right)$$

Phase of the scattering amplitude

Polarization factor between momentum transfer and phonon's polarization vector

phonon frequency

delta-function in ω

External probe-photon

22

Entropy fluctuations, $\Delta\omega_R \sim \alpha q^2$

Concentration fluctuations $\Delta\omega_R \sim Dq^2$

Pressure fluctuations

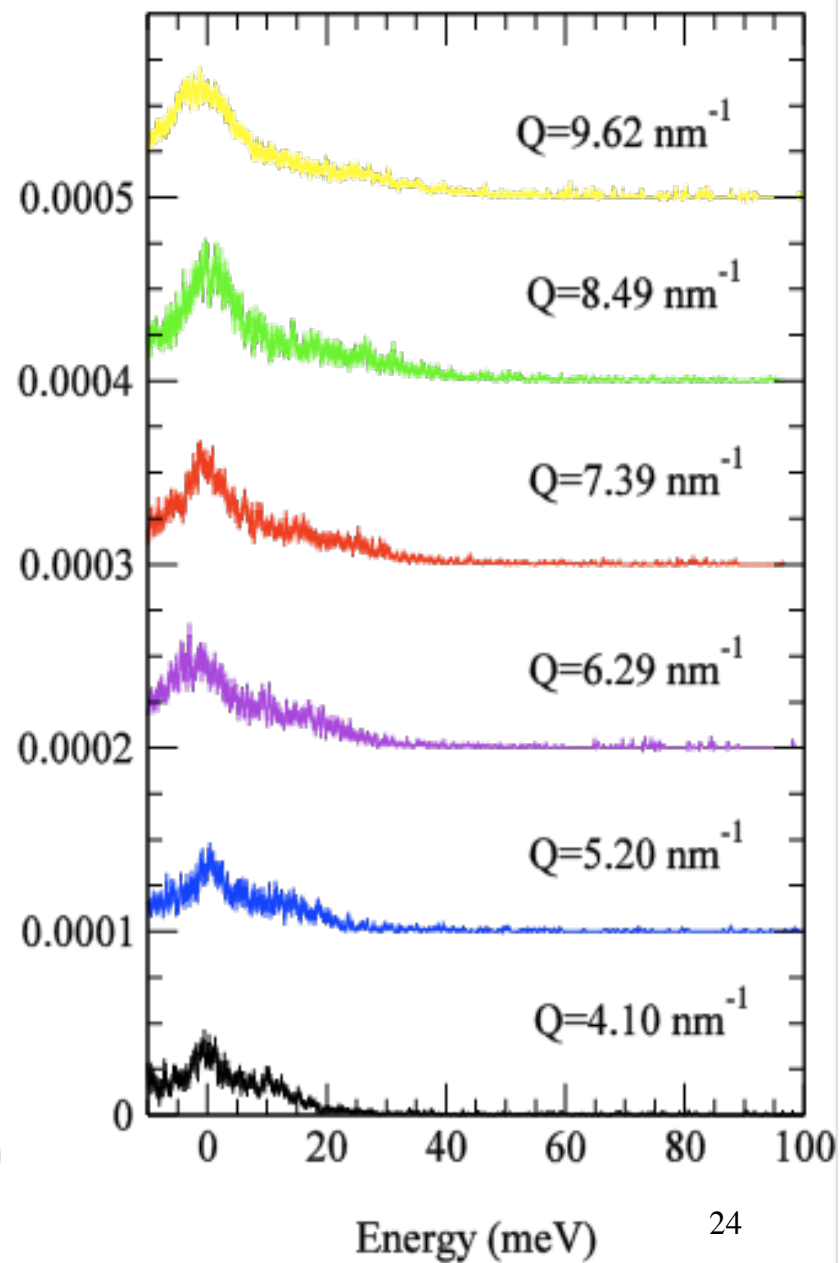$\omega_B(q) = V \cdot q$

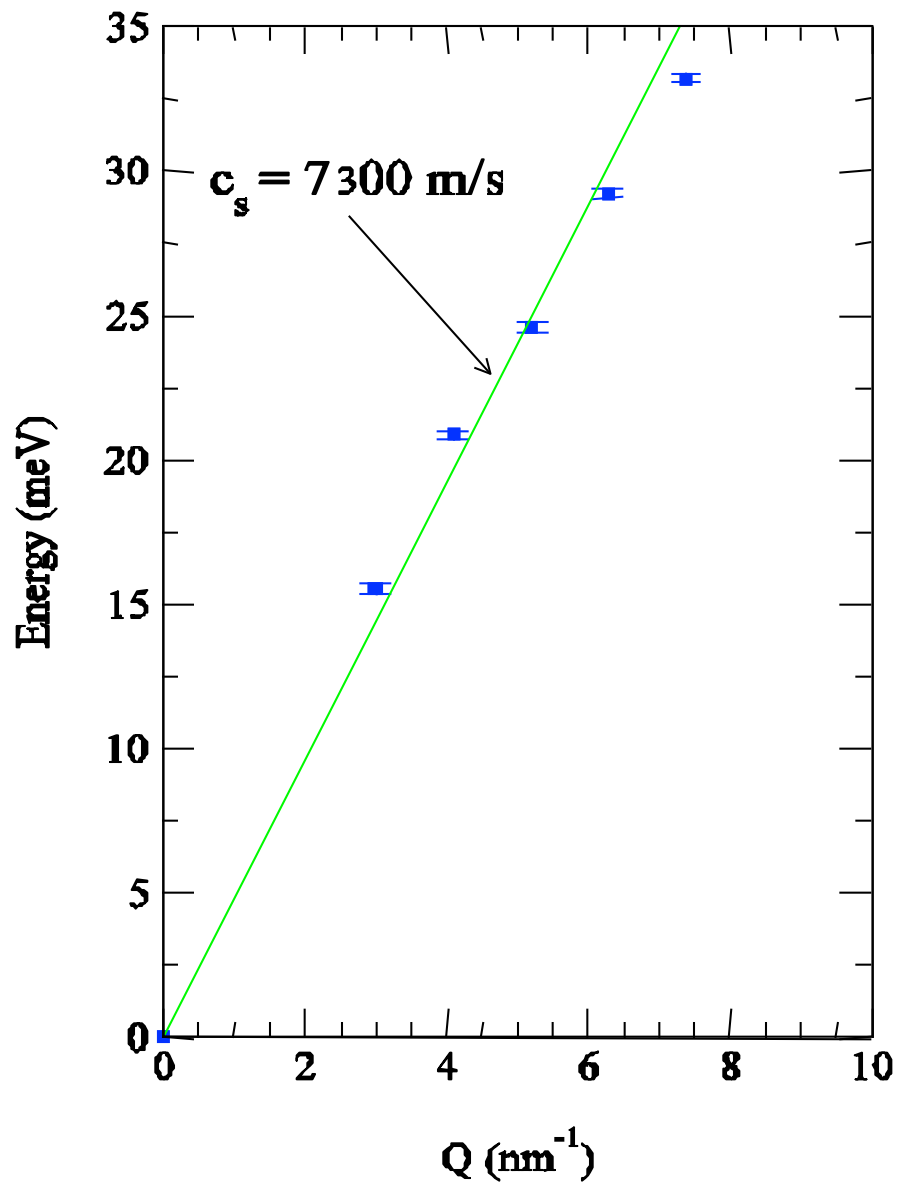$\Delta\omega_B \sim Vq^2$

Hot Solid Silicon
T=1300 C^o

Q=9.62 nm^{-1}

Q=8.49 nm^{-1}

Q=7.39 nm^{-1}

Q=6.29 nm^{-1}

Q=5.20 nm^{-1}

Q=4.10 nm^{-1}

Arb. Unit

Energy (meV)
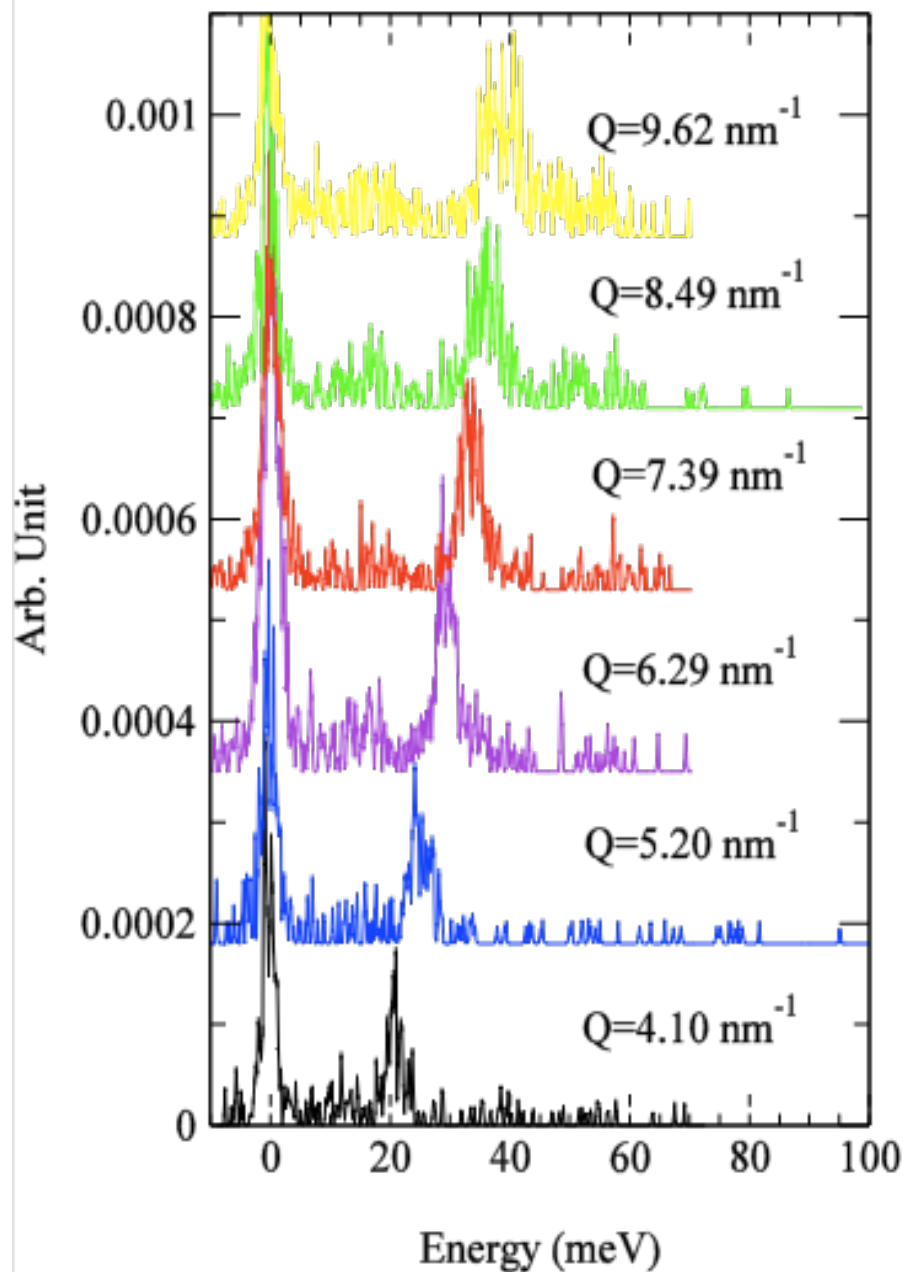
Supercooled Silicon
T=1300 C^o

Q=9.62 nm^{-1}

Q=8.49 nm^{-1}

Q=7.39 nm^{-1}

Q=6.29 nm^{-1}

Q=5.20 nm^{-1}

Q=4.10 nm^{-1}

Energy (meV)

24

Hot Solid Si
T=1300 C°

$c_s = 7300$ m/s

Supercooled Si
T=1300 C°

$c_s = 4566$ m/s

Energy (meV)

Q (nm⁻¹)
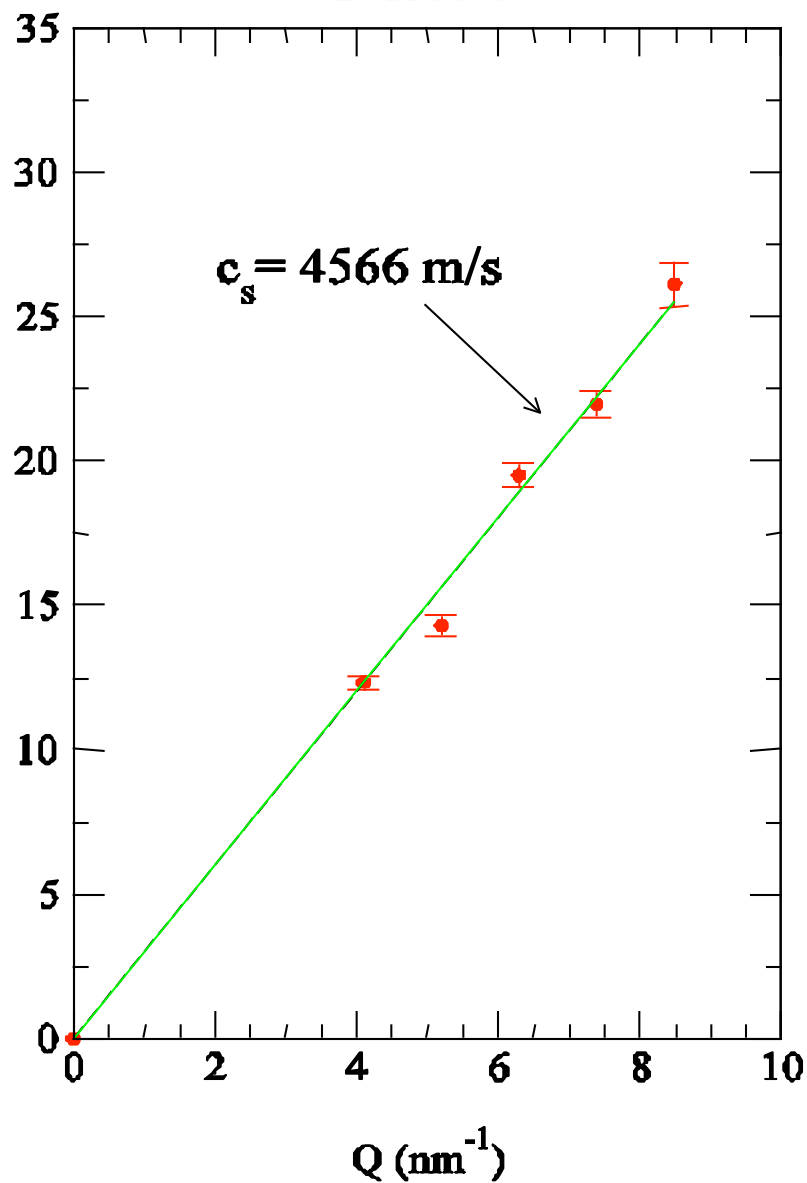
Where is quantum mechanics in all of this?

$$E_{1,n} = \frac{1}{2}J(u_{1,n} - u_{2,n})^2 + \frac{1}{2}J(u_{1,n} - u_{2,n-1})^2$$

Diatomic model

$$E_{2,n} = \frac{1}{2}J(u_{2,n} - u_{1,n})^2 + \frac{1}{2}J(u_{2,n} - u_{1,n+1})^2$$

$$E = \frac{1}{4}\sum_{n,n'}\sum_{j,j'}\phi_{n,n'}^{j,j'}\left(u_{j,n} - u_{j',n'}\right)^2 = \frac{1}{2}\sum_{n,n'}\sum_{j,j'}u_{j,n}\Phi_{n,n'}^{j,j'}u_{j',n'}$$

Generalized model

j, j' :   atoms in the unit cell

n, n' : unit cells in the crystal

$\phi_{j,j'}^{n,n'}$: differential of individual bond energy with respect to displacement

$\Phi_{j,j'}^{n,n'}$: differential of overall bond energy of all lattice

PHONON's: $\phi\omega\nu\acute{\eta}$ (phonē), *sound*

- Phonons are periodic oscillations in condensed systems.

- They are inherently involved in thermal and electrical conductivity.

- They can show anomalous (non-linear) behavior near a phase transition.

- They can carry sound (acoustic modes) or couple to electromagnetic radiation or neutrons (acoustical and optical).

- Have energy of $\hbar\omega$ as quanta of excitation of the lattice vibration mode of angular frequency ω. Since momentum, $\hbar k$, is exact, they are delocalized, collective excitations.

- Phonons are bosons, and they are not conserved. They can be created or annihilated during interactions with neutrons or photons.

- They can be detected by Brillouin scattering (acoustic), Raman scattering, FTIR (optical).

- Their dispersion throughout the BZ can ONLY be monitored with x-rays (IXS), or neutrons (INS).

- Accurate prediction of phonon dispersion require correct knowledge about the force constants: COMPUTATIONAL TECHNIQUES ARE ESSENTIAL.

$$u_{j\ell}(t) = \frac{1}{\sqrt{Nm_j}} \sum_{\mathbf{k},\lambda} \mathbf{e}_{\mathbf{k},\lambda} \exp(i\mathbf{k} \cdot \mathbf{r}_{j\ell}) \, Q(\mathbf{k}, \lambda, t)$$

Fourier relationship between real space and time and reciprocal space and time

$\mathbf{e}_{\mathbf{k},\lambda}$: mode eigenvector

$Q(\mathbf{k}, \lambda, t)$: normal mode coordinate

$$\dot{u}_{j\ell}(t) = \frac{-i}{\sqrt{Nm_j}} \sum_{\mathbf{k},\lambda} \omega_{\mathbf{k},\lambda} \mathbf{e}_{\mathbf{k},\lambda} \exp(i\mathbf{k} \cdot \mathbf{r}_{j\ell}) \, Q(\mathbf{k}, \lambda, t)$$

Velocity

$$\frac{1}{2} \sum_{j,\ell} m_j |\dot{\mathbf{u}}_{j\ell}|^2 = \frac{1}{2} \sum_{\mathbf{k},\lambda} \omega_{\mathbf{k},\lambda}^2 |Q(\mathbf{k}, \lambda)|^2$$

Kinetic energy

$$\frac{1}{2} \sum_{\substack{j,j' \\ \ell,\ell'}} \mathbf{u}_{j\ell}^T \cdot \Phi_{\ell,\ell'}^{j,j'} \cdot \mathbf{u}_{j'\ell'} = \frac{1}{2} \sum_{\mathbf{k},\lambda} \omega_{\mathbf{k},\lambda}^2 |Q(\mathbf{k}, \lambda)|^2$$

Potential energy (via Virial theorem)

$$\frac{1}{2} \sum_{j,\ell} m_j |\dot{\mathbf{u}}_{j\ell}|^2 + \frac{1}{2} \sum_{\substack{j,j' \\ \ell,\ell'}} \mathbf{u}_{j\ell}^T \cdot \Phi_{\ell,\ell'}^{j,j'} \cdot \mathbf{u}_{j'\ell'} = \sum_{\mathbf{k},\lambda} \omega_{\mathbf{k},\lambda}^2 |Q(\mathbf{k}, \lambda)|^2.$$

Total energy, in terms of normal mode coordinates

$$\omega^2 \mathbf{e} = \mathbf{D}(\mathbf{k}) \cdot \mathbf{e} \quad \Rightarrow \quad \omega^2 = \mathbf{e}^{\mathrm{T}} \cdot \mathbf{D}(\mathbf{k}) \cdot \mathbf{e}$$
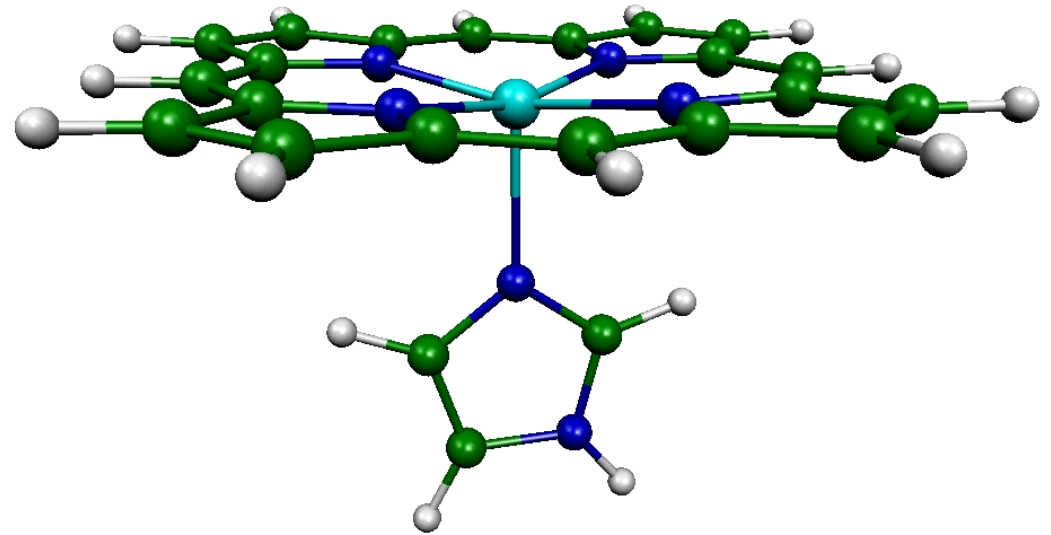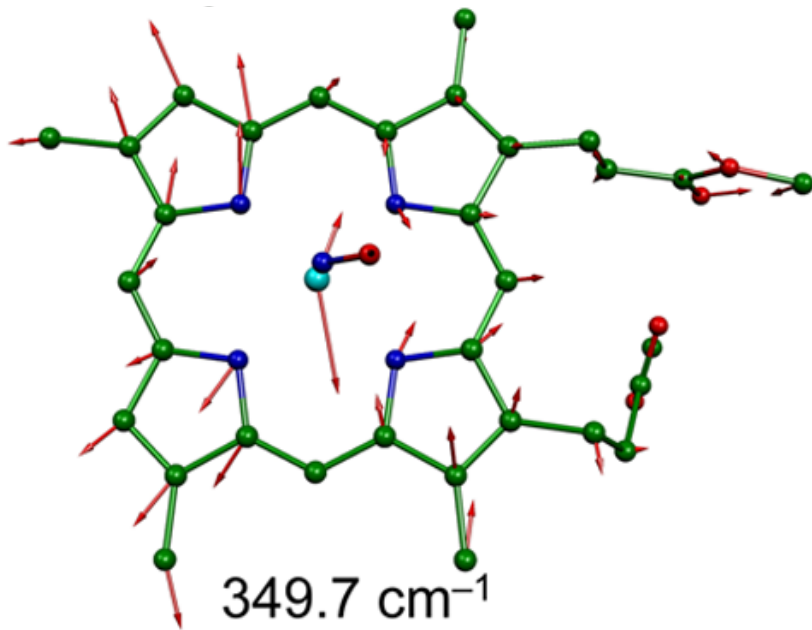
Eigenvalue eqⁿ.

$$D_{j,j'}(\mathbf{k}) = \frac{1}{\sqrt{m_j m_{j'}}} \sum_{n'} \Phi_{0,n'}^{j,j'} \exp\left(i\mathbf{k} \cdot (\mathbf{r}_{j,0} - \mathbf{r}_{j',n'})\right)$$
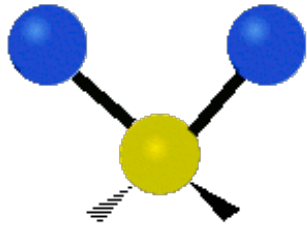
Dynamical matrix

$$\mathbf{e}_\lambda^{\mathrm{T}} \cdot \mathbf{e}_\lambda = 1; \quad \mathbf{e}_{\lambda'}^{\mathrm{T}} \cdot \mathbf{e}_\lambda = \delta_{\lambda',\lambda}$$

Eigenvalues are orthonormal..

349.7 cm⁻¹
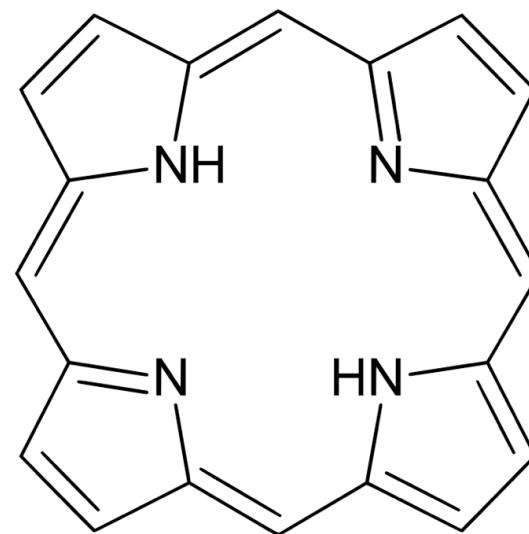
symmetrical
stretching

asymmetrical
stretching
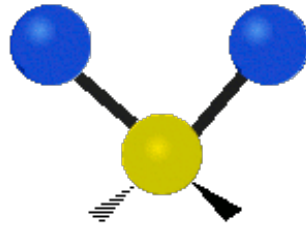
scissoring
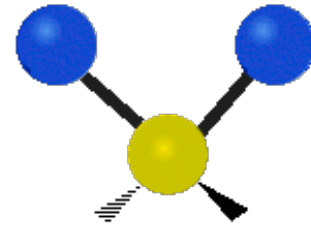
rocking

wagging

twisting

acoustic modes

doming

Fe-N_{pyr}

Fe-Br

Fe-Cl

Fe(P)(Br)
Fe(P)(Cl)

vib. density of states (cm)

$E - E_0/hc$ (cm^{-1})

31
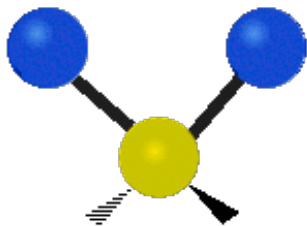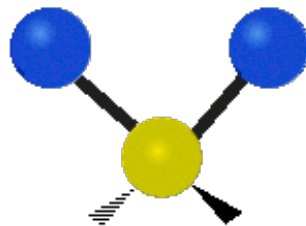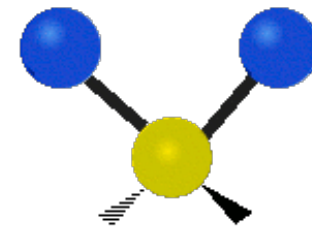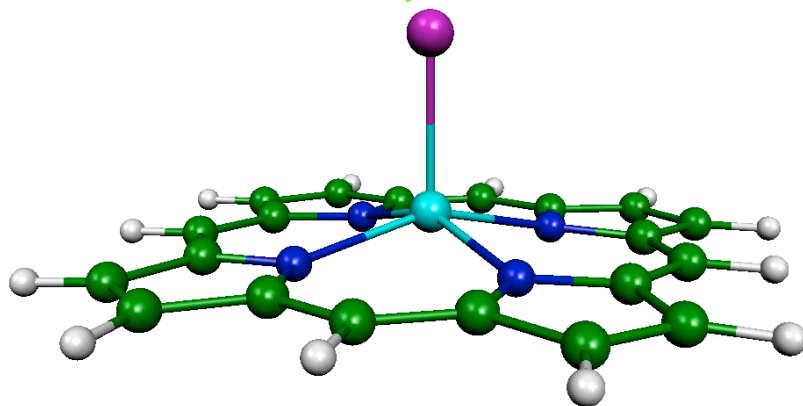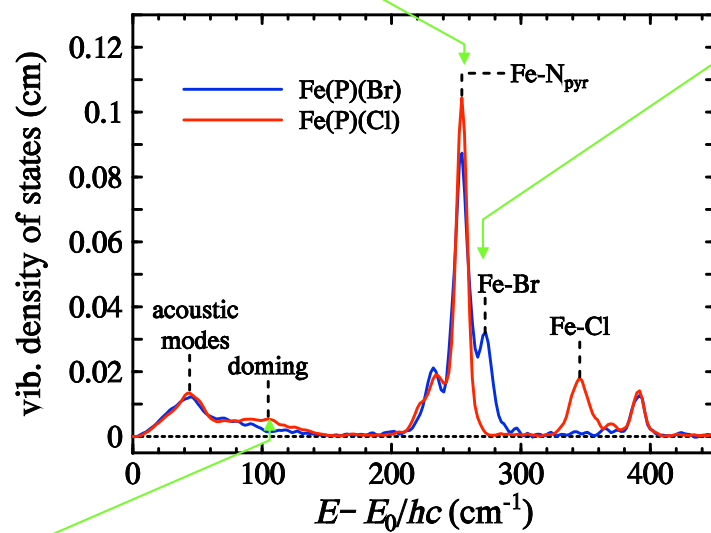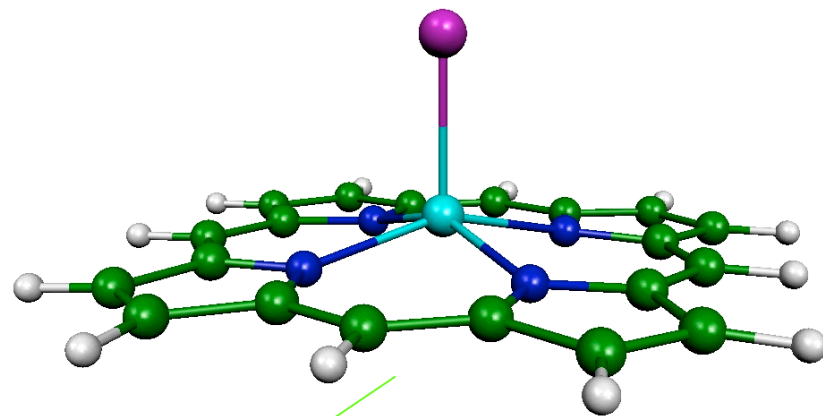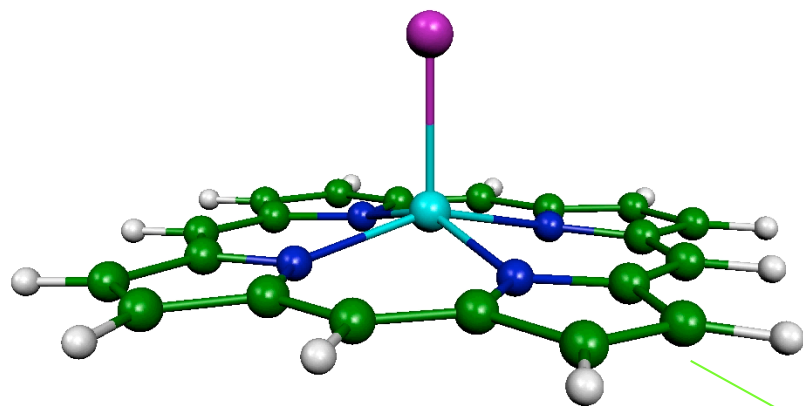
PHONONS (cont'd)

$$E_n = \left(n + \frac{1}{2}\right)\hbar\omega$$

Energy of a single oscillation as a function of number of phonons. The second term +1/2 is the "zero-point" energy.

$$E = \sum_{\mathbf{k},\lambda} \omega_{\mathbf{k},\lambda}^2 \left|Q\left(\mathbf{k},\lambda\right)\right|^2 = \sum_{\mathbf{k},\lambda} \left(n_{\mathbf{k},\lambda} + \frac{1}{2}\right)\hbar\omega_{\mathbf{k},\lambda}.$$

Total energy, in terms of normal mode coordinates

$$\langle n(\omega_{\mathbf{k},\lambda})\rangle = \frac{1}{\exp(\hbar\omega_{\mathbf{k},\lambda}/k_{\mathrm{B}}T) - 1}$$

Bose-Einstein statistics for average number of modes at a given temperature

$$\mathcal{H} = \frac{1}{2}\sum_{j,\ell} m_j \left|\dot{\mathbf{u}}_{j\ell}\right|^2 + \frac{1}{2}\sum_{\substack{j,j' \\ \ell,\ell'}} \mathbf{u}_{j\ell}^T \cdot \Phi_{\ell,\ell'}^{j,j'} \cdot \mathbf{u}_{j'\ell'}$$

Hamiltonian of the system:

$H = Kin. En. + Pot. En$

Phonon density of states

Many thermodynamic functions like free energy, specific heat, and entropy are additive functions of phonon density of states.

This stems from the notion that the normal modes do not interact in the harmonic approximation.

Phonon density of states is the number of modes in a unit energy interval.

$$c_v(T) = 3Nk \int \frac{\hbar^2 \omega^2 e^{\hbar\omega/kT}}{(kT)^2 (1 - e^{\hbar\omega/kT})^2} \cdot g(\omega) \cdot d\omega$$

Vibrational specific heat

Phonon density of states is a key ingredient for many thermodynamic properties

If we choose to write in terms of energy, $\quad E = \hbar\omega, \quad \beta = 1/k_B T$

$$c_v(T) = 3k_B \int (\beta E / 2)^2 \csc h(\beta E) \cdot g(E) \cdot dE$$

Vibrational specific heat

$$S_v(T) = 3k_B \int_0^\infty \left\{ \beta E / 2 \bullet \cot h(\beta E) - \ln\left[2\sin h(\beta E) \right] \right\} \cdot g(E) \cdot dE$$

Vibrational entropy

$$f_{LM} = e^{-E_R \int \{g(E)/2\} \cdot \coth(\beta E/2)} dE$$

Lamb-Mössbauer factor

$$g(E) = \frac{3m}{2\pi^2 \hbar^3 \rho v_D^3} E^2$$

Debye Sound velocity

$$\langle F \rangle = \frac{M}{\hbar^2} \int_0^\infty E^2 g(E) dE$$

Average restoring force constant

And, some thermodynamics

$$\mathcal{Z} = \frac{1}{1 - \exp(-\beta\hbar\omega)}$$

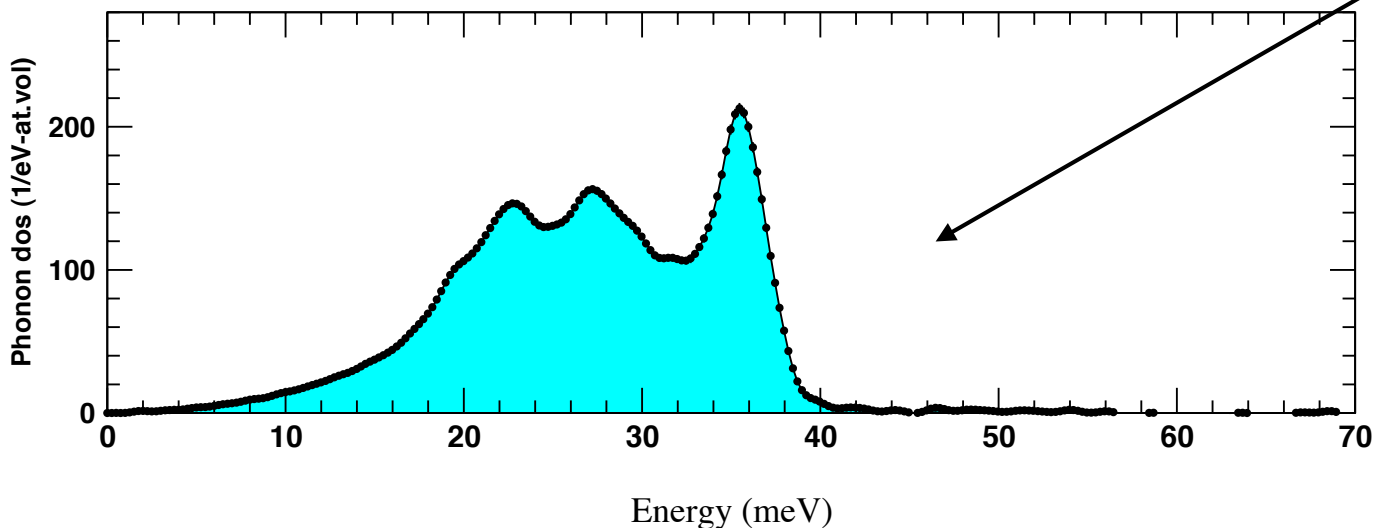Partition function

$$F = -k_{\mathrm{B}} T \ln \mathcal{Z}$$
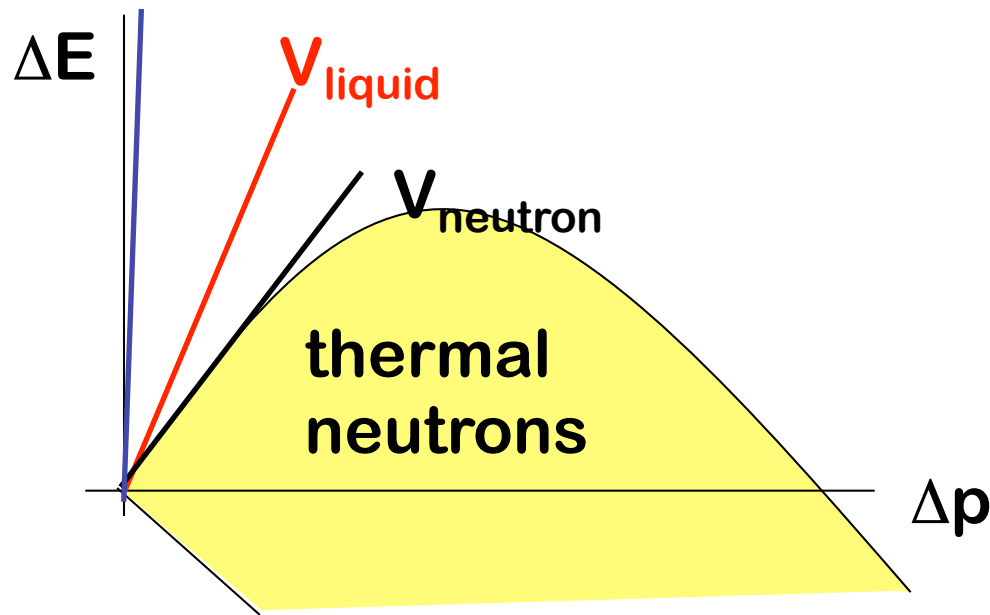
Free energy

$$C = -T \frac{\partial^2 F}{\partial T^2}$$

Heat capacity

$$E = \sum_{\mathbf{k},\lambda} \left(\langle n(\omega_{\mathbf{k},\lambda}) \rangle + \frac{1}{2} \right) \hbar\omega_{\mathbf{k},\lambda} \equiv \int \left(\langle n(\omega) \rangle + \frac{1}{2} \right) \hbar\omega \, g(\omega) \, \mathrm{d}\omega.$$

Energy in terms of
phonon density of states

Why x-rays instead of neutrons or visible light ?

Limited momentum transfer capability of neutrons at low energies favor x-rays to study collective excitations with large dispersion, like sound modes.
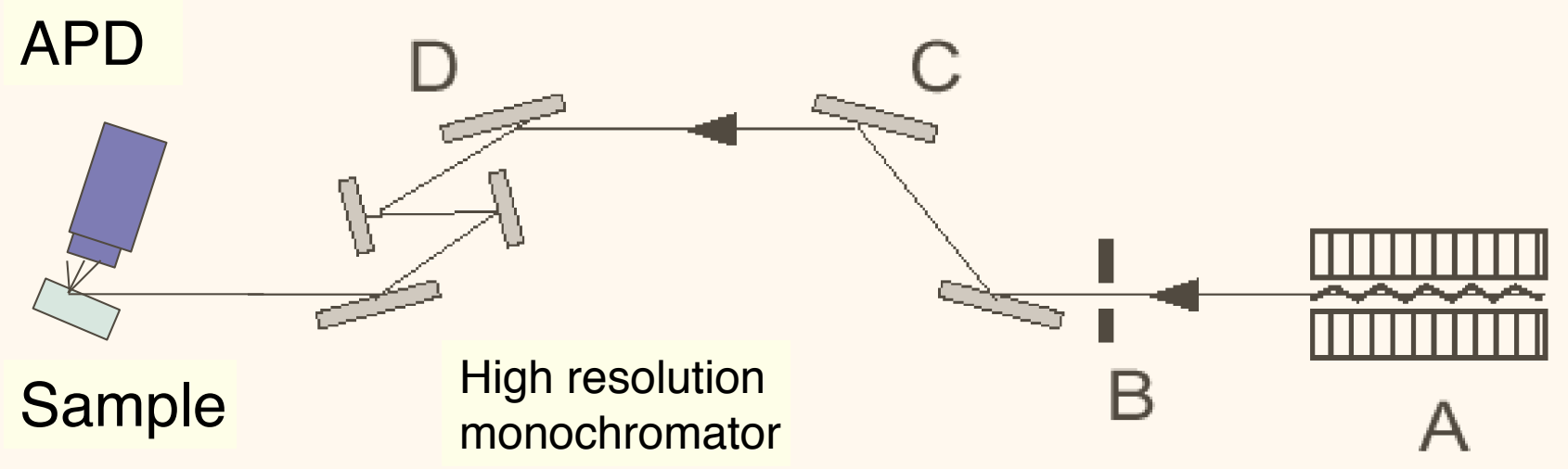
When the sound velocity exceeds that of neutrons in the liquid, x-rays become unique. The low-momentum/high-energy transfer region is only accessible by x-rays.

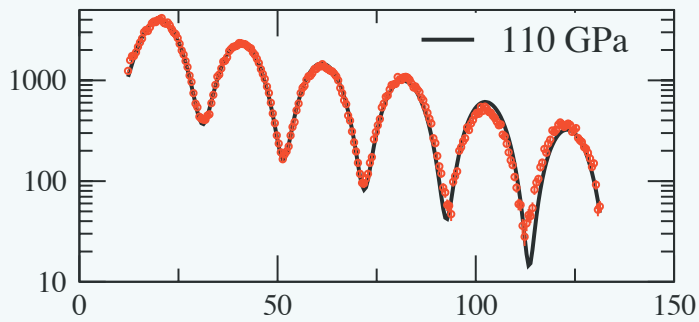# Inelastic X-Ray Scattering: two approaches

IXS: Momentum resolved

6 m horizontal arm

10 cm

~11cm

High resolution monochromator

1 mm

3mm

J

H G F

mirror

D

C

B

A
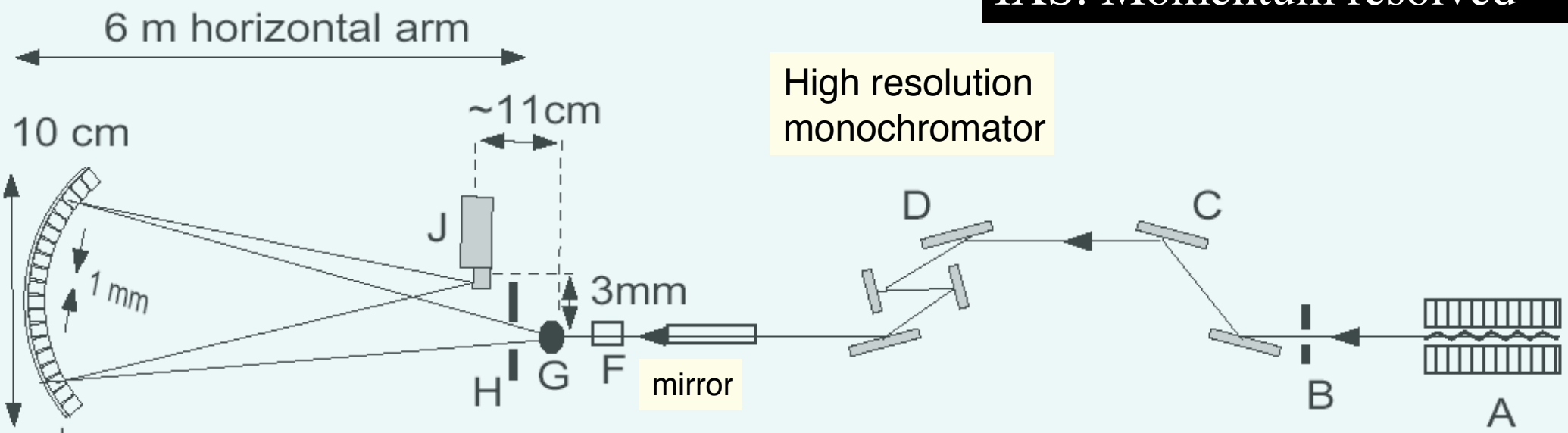
NRIXS: Momentum integrated

APD

D

C

B

A

Sample

High resolution monochromator

Nuclear Resonant Scattering

SMS: Synchrotron Mössbauer Spectroscopy
NFS : Nuclear Forward Scattering

Isomer shift
Quadrupole splitting
Magnetic hyperfine field
- valence state
- local crystallographic symmetry
- magnetic ordering
- relaxation

APD

D   C   B   A

NRIXS: Nuclear Resonant Inelastic X-ray Scattering
NRVS: Nuclear Resonant Vibrational Spectroscopy
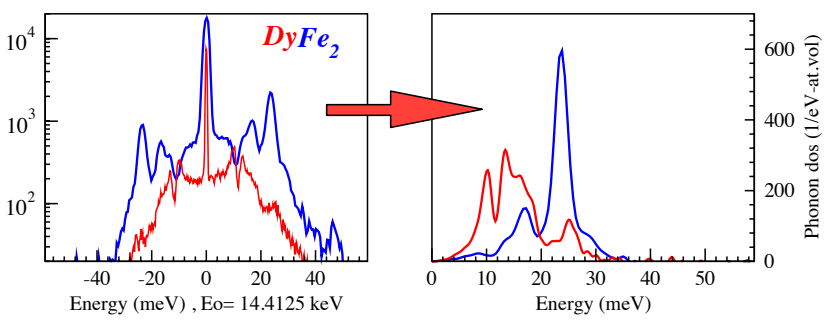
Partial phonon density of states
Recoil-free fraction
- speed of sound
- vibrational modes
- entropy and specific heat
- phonon confinement
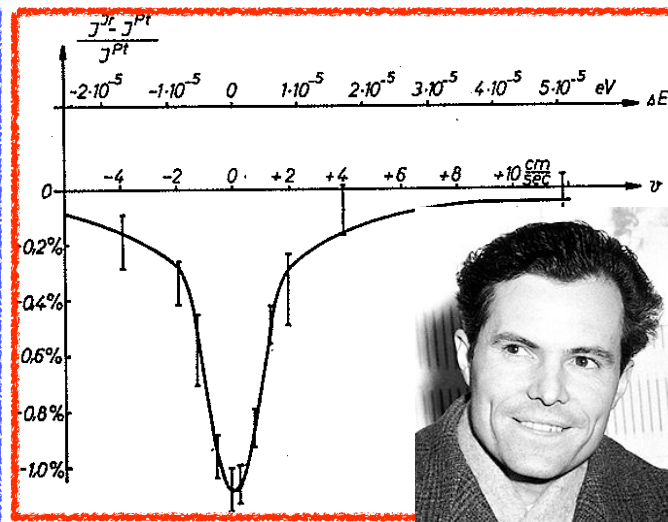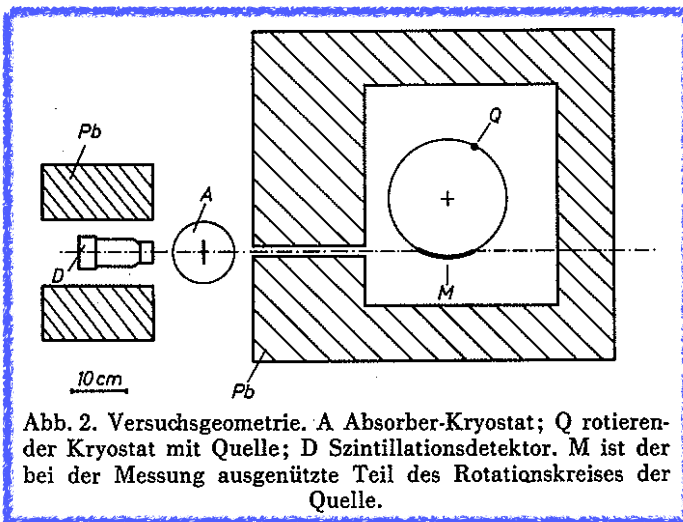- resilience, compressibility
- Debye Temperature

$DyFe_2$

Sample

APD

D   C   B   A
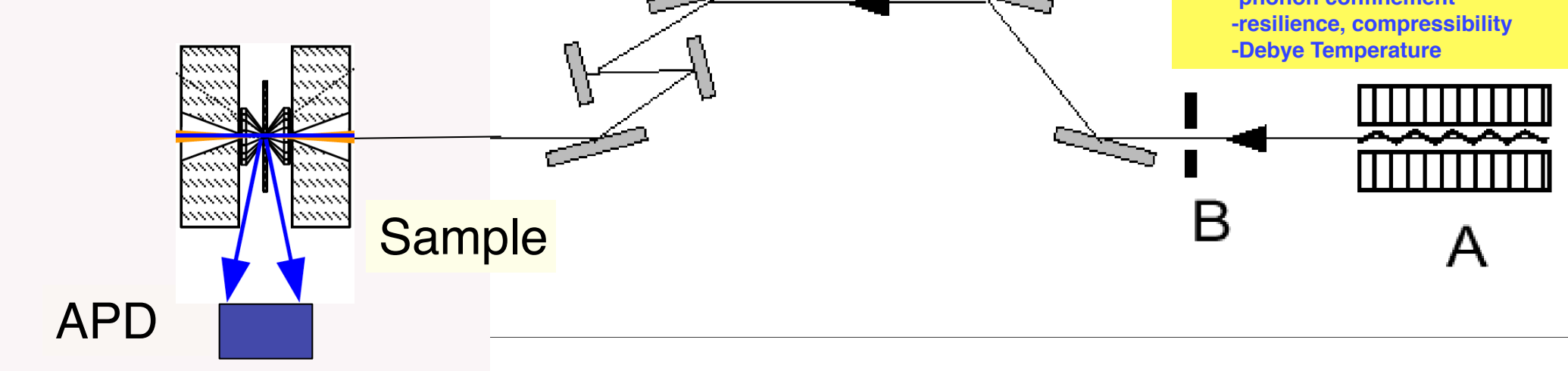
Kernresonanzabsorption von γ-Strahlung in Ir^{191}
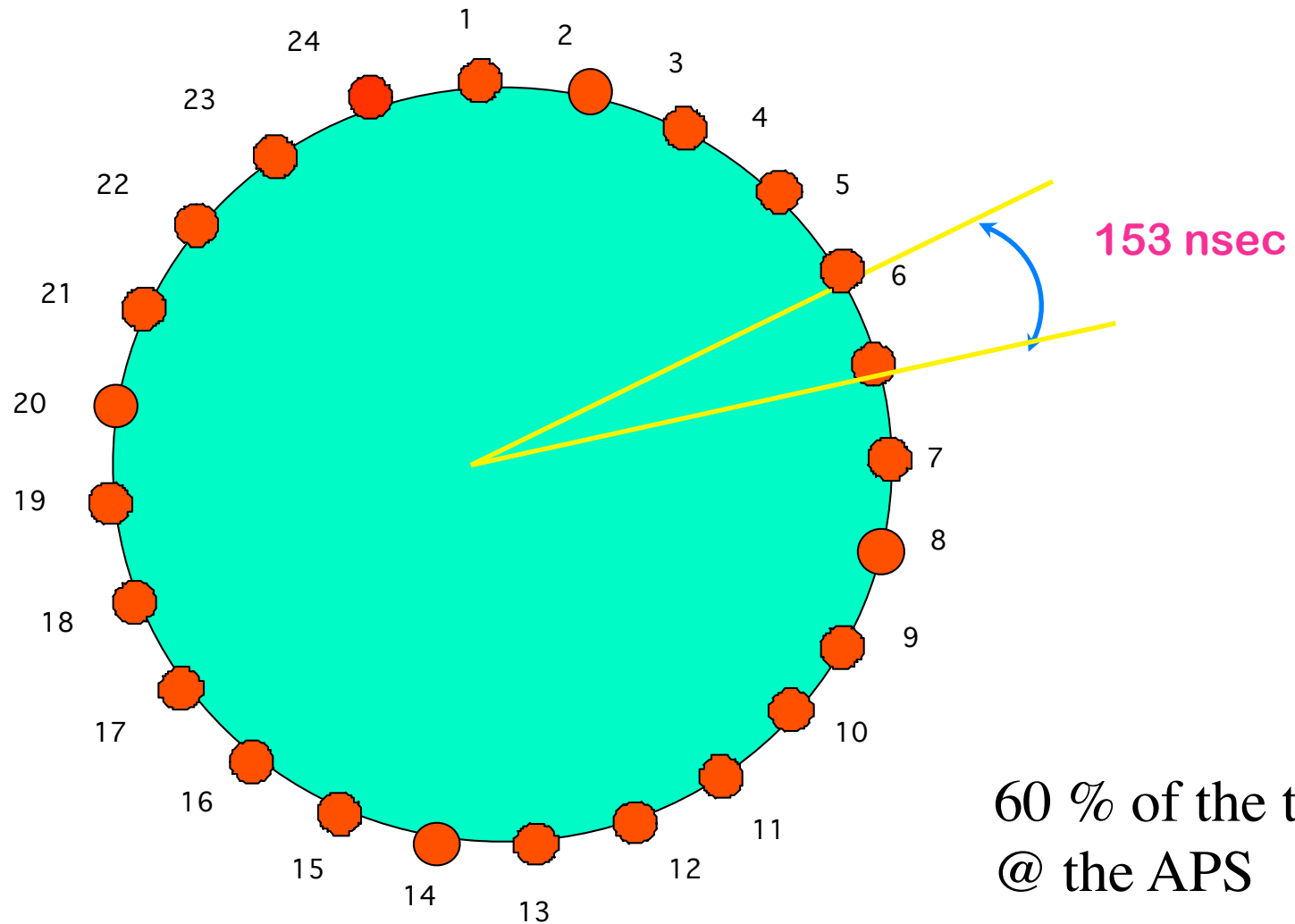
Von Rudolf L. Mössbauer

Aus dem Laboratorium für technische Physik der Technischen Hochschule in München
und dem Institut für Physik im Max-Planck-Institut für medizinische Forschung in Heidelberg

Bei der Emission und Selbstabsorption von weicher γ-Strahlung in Kernen treten bei tiefen Temperaturen in Festkörpern sehr starke Linien mit der natürlichen Linienbreite auf. Diese Linien erscheinen als Folge davon, daß bei tiefen Temperaturen bei einem Teil der Quantenübergänge der γ-Rückstoßimpuls nicht mehr vom einzelnen Kern aufgenommen wird, sondern von dem Kristall als Ganzes. Da die scharfen Emissions- und Absorptionslinien energetisch an der gleichen Stelle liegen, tritt ein sehr starker Resonanzfluoreszenzeffekt auf. Durch eine „Zentrifugen"-Methode, bei der die Emissions- und Absorptionslinien gegeneinander verschoben werden, läßt sich der Fluoreszenzeffekt unterdrücken und so eine unmittelbare Bestimmung der natürlichen Linienbreite von Resonanzlinien vornehmen. Erste Messungen nach dieser Methode ergeben für die Lebenszeit τ des 129 keV-Niveaus in Ir^{191}: $\tau = \left(1{,}4 \begin{array}{c} +0{,}2 \\ -0{,}1 \end{array}\right) \cdot 10^{-10}$ sec.
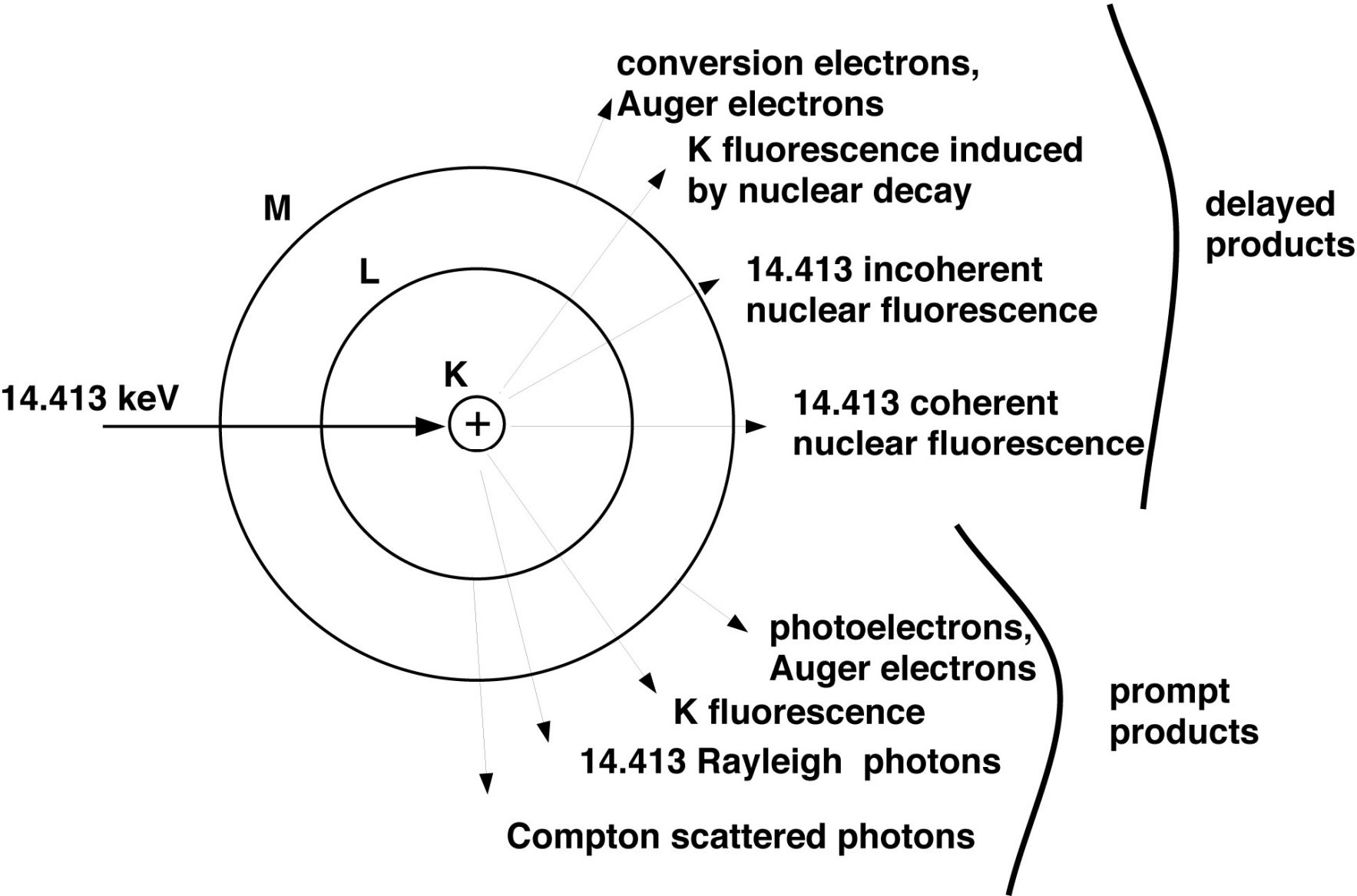

Abb. 2. Versuchsgeometrie. A Absorber-Kryostat; Q rotierender Kryostat mit Quelle; D Szintillationsdetektor. M ist der bei der Messung ausgenützte Teil des Rotationskreises der Quelle.
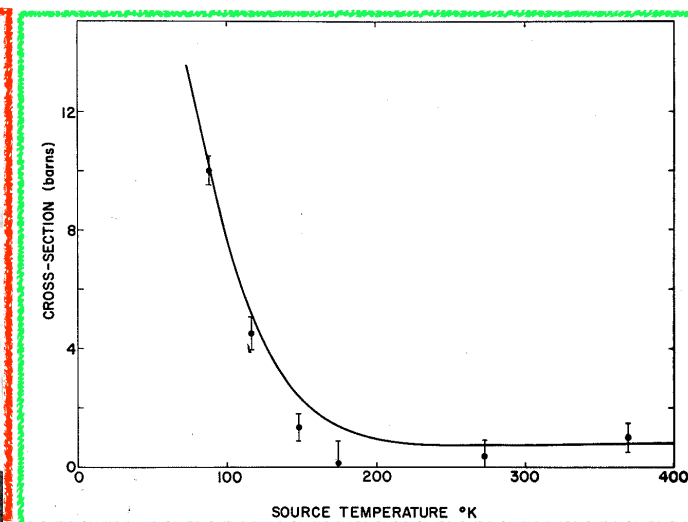
Standard Time structure @ APS

153 nsec

60 % of the time
@ the APS

1 revolution=3.68 µsec =>1296 buckets

Nuclear Resonance and Fallout in ^{57}Fe-decay

conversion electrons,
Auger electrons

K fluorescence induced
by nuclear decay

14.413 incoherent
nuclear fluorescence

14.413 coherent
nuclear fluorescence

delayed
products

M

L

K

14.413 keV

photoelectrons,
Auger electrons

K fluorescence

14.413 Rayleigh photons

Compton scattered photons

prompt
products

Detection of nuclear decay
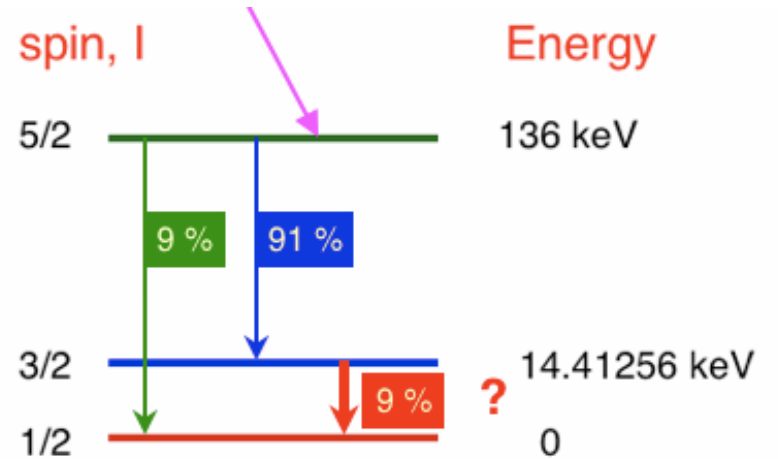
Level Diagram
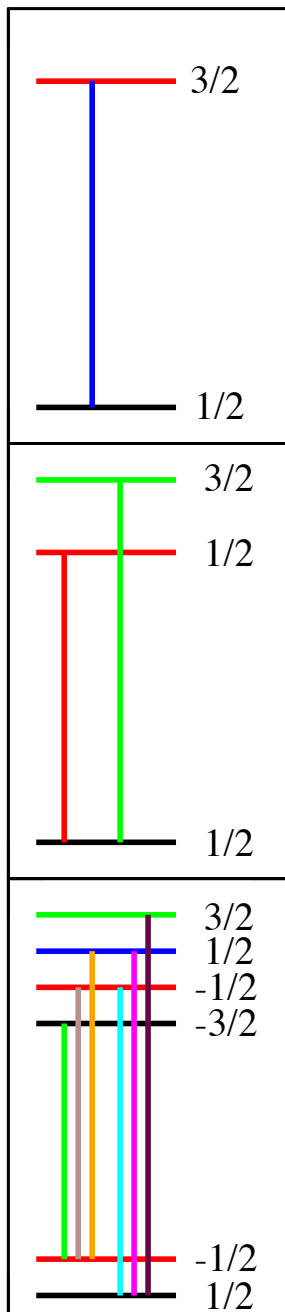
Energy domain

Time domain (SMS or NFS)

3/2

1/2

3/2

1/2

1/2

3/2
1/2
-1/2
-3/2

-1/2

1/2

-6 -4 -2 0 2 4 6

energy(mm/s)

0   100   200   300   400   500

time (ns)

44
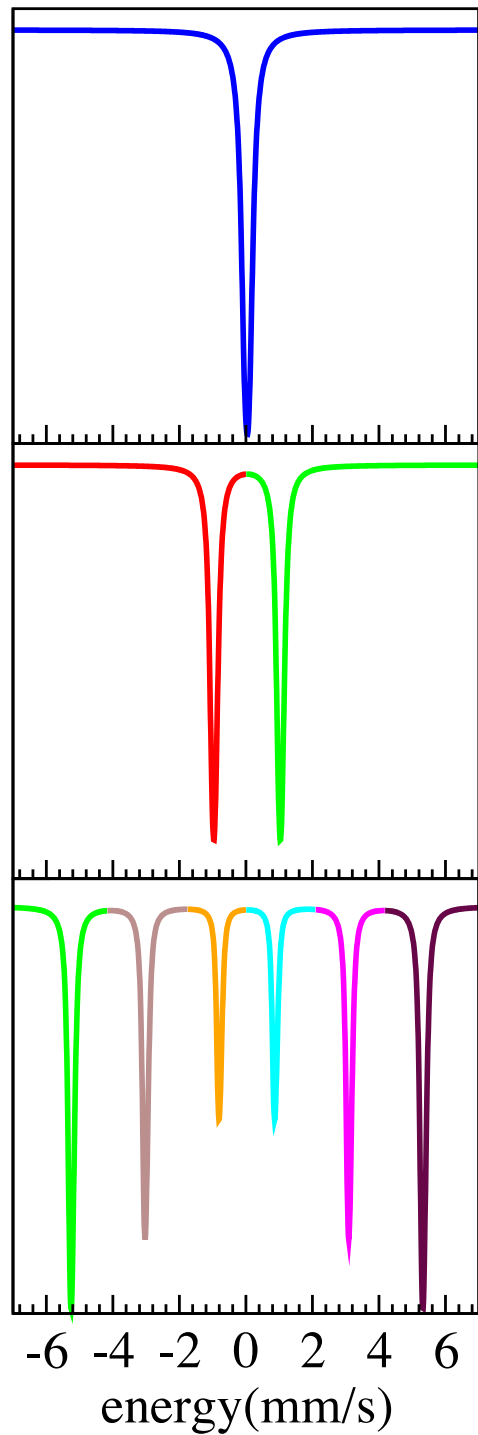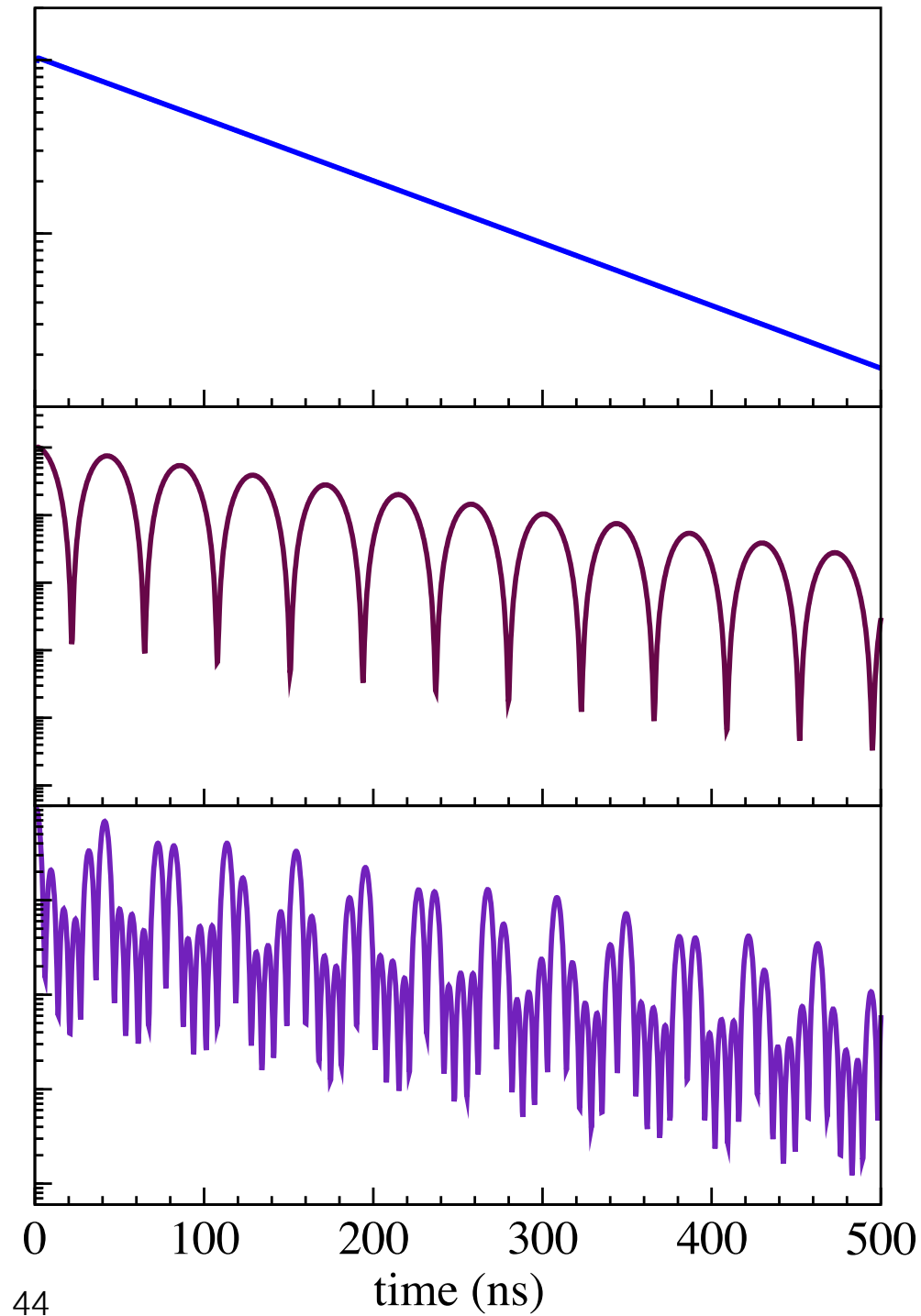
α (bcc-Fe) to ε (fcc-Fe) transition under pressure by synchrotron Mössbauer spectroscopy

remaining % α

Pressure (GPa)

APD detector

Sample

High resolution Monochromator

High Heat Load Monochromator

White beam slits

Undulator

$\Delta E \sim 10$ neV

$\Delta E \sim 1$ meV

$\Delta E \sim 1$ eV

$\Delta E \sim 150$ eV

$\Delta E \sim 500$ keV

1Hz -10^5 Hz

5×10^9 Hz

10^{13} Hz

Early dreamers..

Zero phonon "Mössbauer pip"
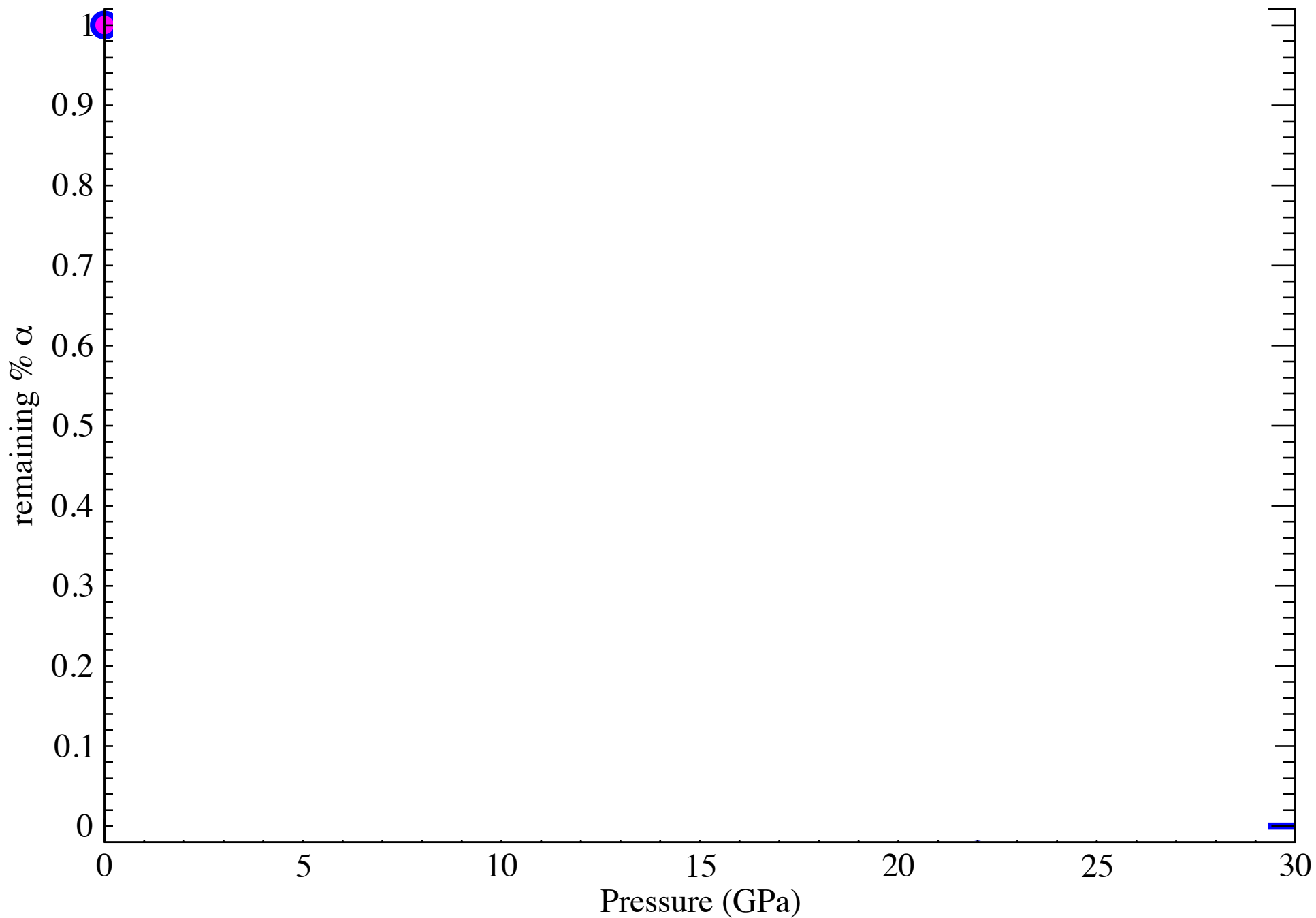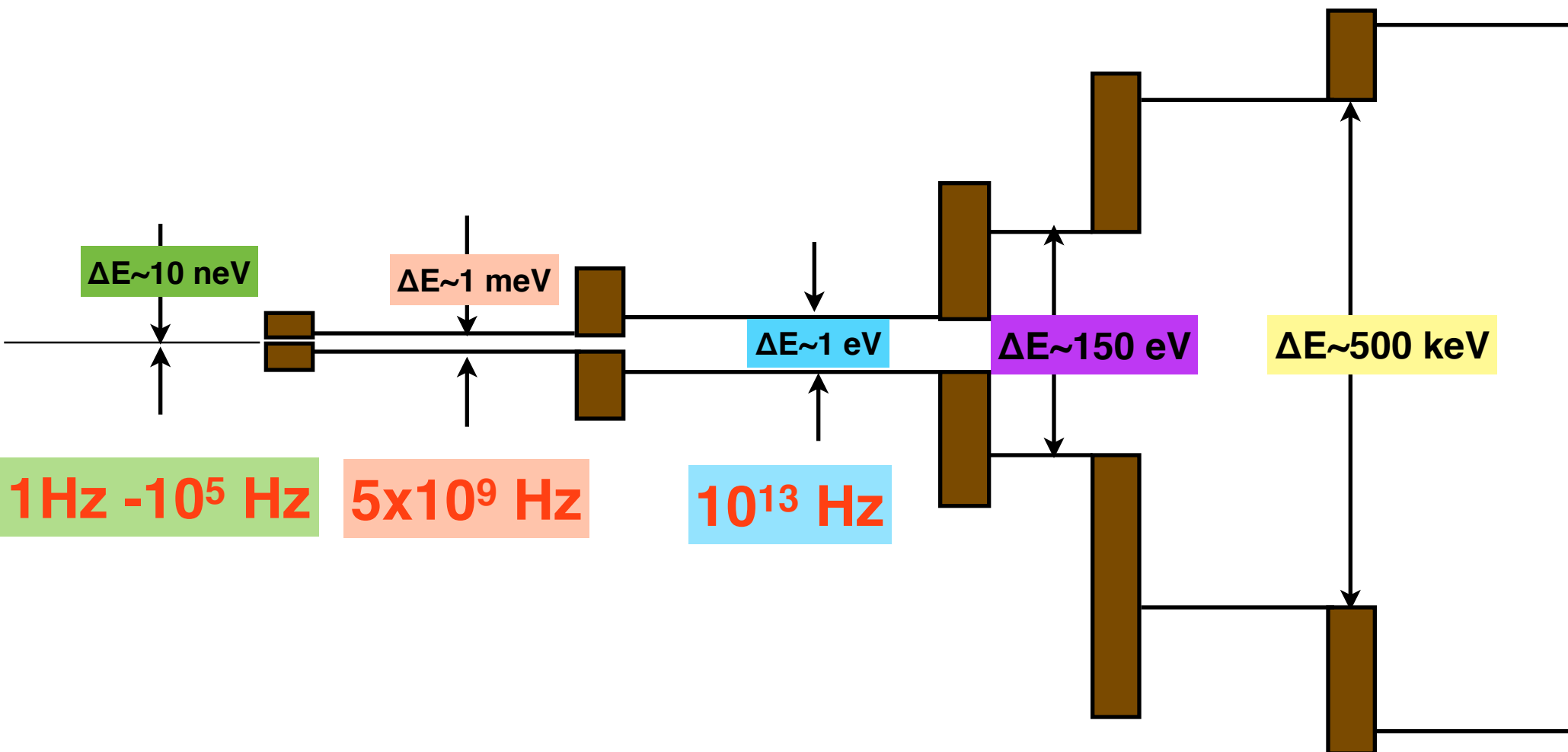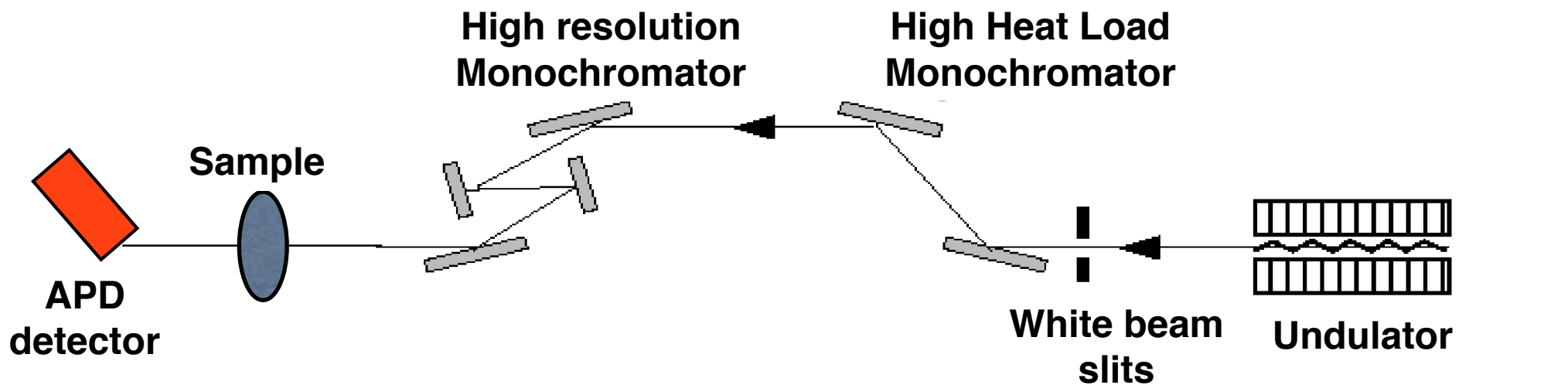
Visualized by W. Vischer at Los Alamos & K. S. Singwi at Argonne (1960), but only properly observed after synchrotron radiation based tunable monochromators are realized.
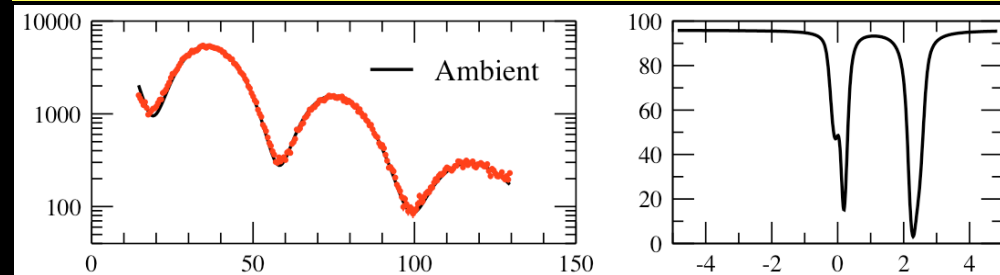(W. Sturhahn et al, PRL , 74 (1995) p. 3832)

Singwi (1967)

Visualized by Stan Ruby (1974) at Argonne and properly observed by E. Gerdau (Hamburg).
(S. L Ruby. J. de Physique 35 (1974) C6-209

5 neV + mono. resolution

Phonon annihilation

Phonon creation

-    0   +

Energy (~ meV)

Phonon Density of States Measured by Inelastic Nuclear Resonant Scattering

W. Sturhahn, T. S. Toellner, and E. E. Alp

Advanced Photon Source, Argonne National Laboratory, Argonne, Illinois 60439

X. Zhang and M. Ando

Photon Factory, National Laboratory for High Energy Physics, Oho 1-1, Tsukuba, Ibaraki 305, Japan

Y. Yoda and S. Kikuta

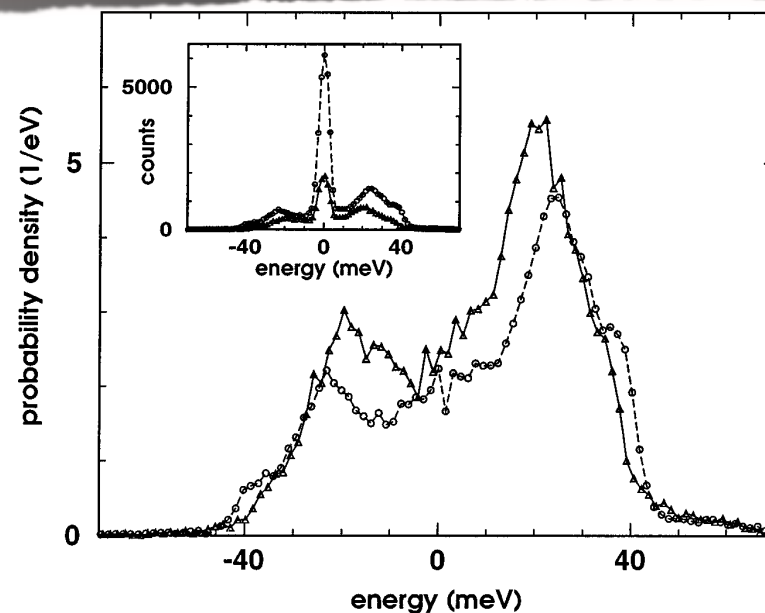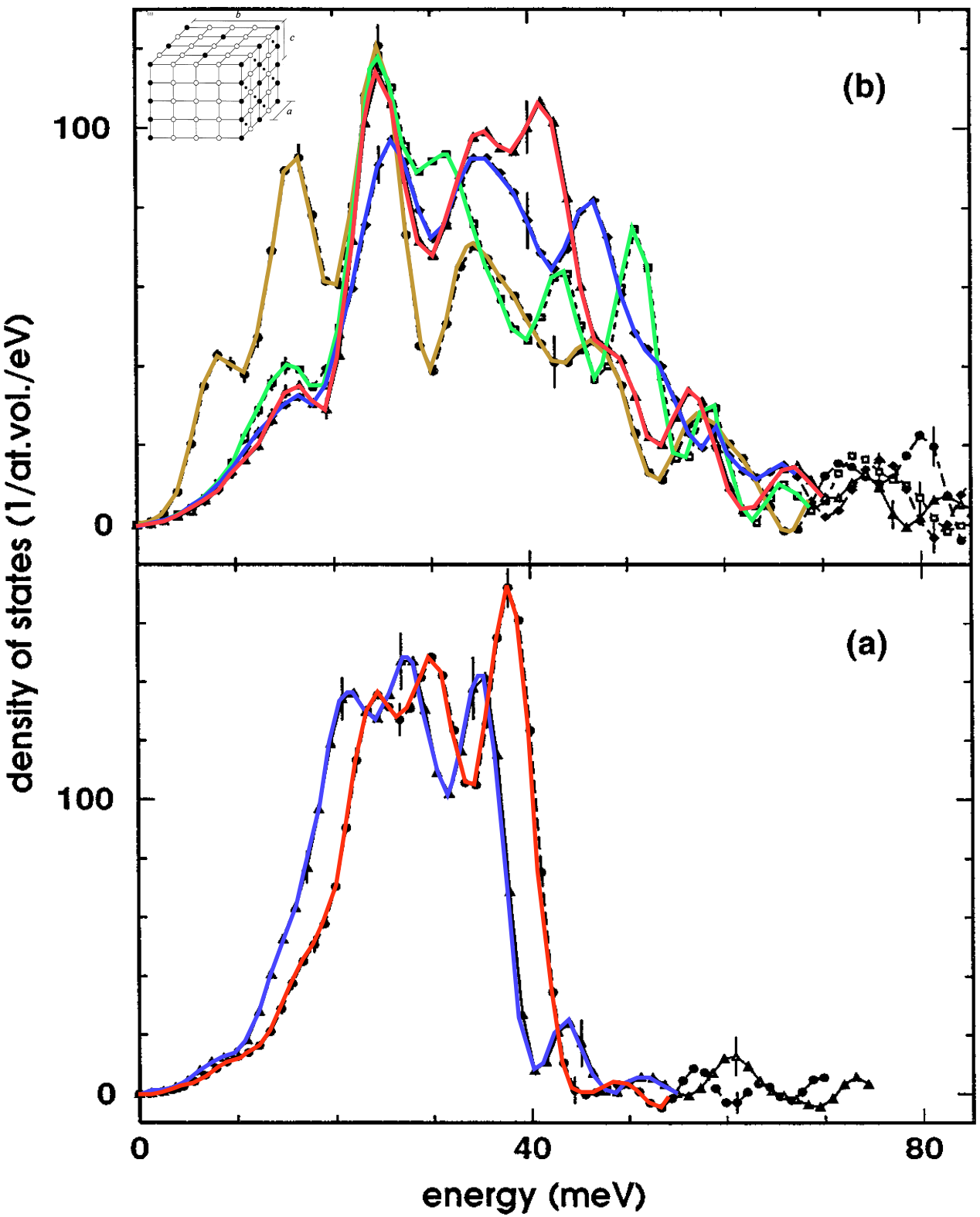*Department of Applied Physics, Faculty of Engineering, The University of Tokyo, Hongo 7-3-1, Bunkyo-ku, Tokyo 113, Japan*

M. Seto

Research Reactor Institute, Kyoto University, Sennan-gun, Osaka 590-04, Japan

C. W. Kimball and B. Dabrowski

Department of Physics, Northern Illinois University, De Kalb, Illinois 60115
(Received 16 December 1994)

> 400 citations

48

$Sr_2Fe_2O_5$ — Brownmillerite

$Sr_2Fe_2O_{5.5}$ — Orthorombic perovskite

$Sr_2Fe_2O_{5.75}$ — Tetragonal perovskite

$Sr_2Fe_2O_6$ — Cubic perovskite

bcc-iron

stainless steel, 304

Phonons in Nanocrystalline ^{57}Fe
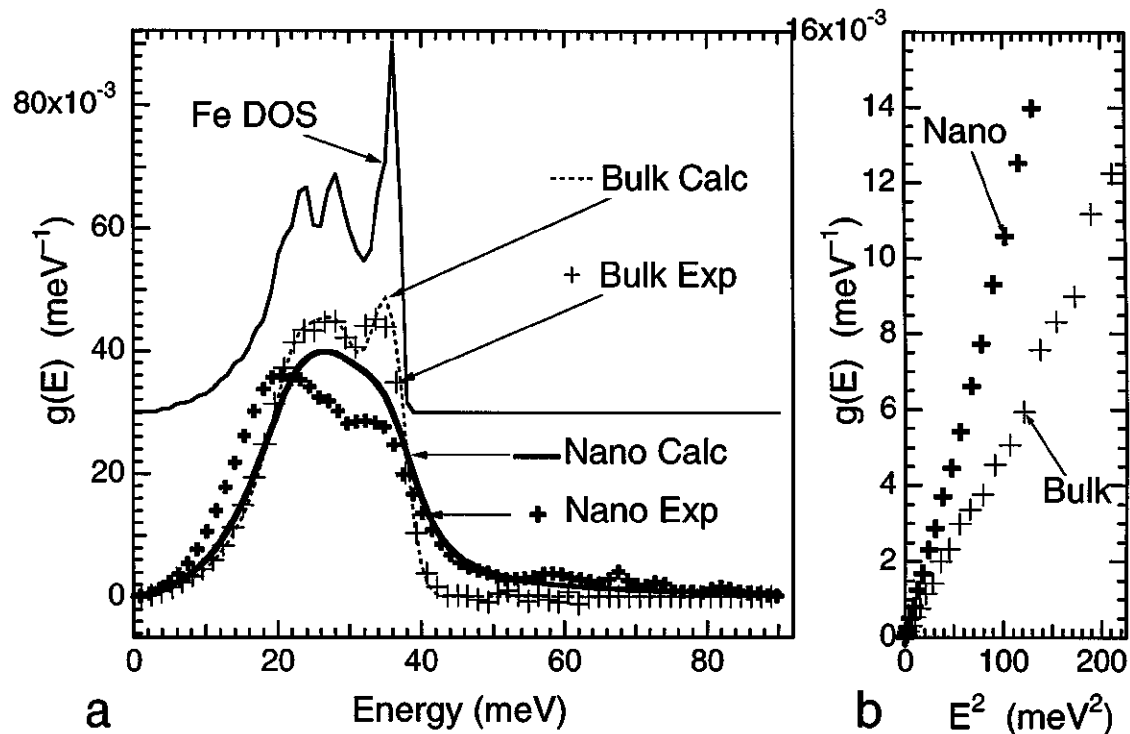
B. Fultz,[1] C. C. Ahn,[1] E. E. Alp,[2] W. Sturhahn,[2] and T. S. Toellner[2]

[1]*Division of Engineering and Applied Science, 138-78, California Institute of Technology, Pasadena, California 91125*
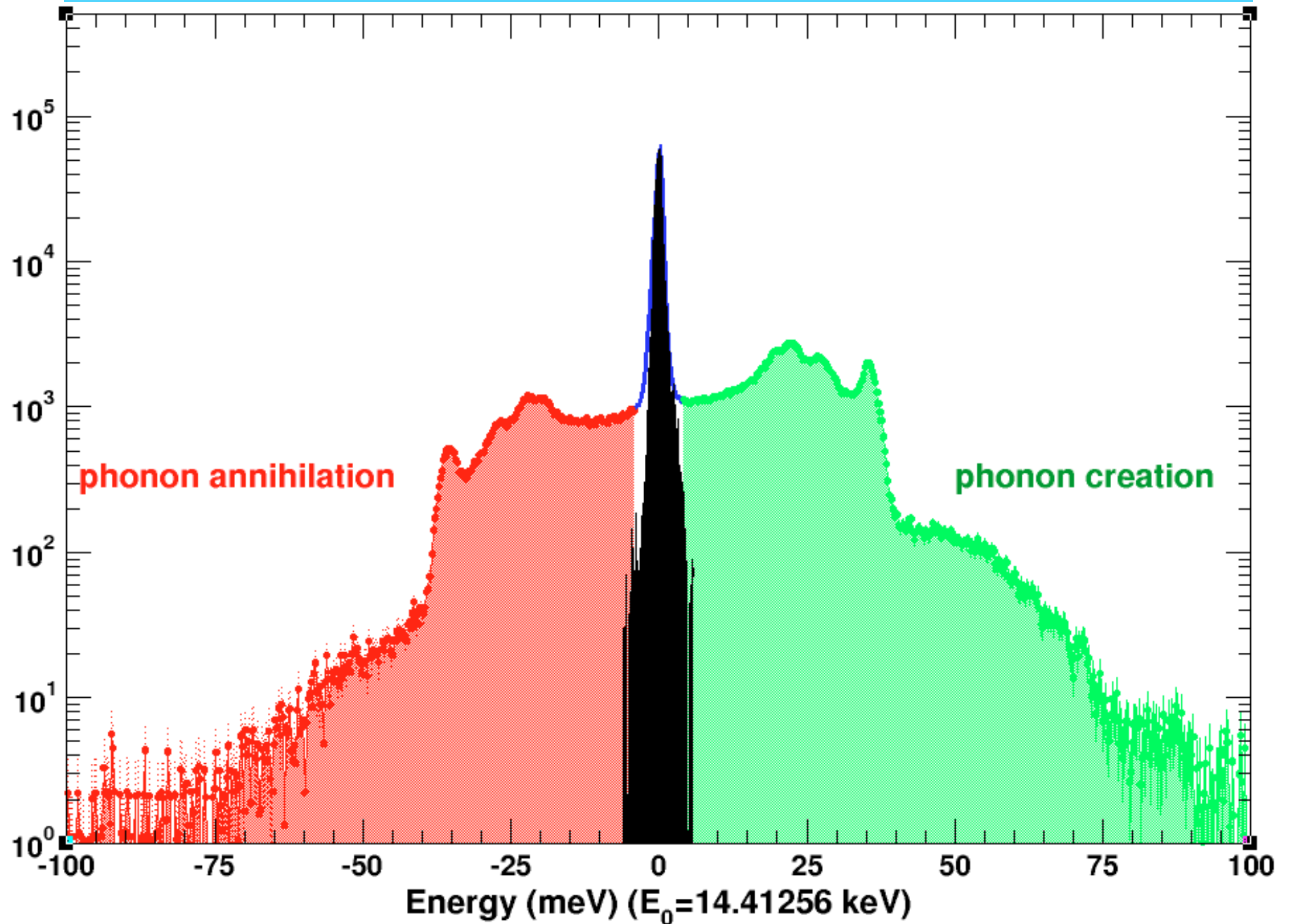[2]*Advanced Photon Source, Argonne National Laboratory, Argonne, Illinois 60439*

(Received 13 March 1997)

We measured the phonon density of states (DOS) of nanocrystalline Fe by resonant inelastic nuclear γ-ray scattering. The nanophase material shows large distortions in its phonon DOS. We attribute the high energy distortion to lifetime broadening. A damped harmonic oscillator model for the phonons provides a low quality factor, Q_u, averaging about 5, but the longitudinal modes may have been broadened most. The nanocrystalline Fe also shows an enhancement in its phonon DOS at energies below 15 meV. The difference in vibrational entropy of the bulk and nanocrystalline Fe was small, owing to competing changes in the nanocrystalline phonon DOS at low and high energies.
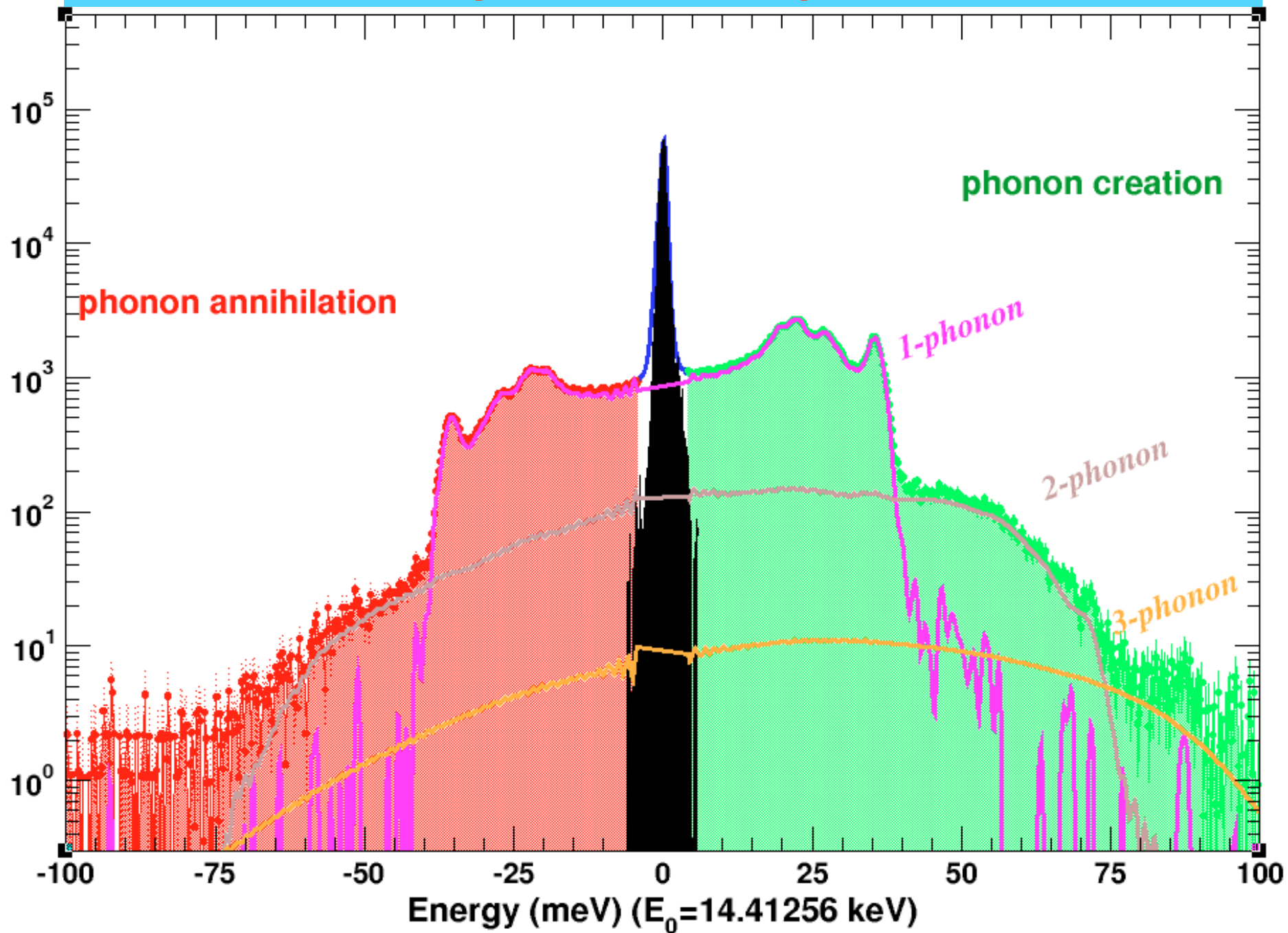
Phonon excitation probability
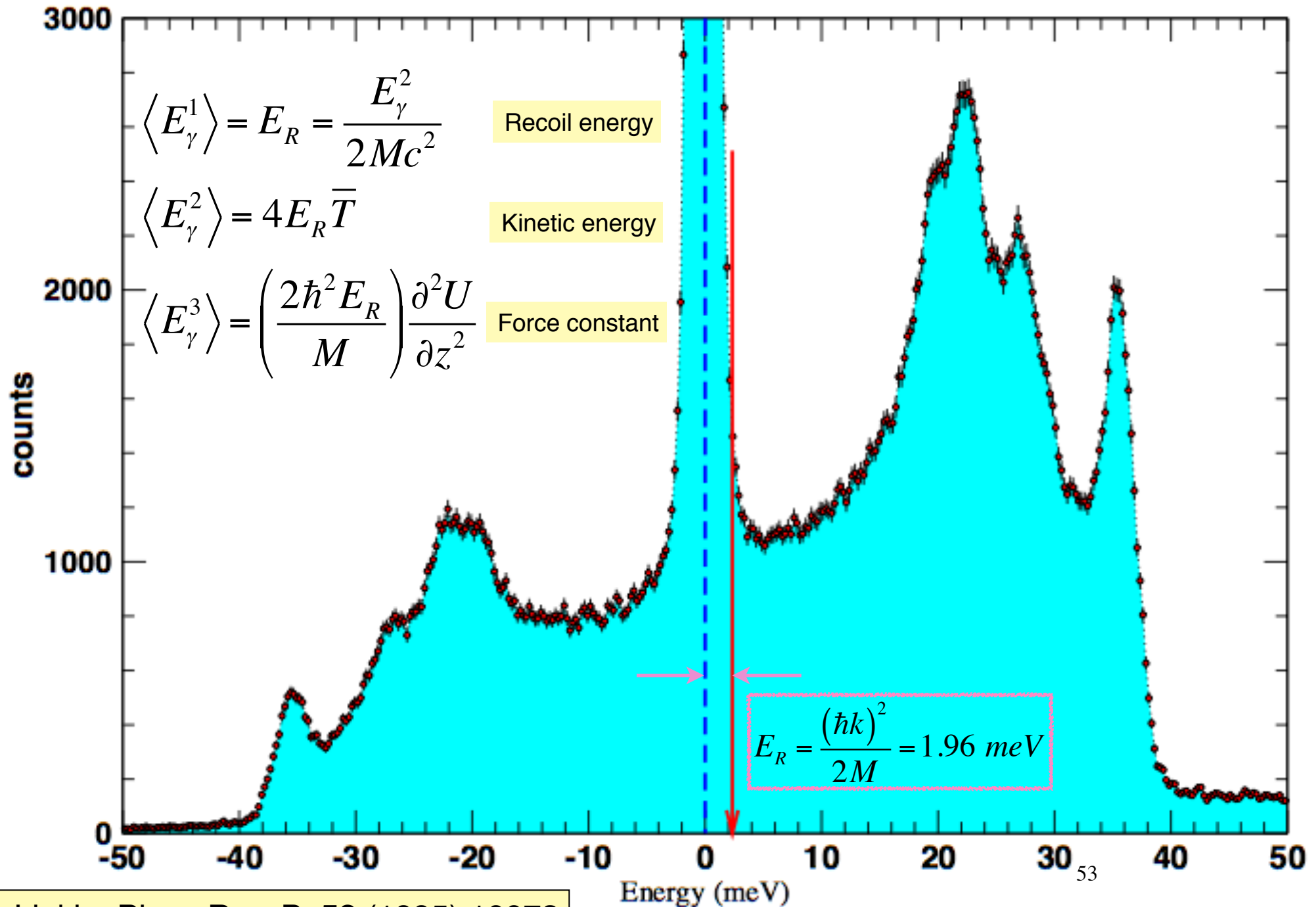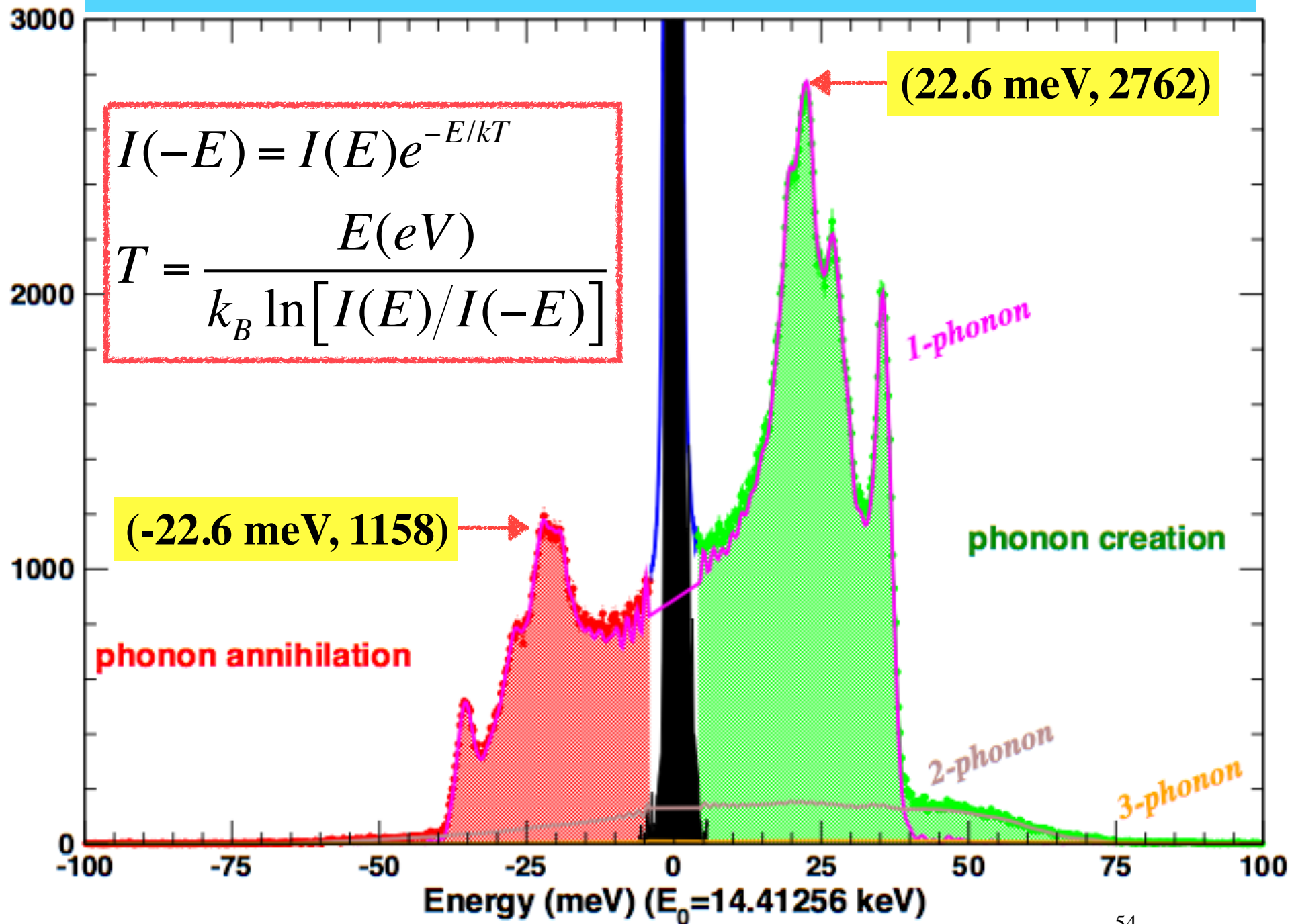

phonon annihilation

phonon creation

Energy (meV) (E_0=14.41256 keV)

Multi-phonon decomposition

phonon creation

phonon annihilation

1-phonon

2-phonon

3-phonon

Energy (meV) (E_0=14.41256 keV)

Lipkin's sum rules related to phonon excitation probability

$$\langle E_\gamma^1 \rangle = E_R = \frac{E_\gamma^2}{2Mc^2}$$

Recoil energy

$$\langle E_\gamma^2 \rangle = 4E_R \overline{T}$$

Kinetic energy

$$\langle E_\gamma^3 \rangle = \left(\frac{2\hbar^2 E_R}{M} \right) \frac{\partial^2 U}{\partial z^2}$$

Force constant

$$E_R = \frac{(\hbar k)^2}{2M} = 1.96 \ meV$$

counts

Energy (meV)

53

H. Lipkin, Phys. Rev. B, **52** (1995) 10073

Detailed Balance

$$I(-E) = I(E)e^{-E/kT}$$

$$T = \frac{E(eV)}{k_B \ln\left[I(E)/I(-E)\right]}$$

(22.6 meV, 2762)

(-22.6 meV, 1158)

1-phonon

phonon creation

phonon annihilation

2-phonon

3-phonon

Energy (meV) (E_0=14.41256 keV)

54

Detailed Balance

$$I(-E) = I(E)e^{-E/kT}$$

$$k_B = 8.6173 \cdot 10^{-2} \, meV / K$$

$$E = 22.6 \, meV$$

$$I(-E) = 1158, \quad I(E) = 2762$$

$$T = \frac{E(eV)}{k_B \ln\left[I(E)/I(-E)\right]} = 297.03K$$

1-phonon

phonon creation

phonon annihilation

2-phonon

3-phonon

Energy (meV) (E$_0$=14.41256 keV)

55

Temperature dependence of phonon excitation probability

Chumakov, et al, Phys. Rev. B 54 (1996) 9596.

$$g(E) = \frac{\tilde{m}}{2\pi^2 \hbar^3 \rho} \frac{1}{v_D^3} E^2$$

bcc-Fe

TA-1

TA-2

LA

θ_D

Fe phonon density of states (1/eV-atomic vol)

Energy (meV)

57
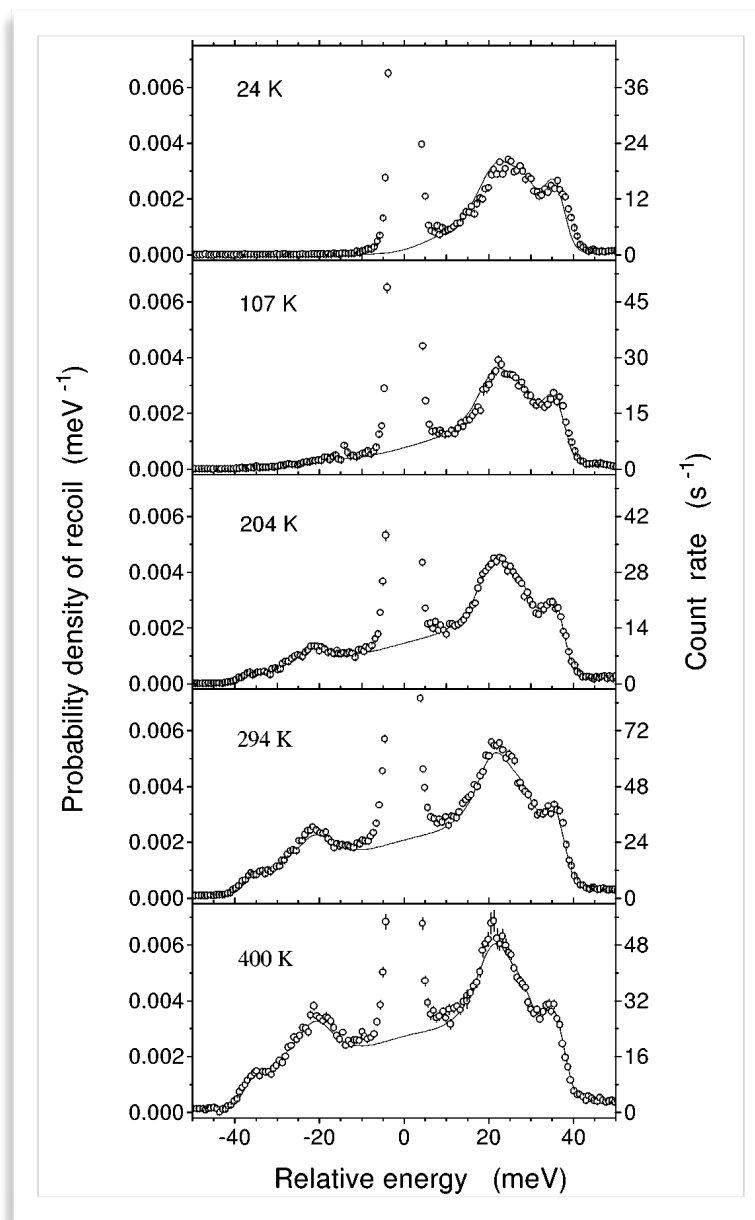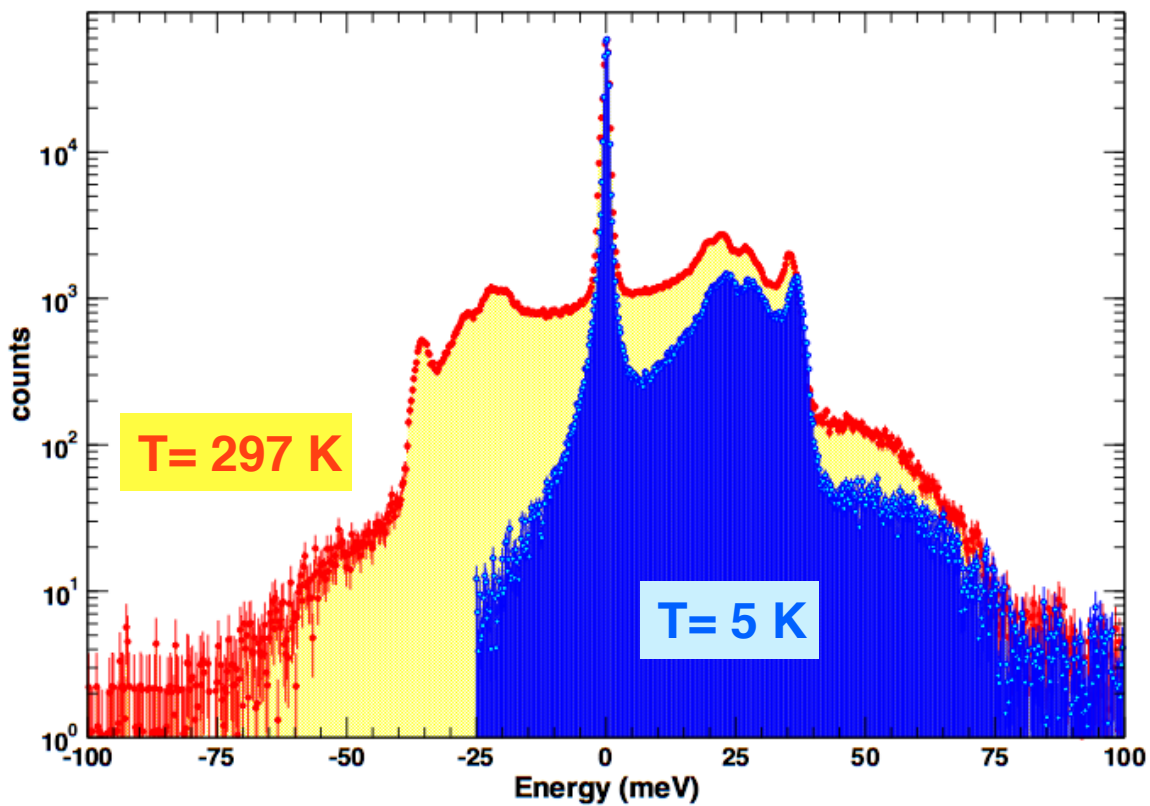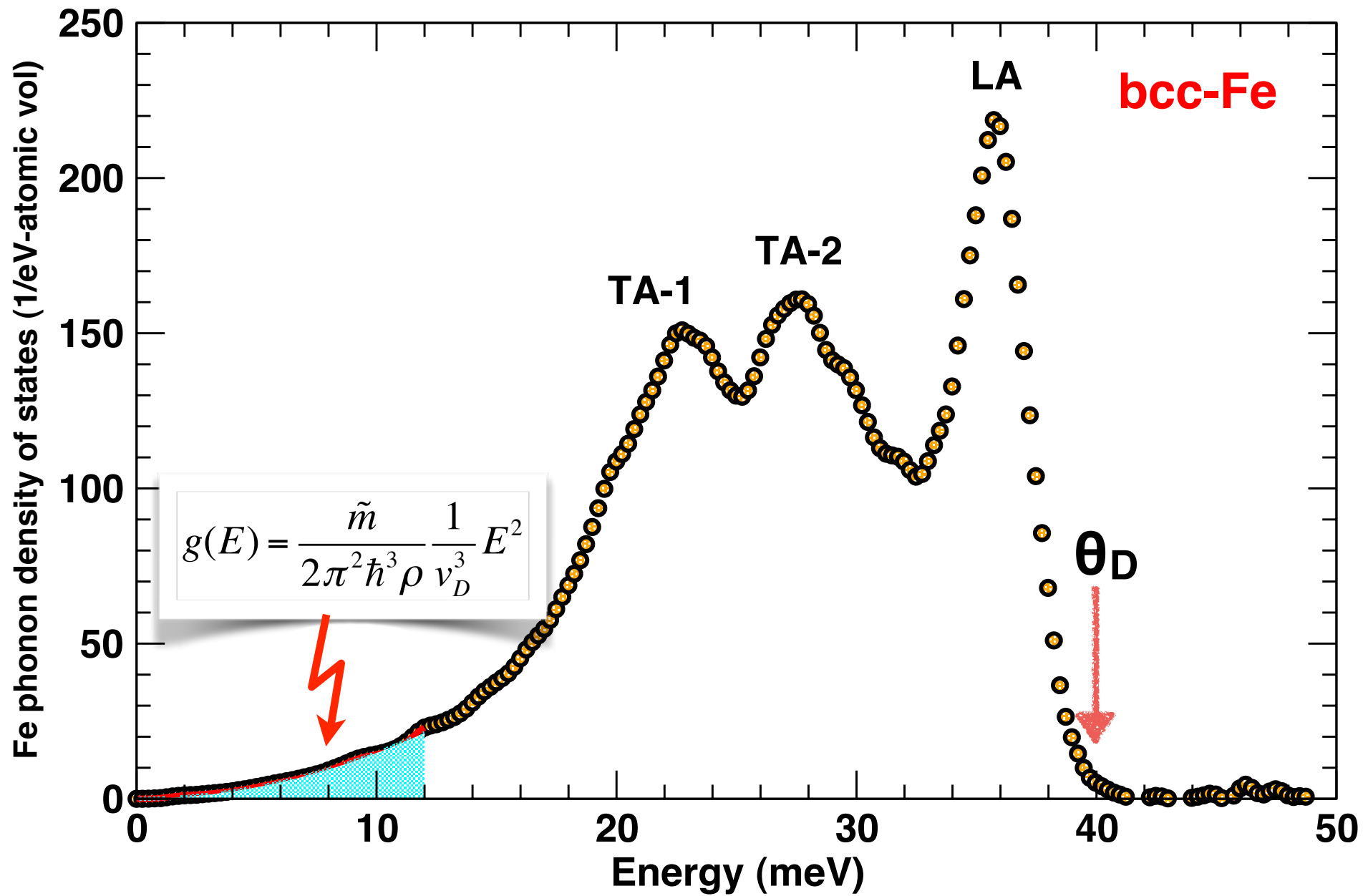
Measurement of v_D, Debye sound velocity allows to resolve longitudinal and shear sound velocity, provided that bulk modulus and density, is independently and simultaneously measured by x-ray diffraction.
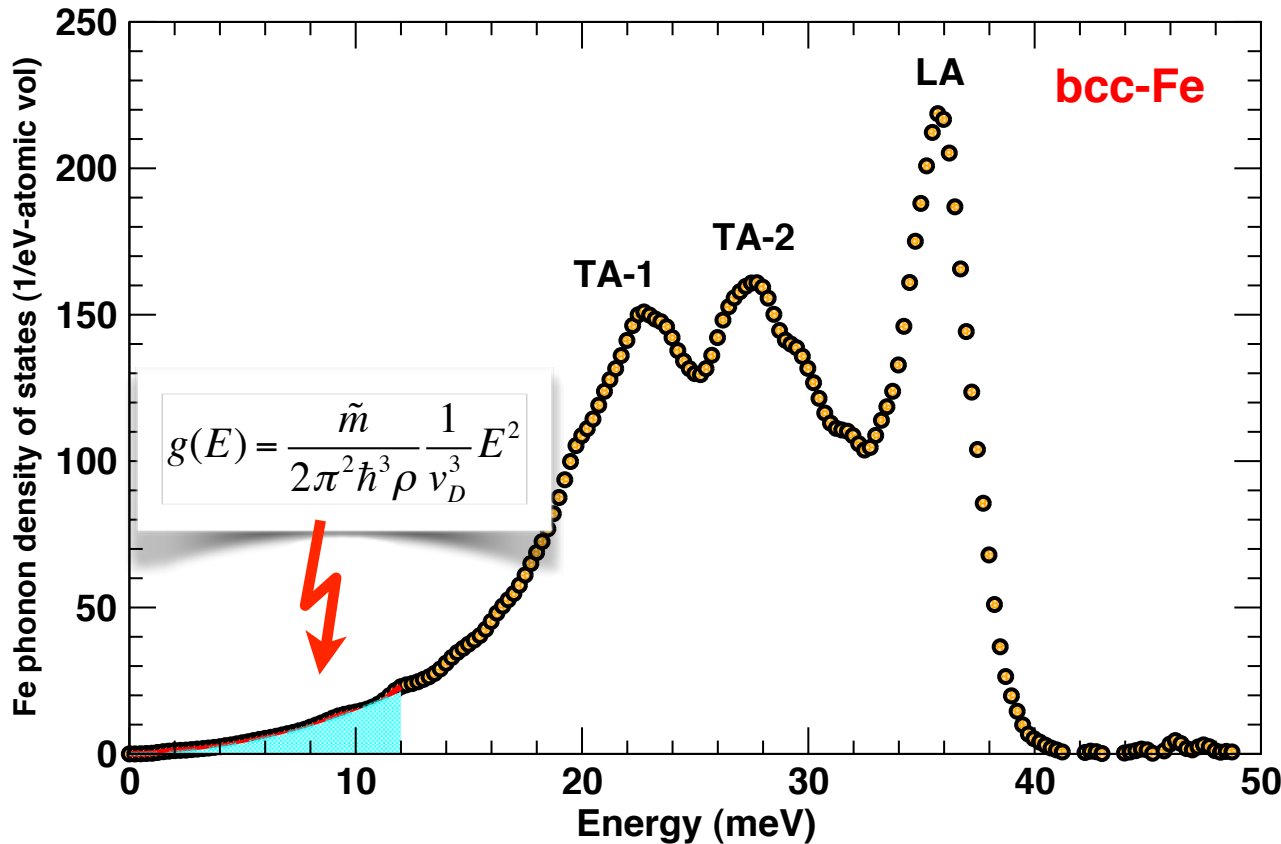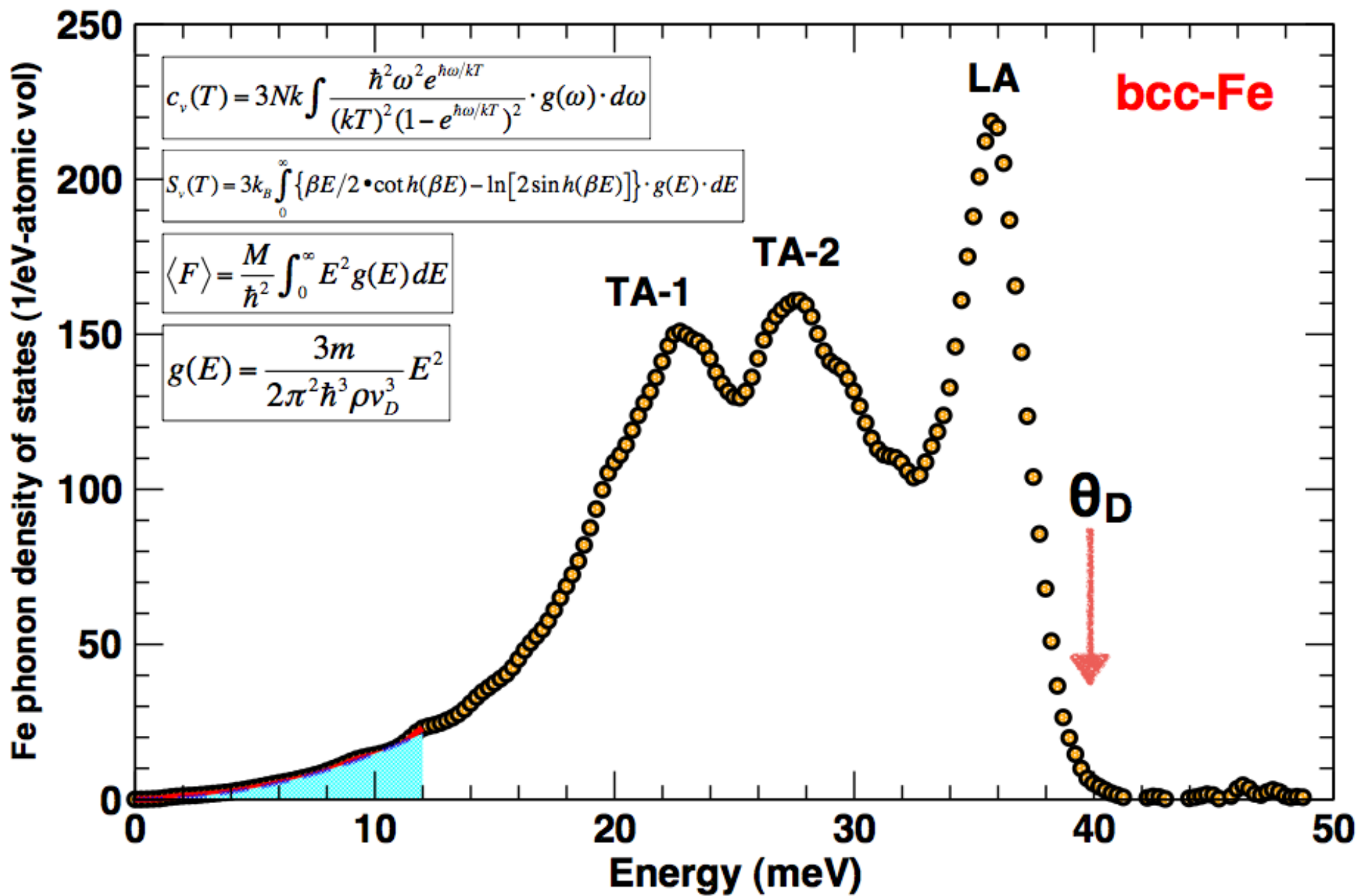
$$\frac{K_S}{\rho} = V_P^2 - \frac{4}{3}V_S^2$$

$$\frac{G}{\rho} = V_S^2$$

$$\frac{3}{V_D^3} = \frac{1}{V_P^3} + \frac{2}{V_S^3}$$

$$g(E) = \frac{\tilde{m}}{2\pi^2\hbar^3\rho}\frac{1}{v_D^3}E^2$$

LA

bcc-Fe

TA-2

TA-1

Fe phonon density of states (1/eV-atomic vol)

Energy (meV)

K_S : adiabatic bulk modulus
G : shear modulus
V_P : compression wave velocity
V_S : shear wave velocity
V_D : Debye sound velocity
P : density

K (GPa)	ρ (g/cc)	V_D (m/s)	V_P (m/s)	V_S (m/s)	G (GPa)
165 ± 1	8.01	3510 ± 12	5813 ± 13	3146 ± 11	79.3 ± 0.6

$$c_v(T) = 3Nk \int \frac{\hbar^2 \omega^2 e^{\hbar\omega/kT}}{(kT)^2 (1-e^{\hbar\omega/kT})^2} \cdot g(\omega) \cdot d\omega$$

$$S_v(T) = 3k_B \int_0^\infty \left\{ \beta E/2 \bullet \cot h(\beta E) - \ln\left[2\sin h(\beta E)\right]\right\} \cdot g(E) \cdot dE$$

$$\langle F \rangle = \frac{M}{\hbar^2} \int_0^\infty E^2 g(E)\, dE$$

$$g(E) = \frac{3m}{2\pi^2 \hbar^3 \rho v_D^3} E^2$$

LA

bcc-Fe

TA-1

TA-2

θ_D

Phonon density of states

$$g(k)\,dk = \frac{V}{(2\pi)^3}\,4\pi k^2\,dk.$$

Number of wave vectors in a spherical shell of radius k per unit volume of reciprocal space.

$$g(\omega) = \frac{3V}{2\pi^2 c^3}\,\omega^2$$

Phonon density of states has a quadratic dependence on frequency, and inversely proportional to the cube of sound velocity.
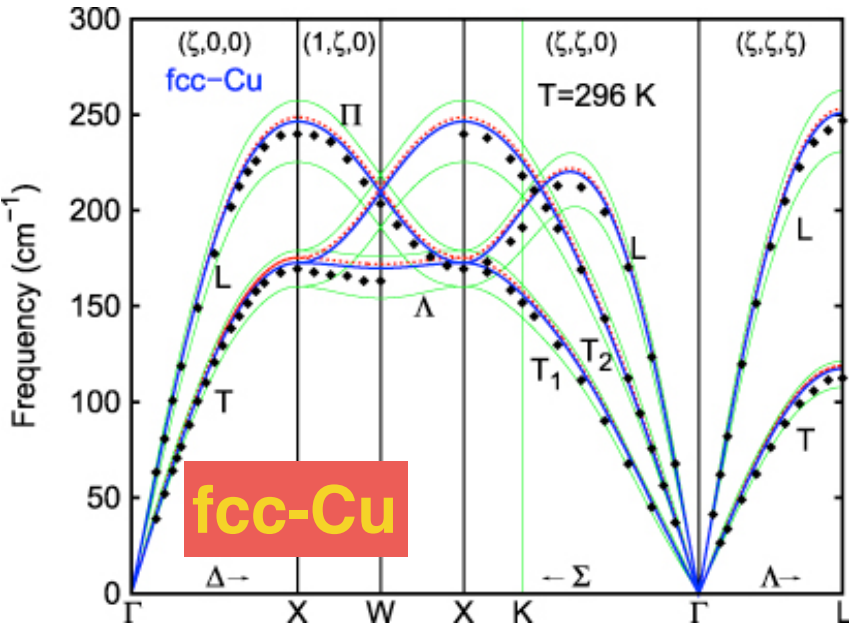
Debye model

pure iron

Fe-TPP-NO

acoustic modes $\Sigma e_{Fe}^2 = 0.25$

DyFe$_3$

Dy 0 GPa   Fe 0 GPa

bcc-Fe

α-Fe
$T = 296\,K$

$\leftarrow \theta_D$

Phonon dos (1/eV/at.vol)

Energy (meV)

• NRIXS
— INS+BvK

fcc-Cu
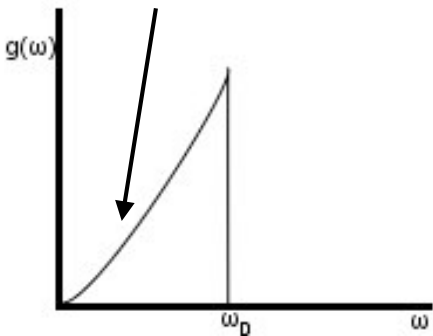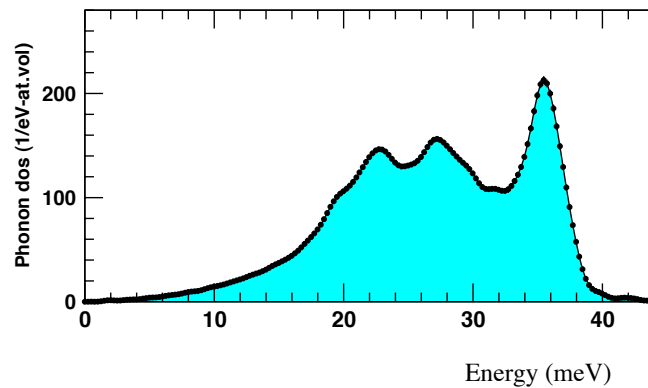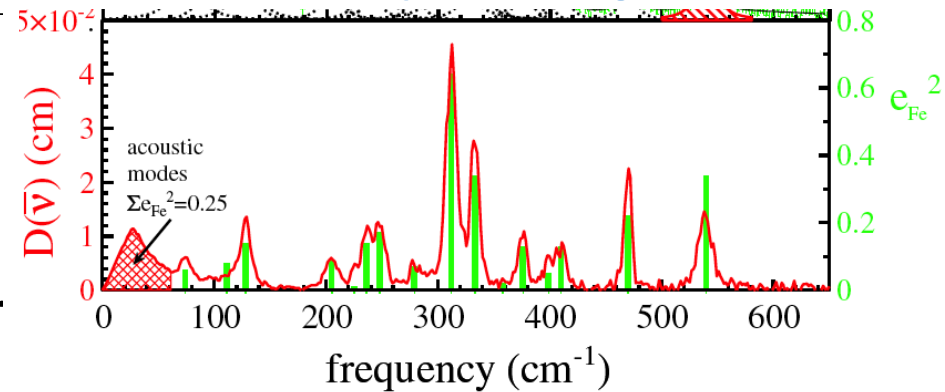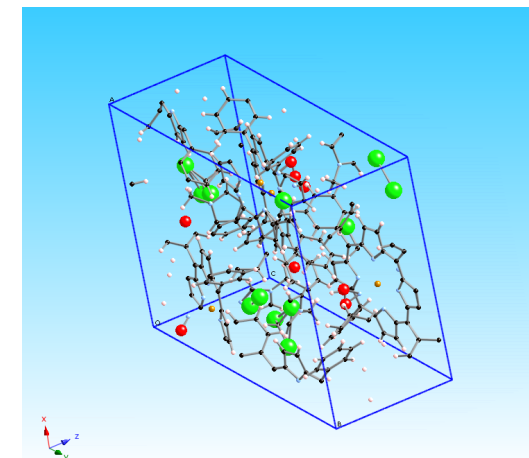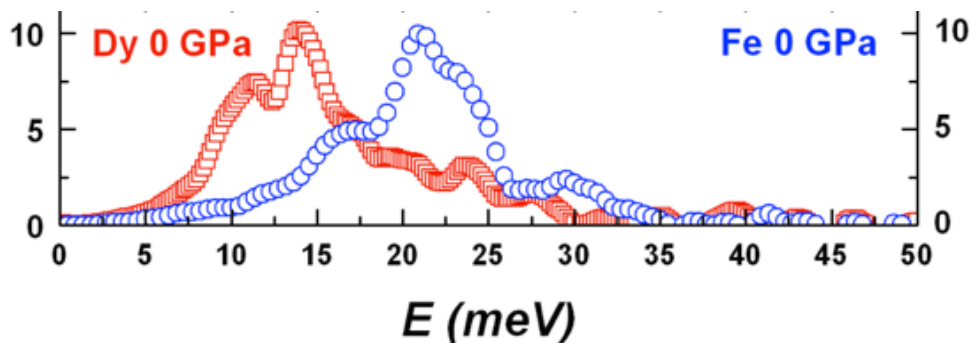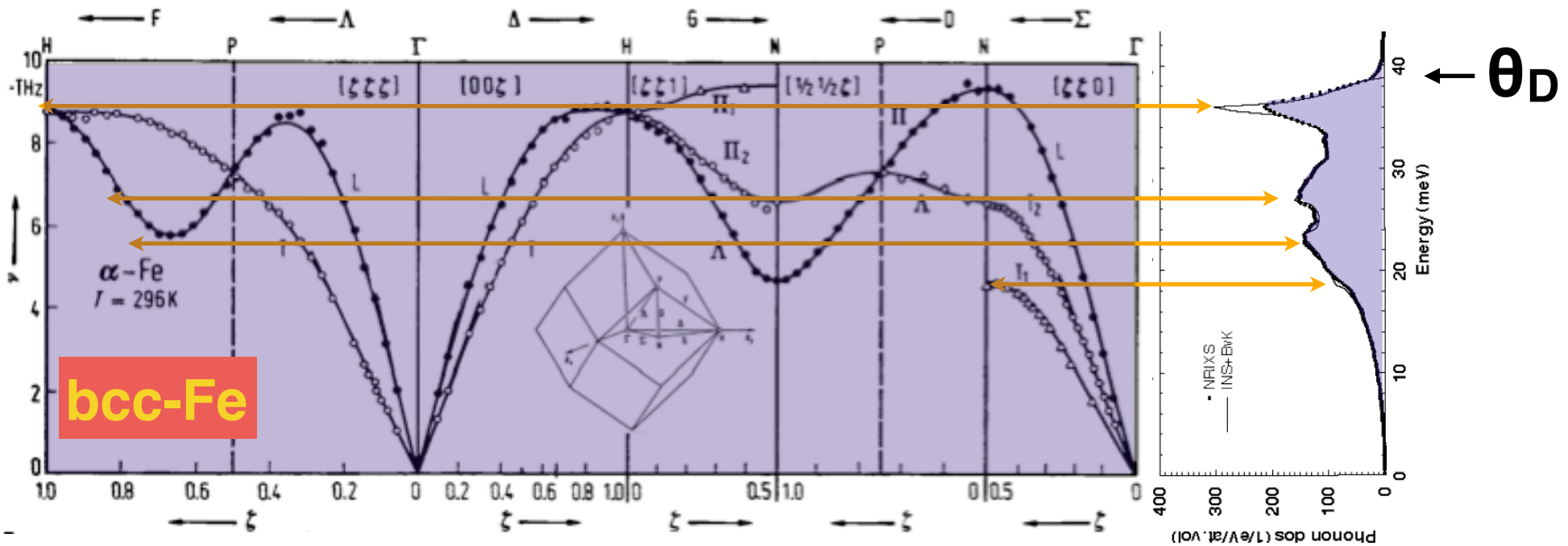
Let's assume that the acoustic modes have a linear relationship between frequency and wave vector:
$$\omega = ck$$, where **c** is average sound velocity

Maximum frequency cut off is at Debye energy: e.g. for Cu, this frequency is 240 cm^{-1} (~ 30 meV). Considering 1 meV = 11.605 K=8.065 cm^{-1}, this corresponds to 348 K, which is close to 344 K.
For Fe, the measured cut-off value is ~ 39.5 meV, which corresponds to 458 K, very close to reported 460 K.

Phonon density of states of iron under high pressure

153 GPa

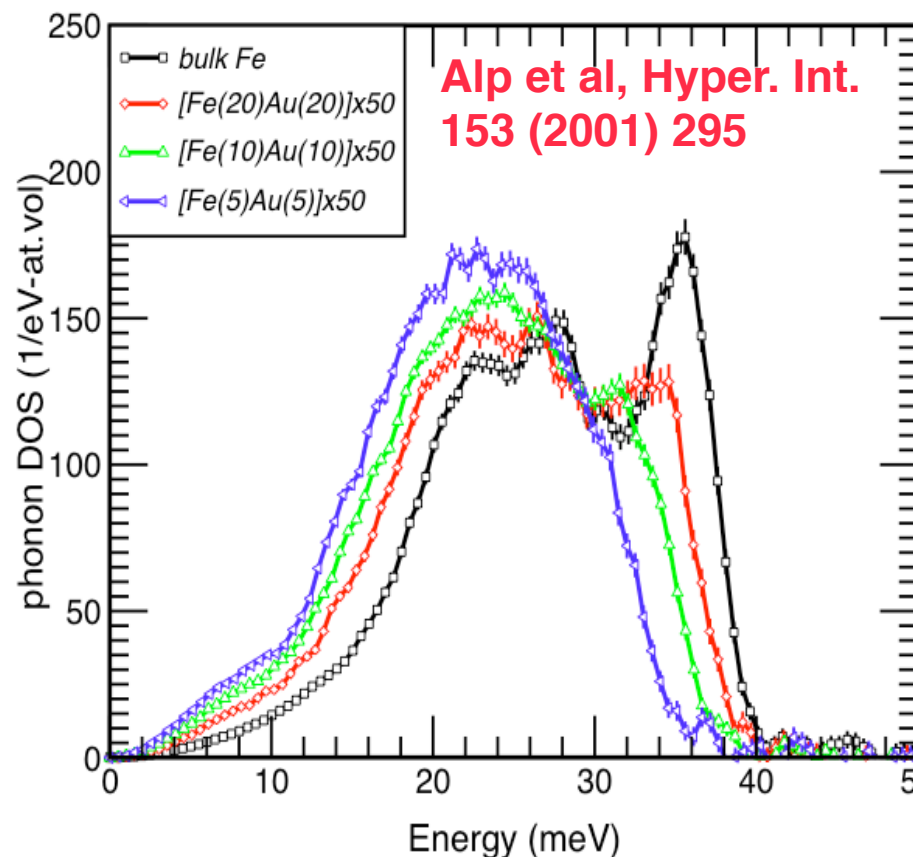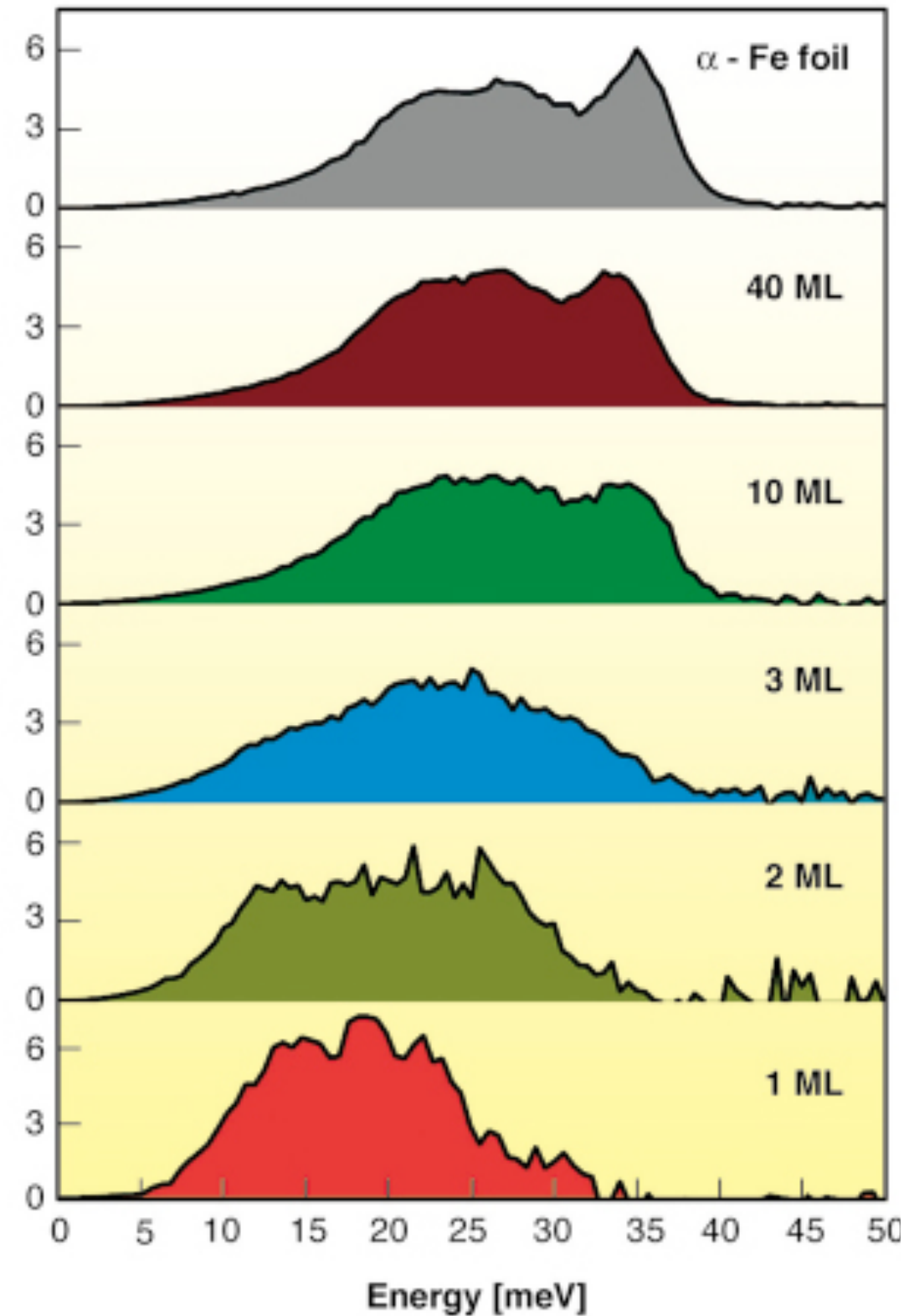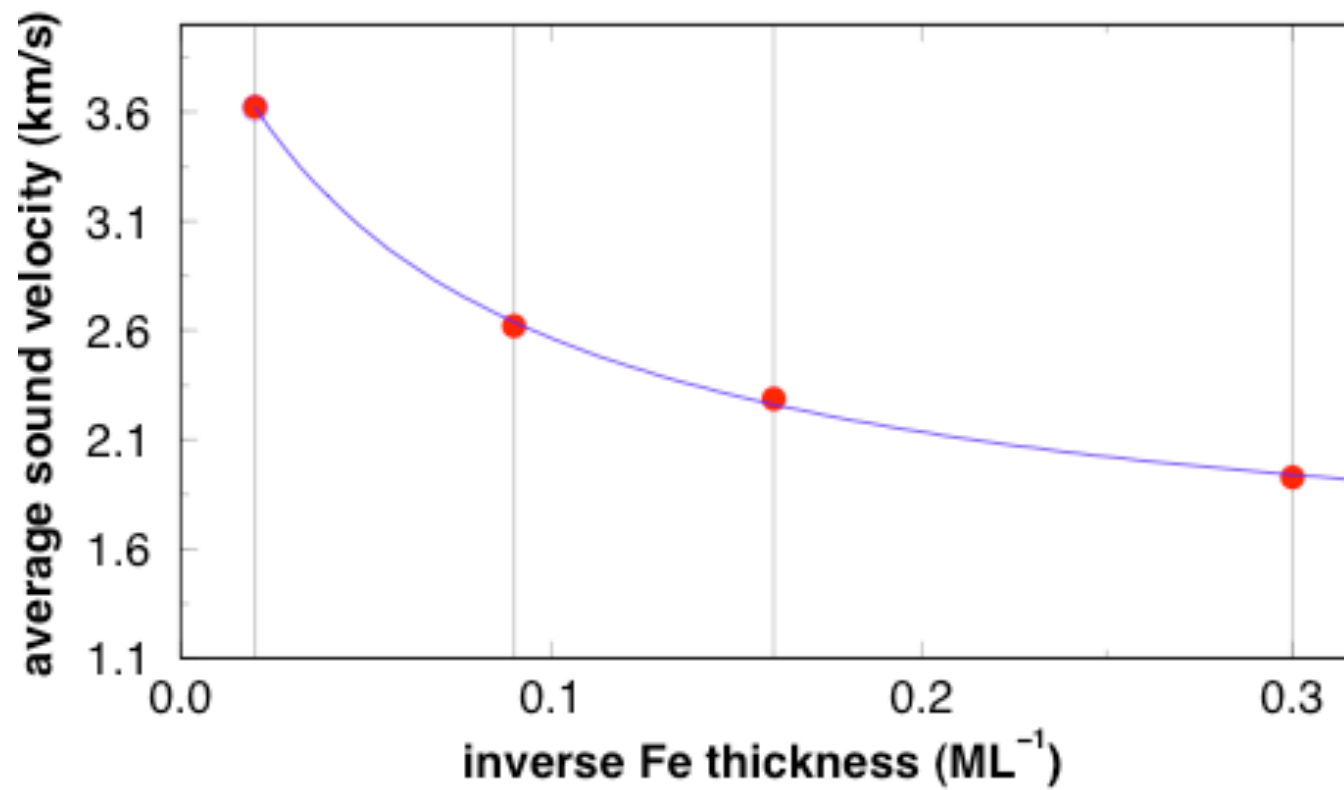phonon density of states (1/eV)

DOS/E^2 (10^6/eV^3)

Energy (meV)

Θ_D(K) — *Debye Temp*

E_k(meV) — *Kinetic Energy*

E_z(meV) — *Zero pt. Energy*

S_{vib}(k$_B$) — *Vib. Entropy*

C_{vib}(k$_B$) — *Vib. Sp.Heat*

Pressure (GPa)

H.K. Mao, et al, Science, 292 (2001) 914

V. Struzhkin, et al, PRL 87 (2001) 255501
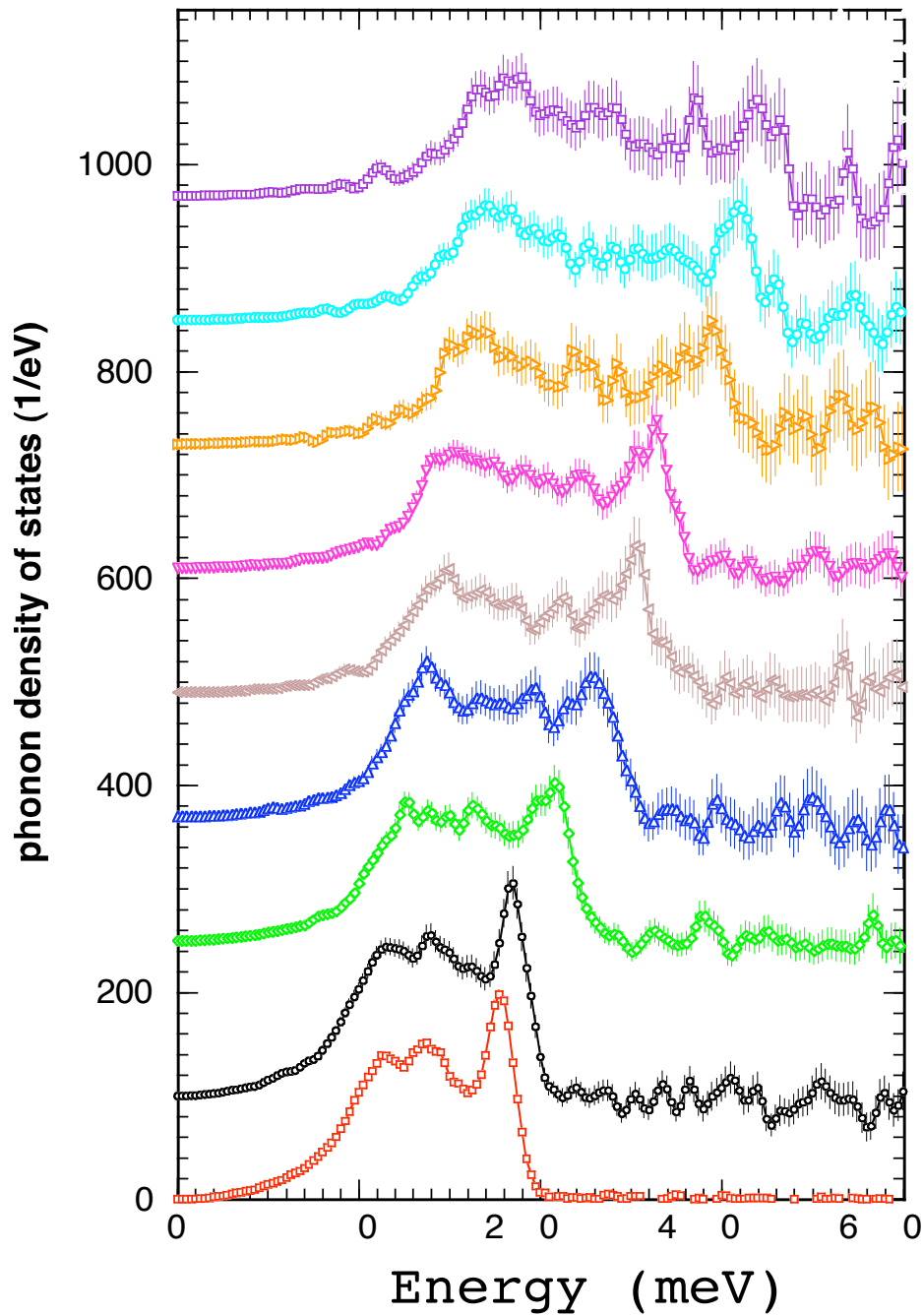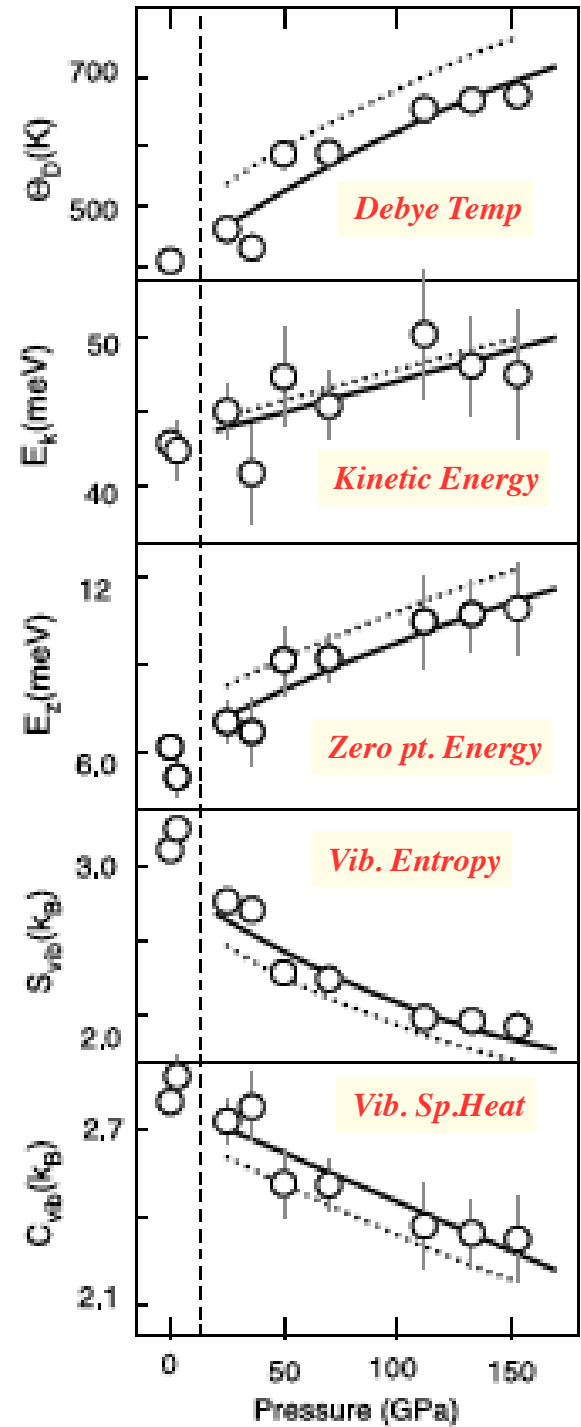
Fe films deposited on W(110)

Transition from the bulk to a single iron monolayer

S. Stankov, R. Röhlsberger, T. Slezak, M. Sladecek, B. Sepiol, G. Vogl, A. I. Chumakov, R. Rüffer, N. Spiridis, J. Lazewski, K. Parlinski, and J. Korecki,
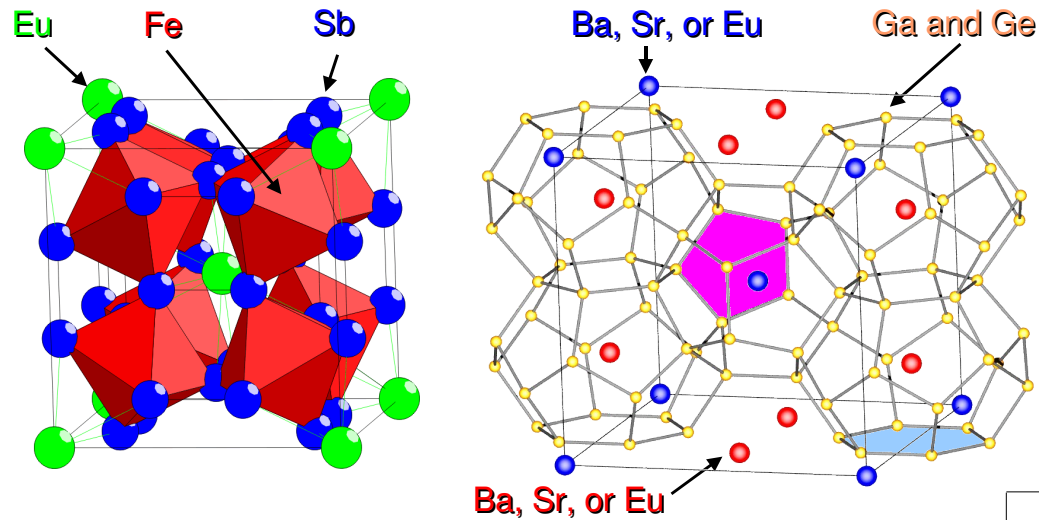
ESRF Highlights 2006

Alp et al, Hyper. Int. 153 (2001) 295

Skutterudites

Eu   Fe   Sb

Ba, Sr, or Eu   Ga and Ge

Ba, Sr, or Eu

EuFe₄Sb₁₂
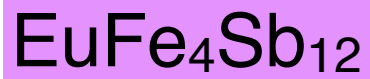
The loosely bound guests affect the characteristics of the vibrations, and change the thermal conductivity

Many elements in modern thermolelectric materials include **Fe**, rare-earth atoms like **Eu, Sm, Dy**, as well as **Sb**, and **Te**. These are all proper Mössbauer resonances we can exploit, and we do..

Courtesy: Raphael Hermann, Jülich

Wavenumber (cm^{-1})

a) ^{121}Sb   ID18, ID22n ESRF

b) ^{151}Eu

c) ^{57}Fe

Nuclide Specific VDOS in EuFe$_4$Sb$_{12}$ (meV^{-1})

Energy (meV)
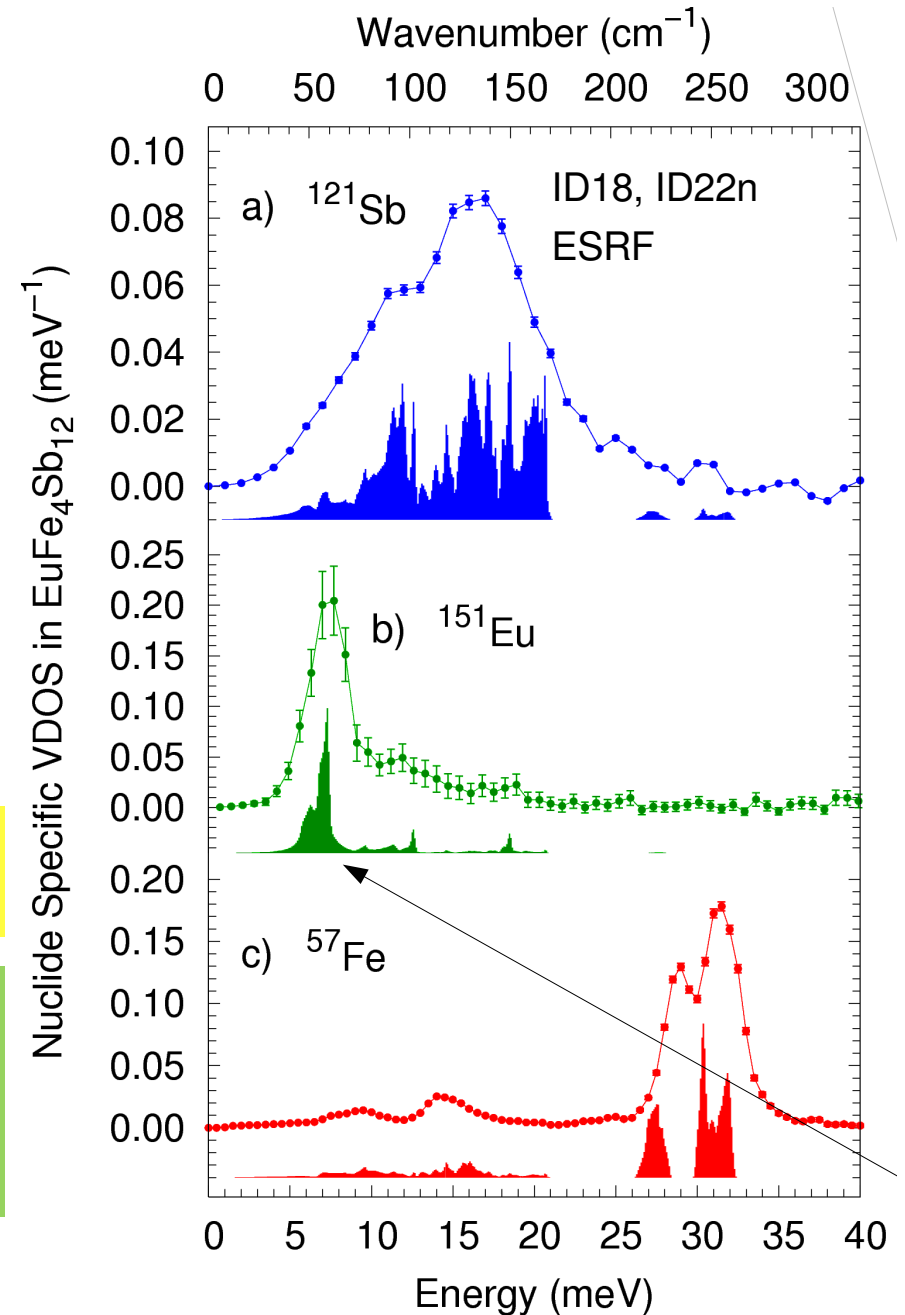
Vibrational dynamics of the host framework in Sn clathrates

Bogdan M. Leu,[1,*] Mihai Sturza,[2] Michael Y. Hu,[1] David Gosztola,[3] Volodymyr Baran,[4] Thomas F. Fässler,[4] and E. Ercan Alp[1]

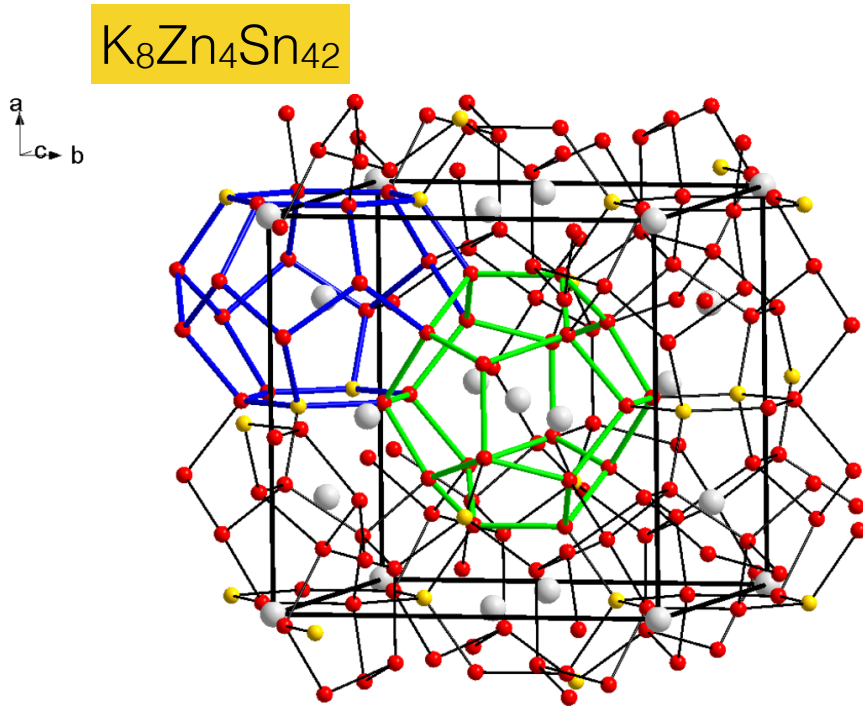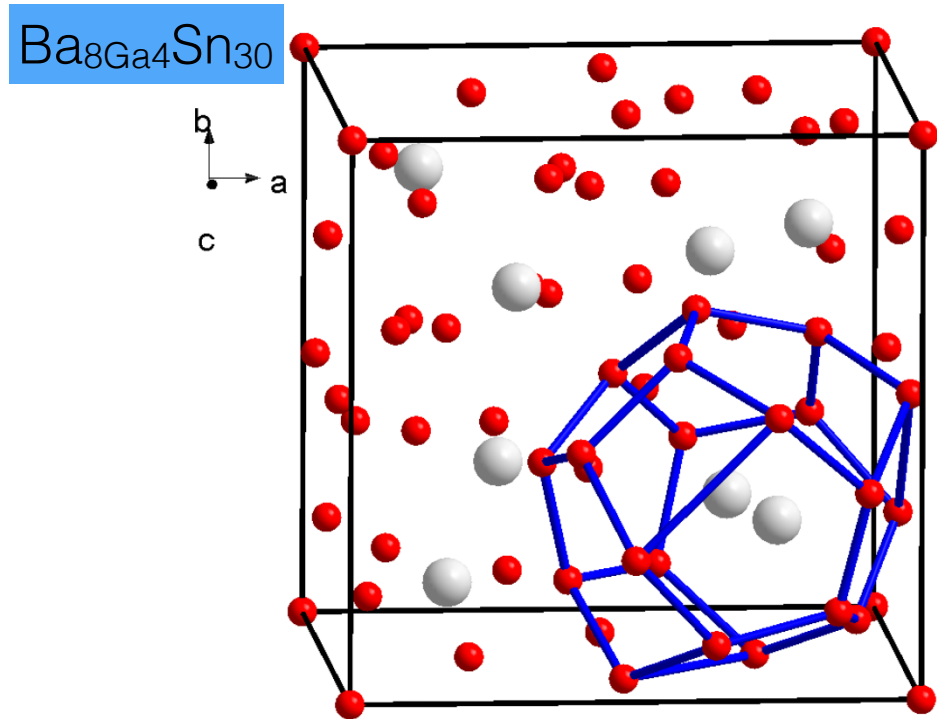$K_8Zn_4Sn_{42}$

$Ba_8Ga_4Sn_{30}$

FIG. 1. (Color online) Structure of type-I clathrate $K_8Zn_4Sn_{42}$. Color scheme: gray = K, yellow = Zn/Sn, red = Sn. One small (pentagonal dodecahedron) and large (tetrakaidecahedron) host framework cage are highlighted in green and blue, respectively.
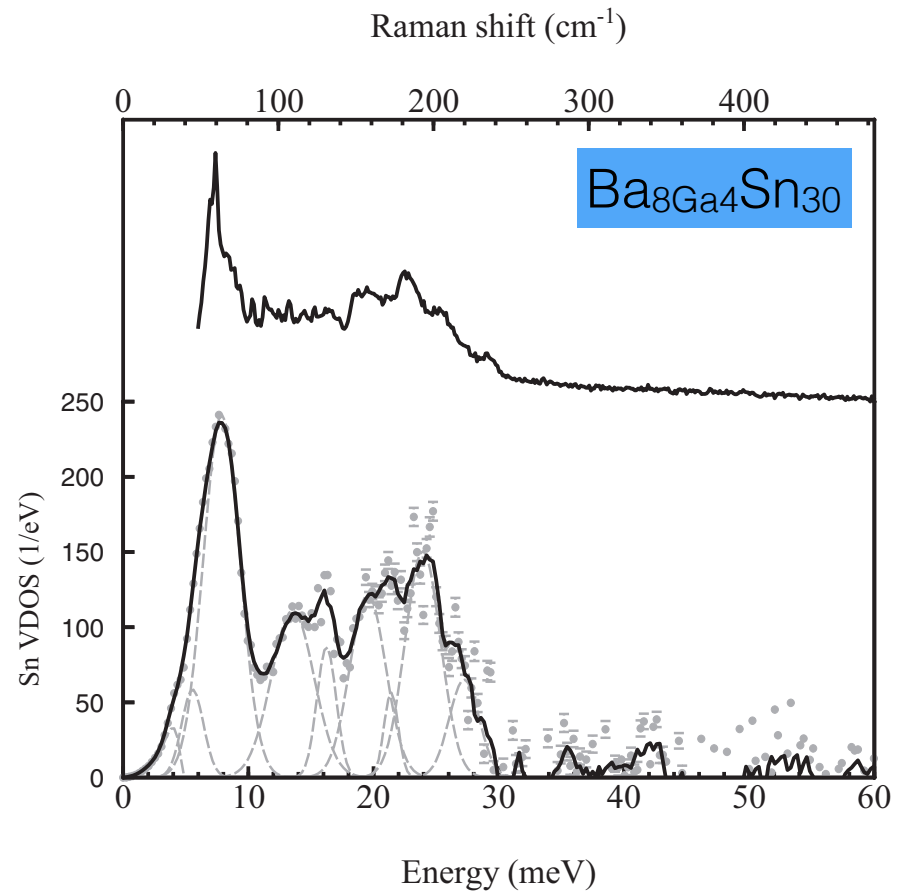
FIG. 2. (Color online) Structure of type-VIII clathrate $Ba_8Ga_{16}Sn_{30}$. Color scheme: gray = Ba, red = Sn/Ga. One host framework cage (pentagonal dodecahedron) is highlighted in blue.

type-I clathrate: pentagonal dodecahedra and tetrakaidecahedra alternating in a 1:3 ratio
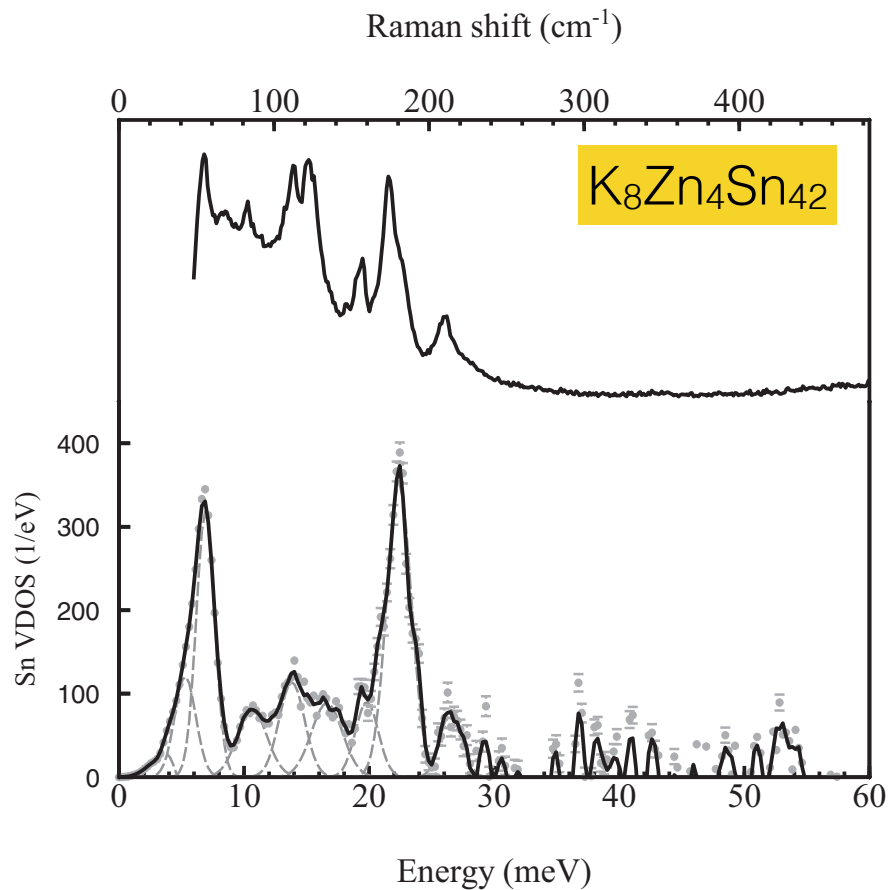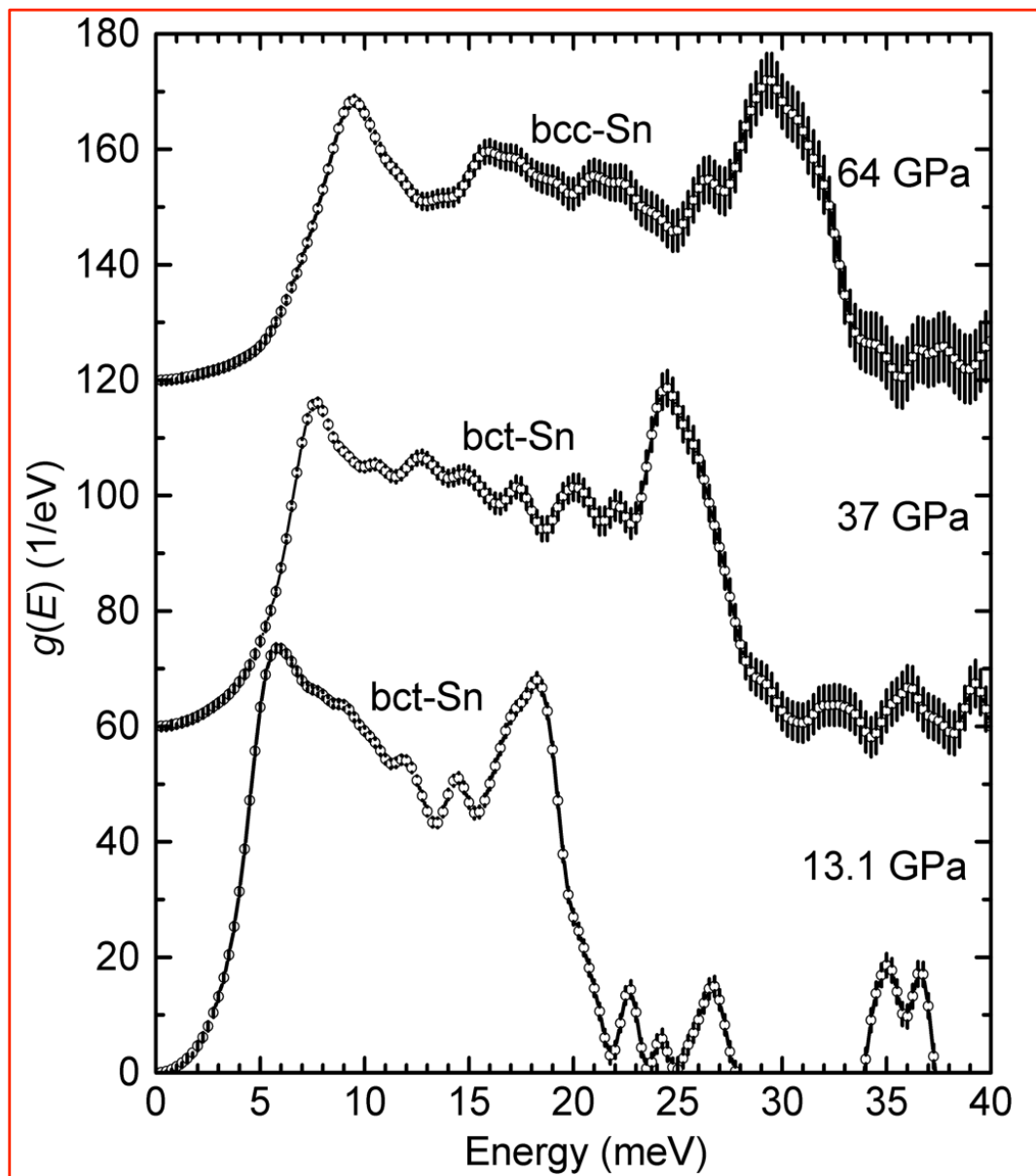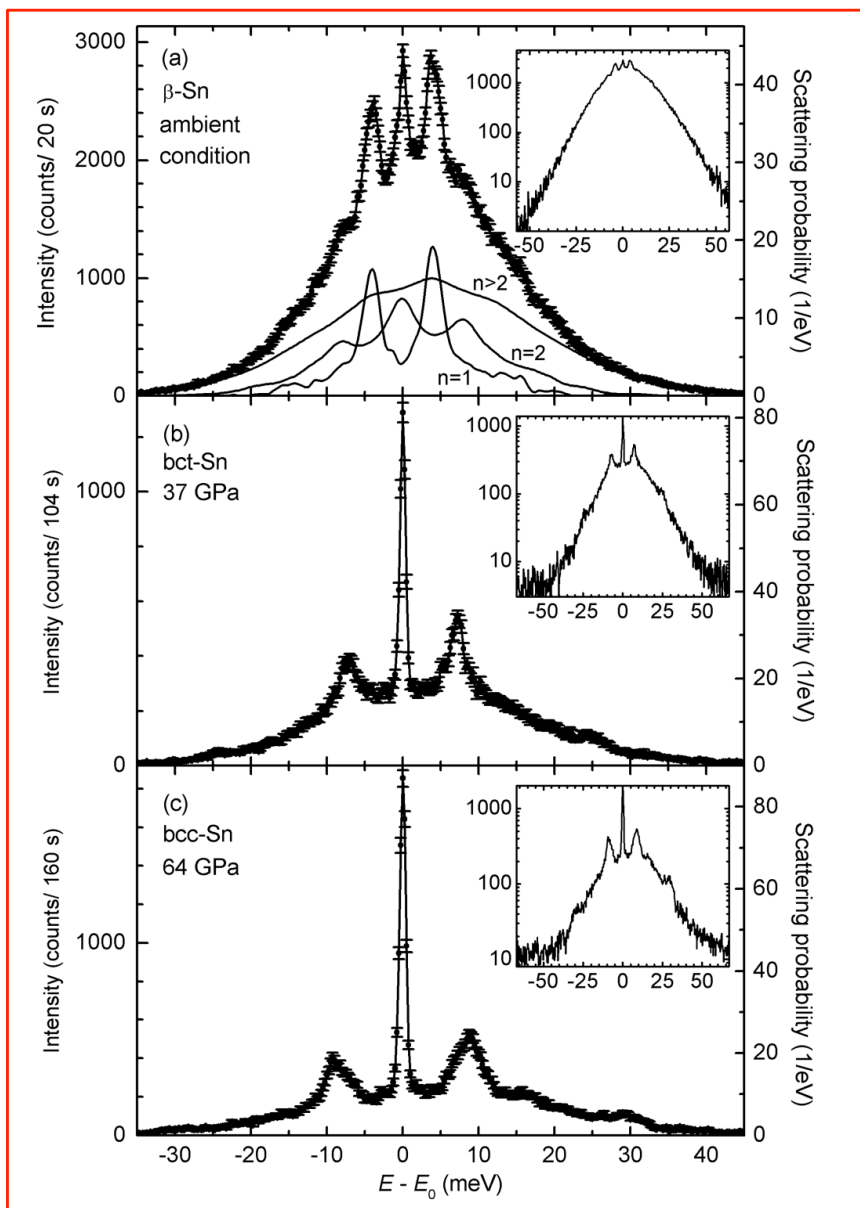
type VIII : pentagonal dodecahedra; however, BGS adopts the type-I clathrate structure at high-temperature

Raman shift (cm^{-1})

K$_8$Zn$_4$Sn$_{42}$

Sn VDOS (1/eV)

Energy (meV)

Temperature (K)

Ba$_8$Ga$_4$Sn$_{30}$

Sn VDOS (1/eV)

Energy (meV)

$\langle z \rangle^2_v (\text{Å}^2)$

K$_8$Zn$_4$Sn$_{42}$

Ba$_8$Ga$_{16}$Sn$_{30}$

Temperature (K)
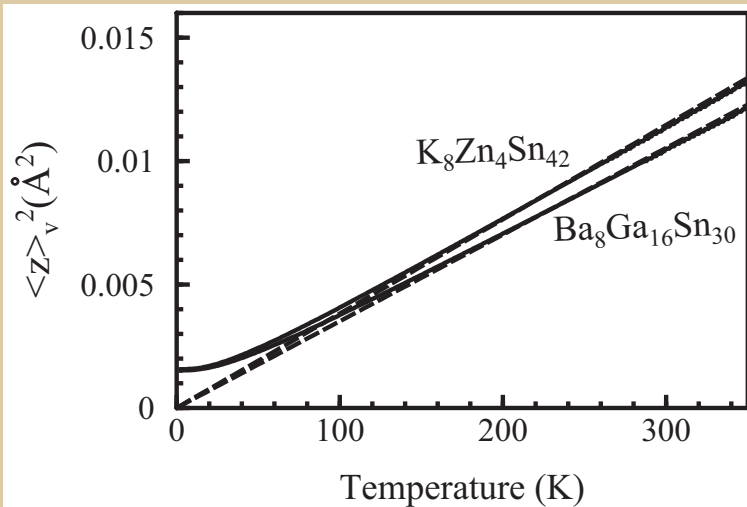
mean square displacement via phonon dos

$$\langle z^2 \rangle_v = \frac{1}{3k^2} \int [2\bar{n}(\bar{v}) + 1] \frac{\bar{v}_R}{\bar{v}} D(\bar{v}) d\bar{v},$$

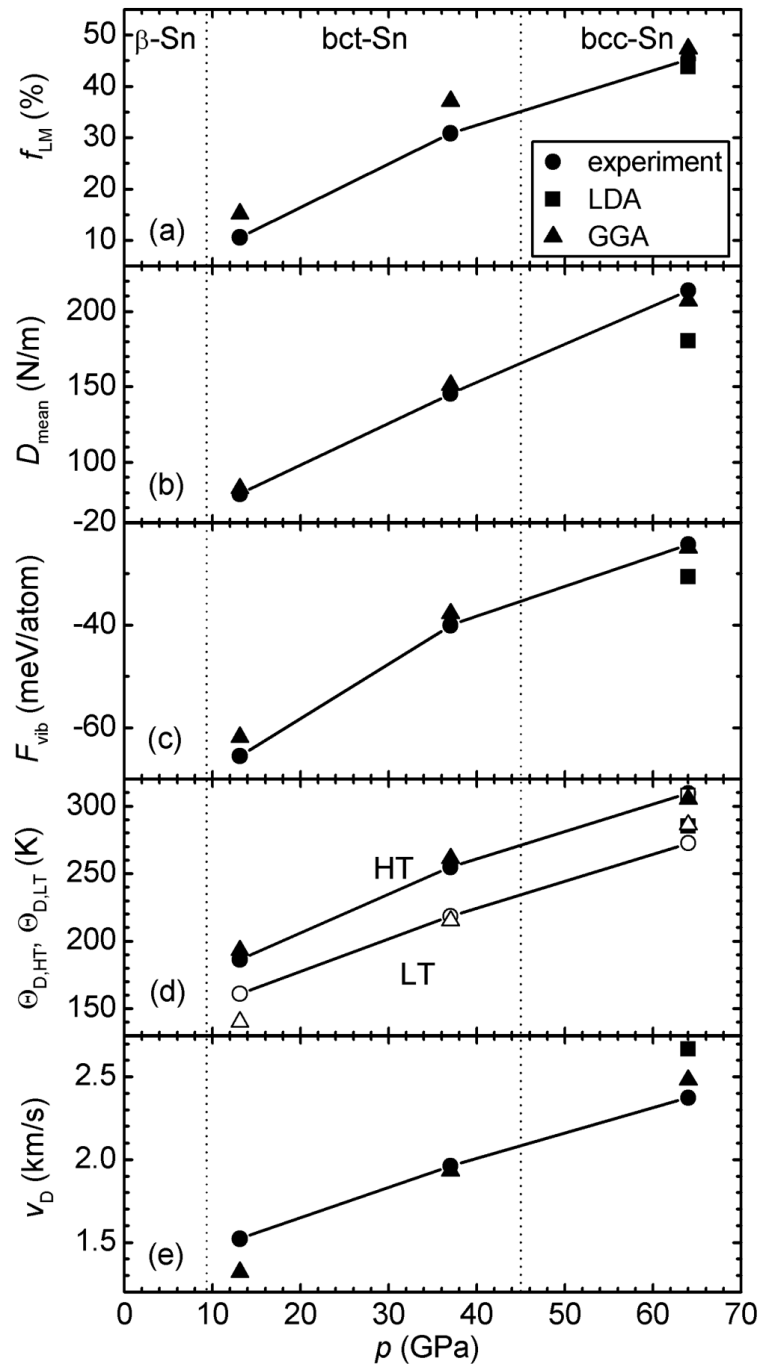3.8×10^{-5} Å^2/K for KZS and 3.5×10^{-5} Å^2/K for BGS.
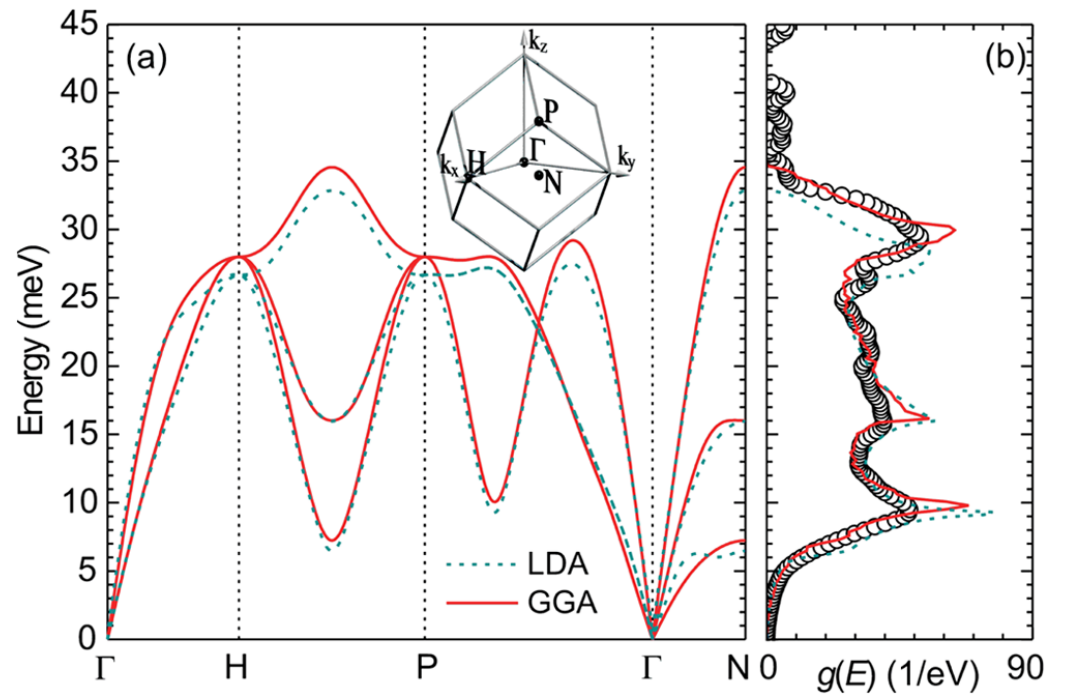
FIG. 3 (color online). (a) Theoretical phonon dispersion relation of bcc-Sn at 64 GPa. The inset shows the Brillouin zone of the bcc-Sn lattice. (b) Comparison between the theoretically calculated phonon DOS (lines) and the experimentally derived phonon DOS at 64 GPa (circles).
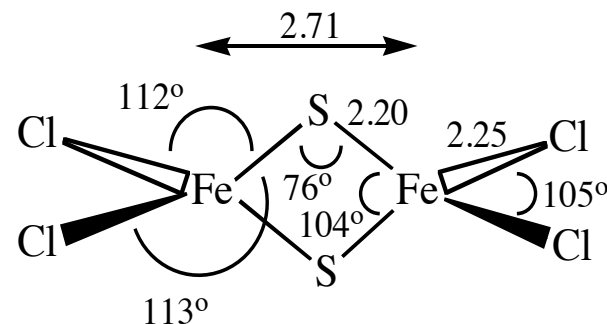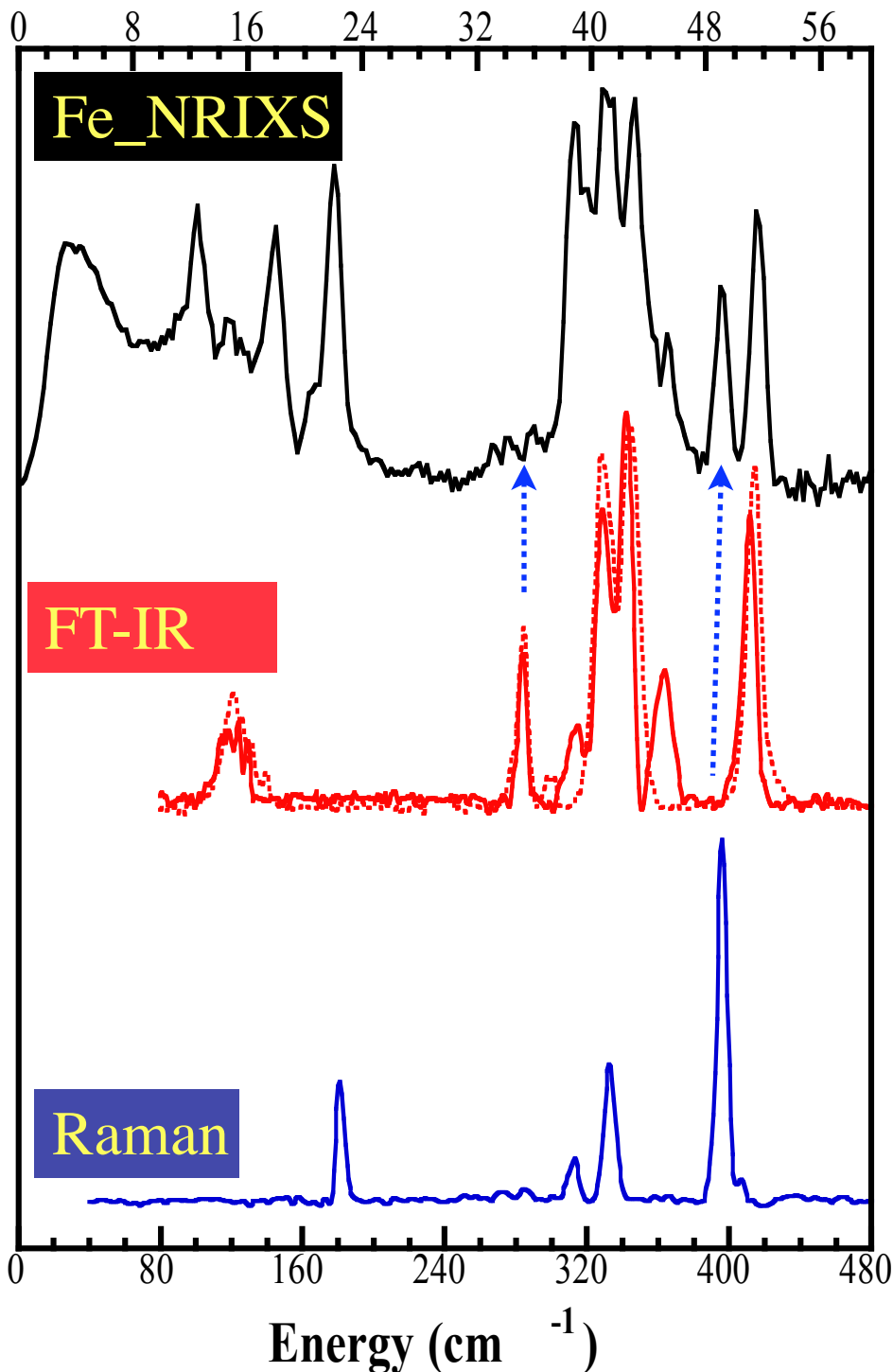
Biology & bio-inorganic chemistry

S. Cramer	University of California-Davis
E. Solomon	Stanford University
T. Sage	Northeastern University
E. Munck	University of Pittsburg
DeBeer George	Cornell University
Nicolai Lehnert	University of Michigan
R. Scheidt	University of Notre Dame

Mb
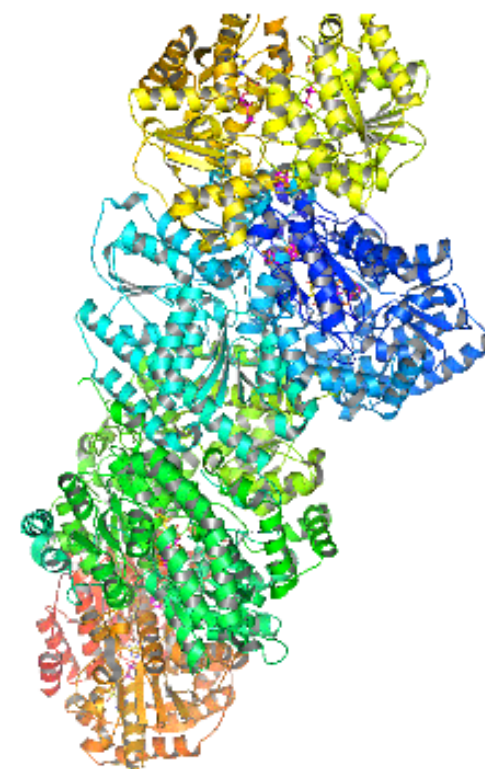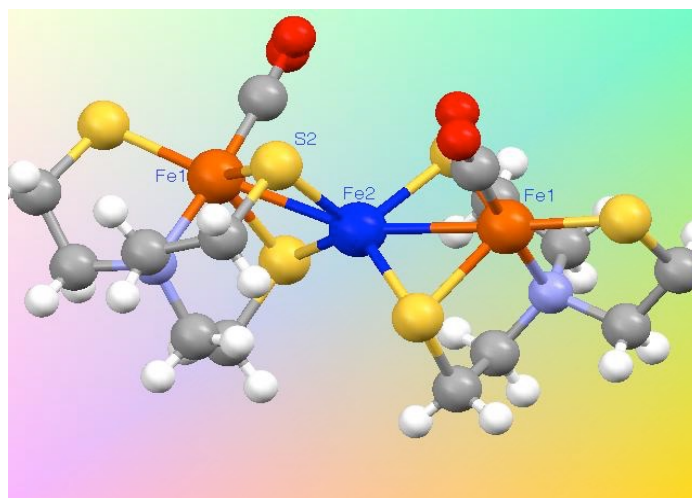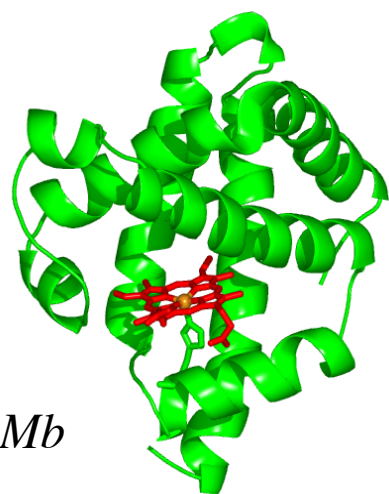
Vibrational spectroscopy of proteins, enzymes and biomimic model porphyrins and cubanes

Energy (meV)

Fe_NRIXS

FT-IR

Raman

Intensity (a.u.)

Energy (cm⁻¹)

[NEt₄]₂[Fe₂S₂Cl₄].
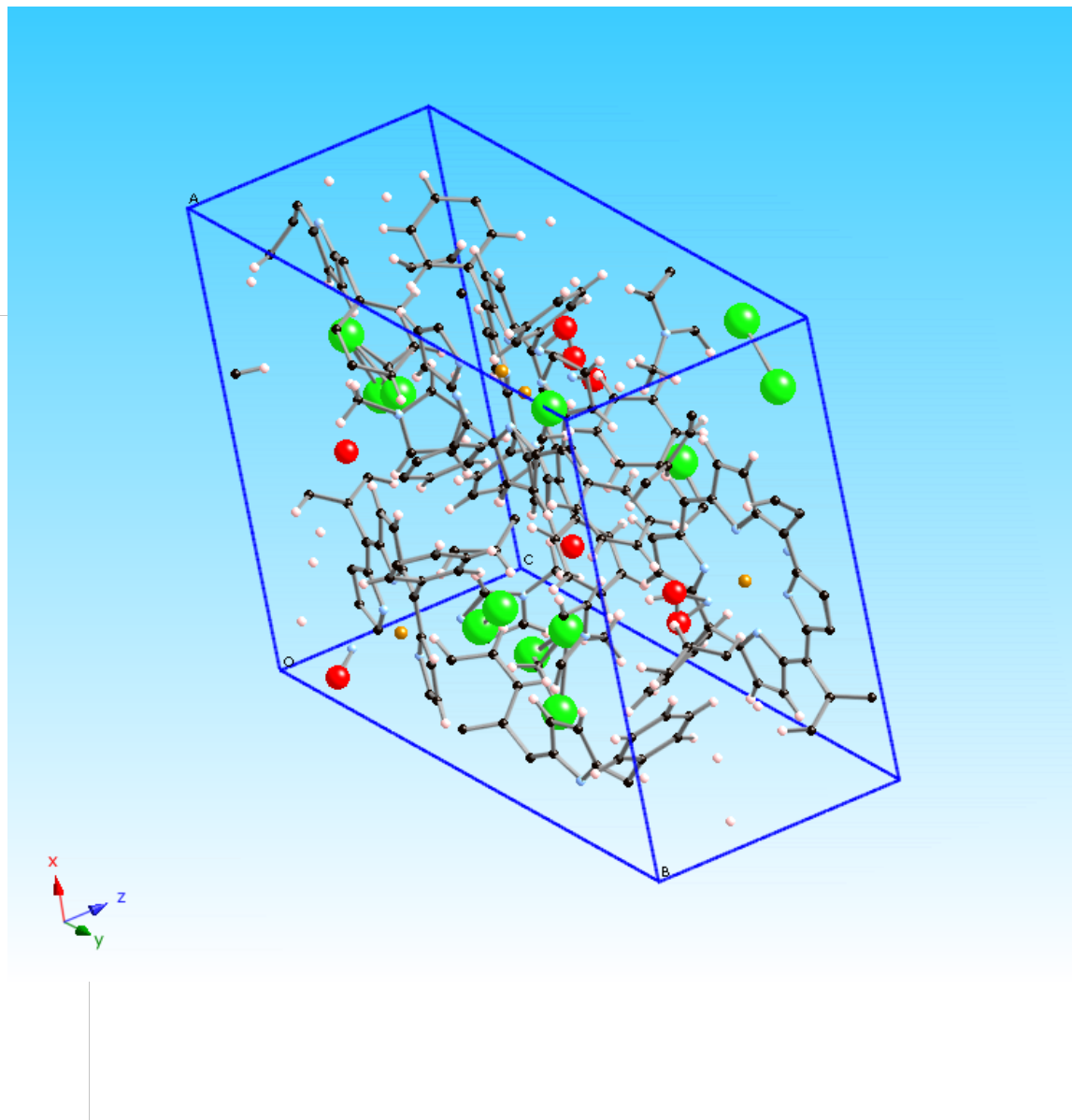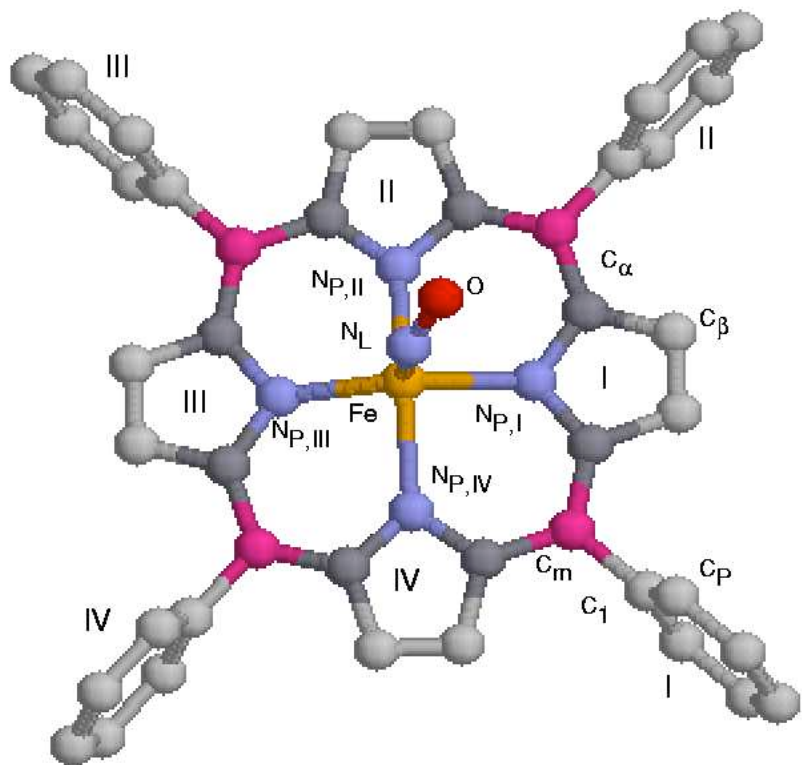

Some unique advantages of NRIXS

1. Low frequency motions: ~ total mass
2. No selection rule except motion of atoms along x-ray propagation
3. Peak intensity ~ mode participation ~ actual displacement
4. No matrix effects or limitations
5. Element and isotope selective
6. No unpredictable cancellations in scattering terms

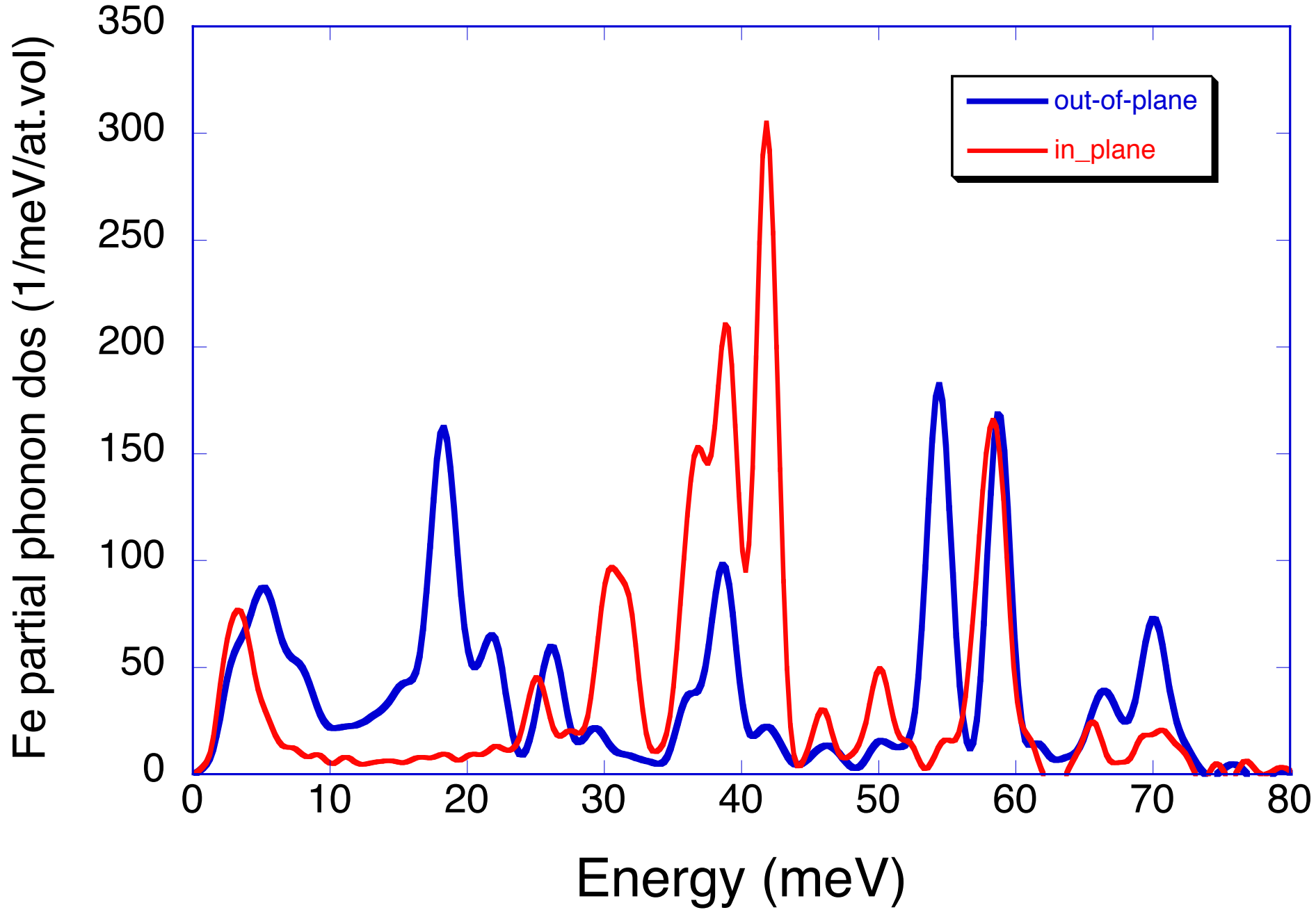$$\phi_\alpha = \frac{1}{3}\frac{\bar{\nu}_R}{\bar{\nu}_\alpha}e^2_{j\alpha}(\bar{n}_\alpha + 1)f$$
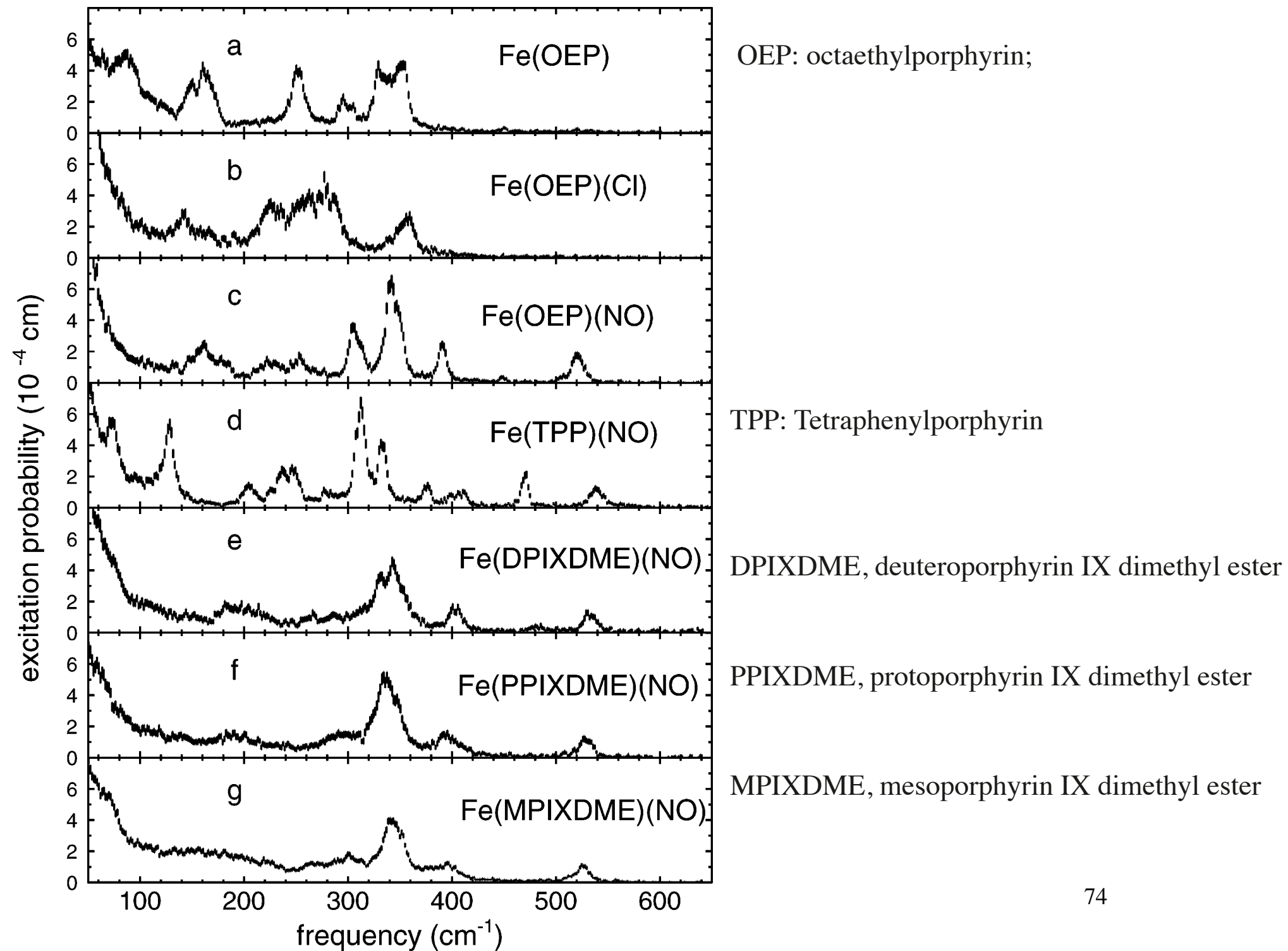
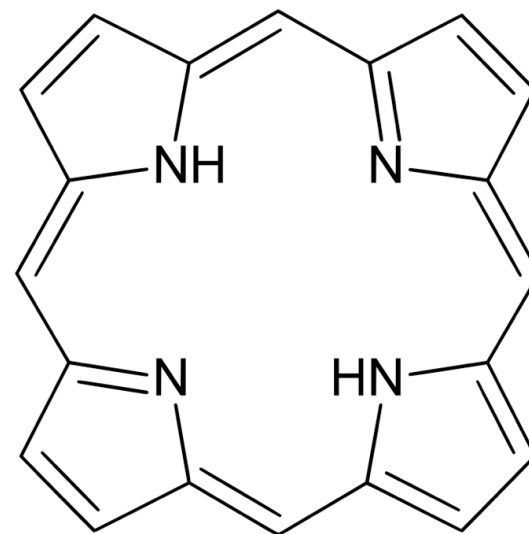Matt Smith, et al, Inorganic Chemistry, 2005, 44, 5562

Porphyrins:	**A**	**B**
Tetraphenylporphyrin (TPP)	Phenyl	H
Octaethylporphyrin (OEP)	H	Ethyl

FeTPP(1MeIm)NO
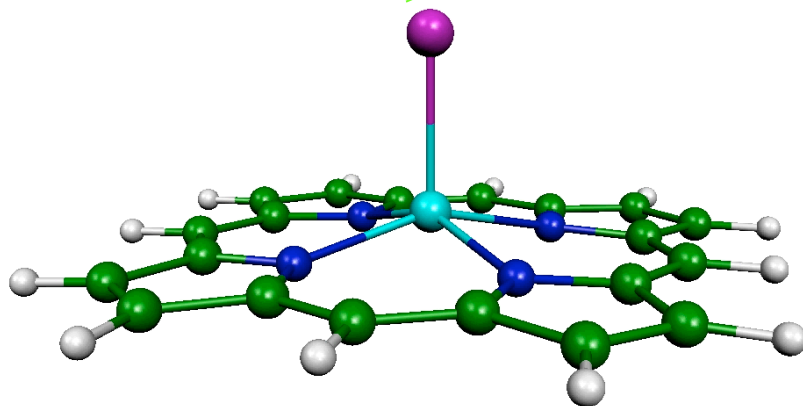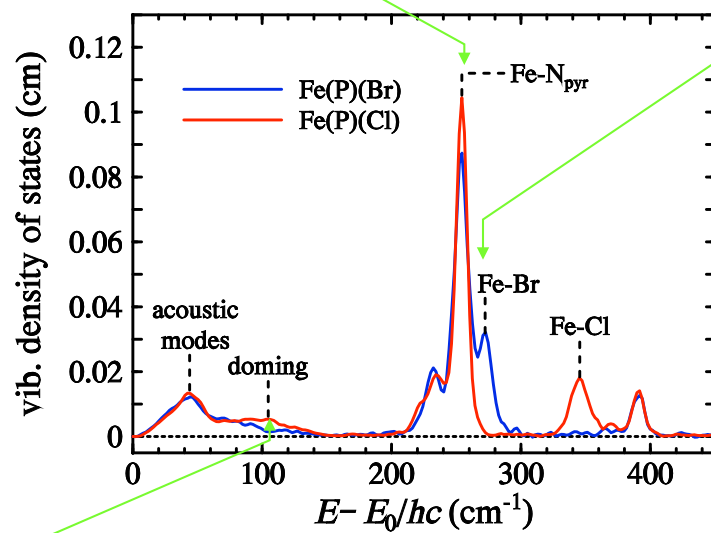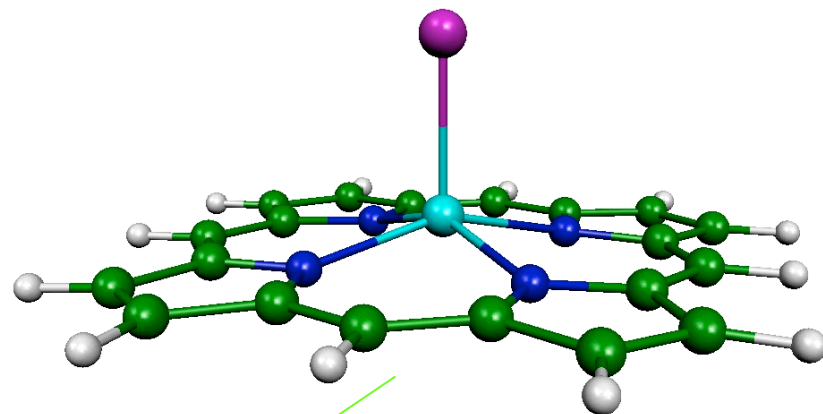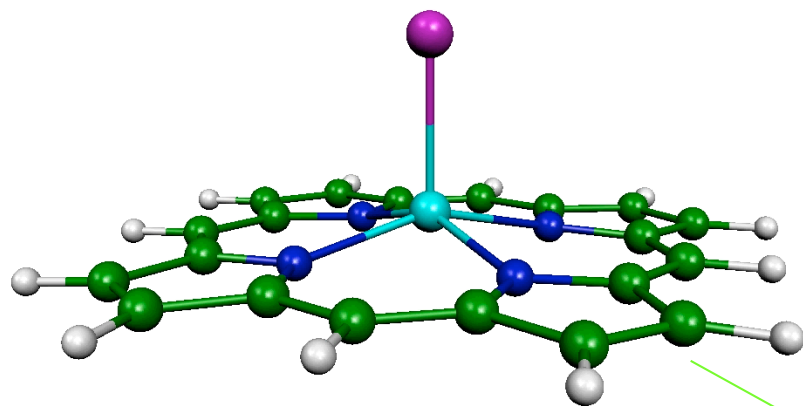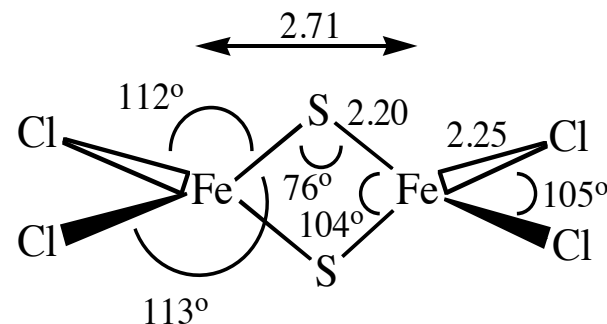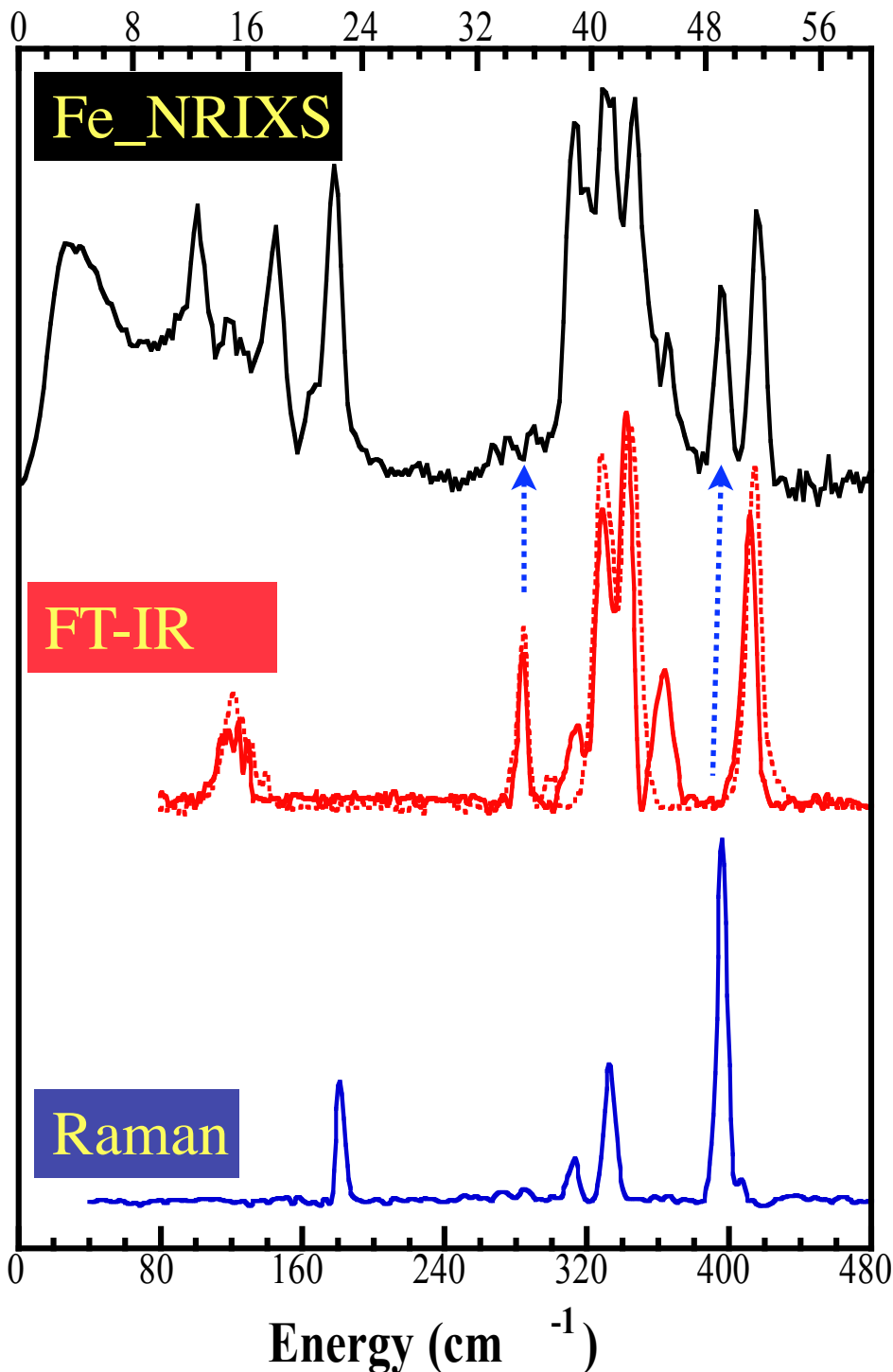
OEP: octaethylporphyrin;

TPP: Tetraphenylporphyrin

DPIXDME, deuteroporphyrin IX dimethyl ester

PPIXDME, protoporphyrin IX dimethyl ester

MPIXDME, mesoporphyrin IX dimethyl ester

74

acoustic modes

doming

Fe-N$_{pyr}$

Fe-Br

Fe-Cl

Fe(P)(Br)
Fe(P)(Cl)

vib. density of states (cm)

$E - E_0/hc$ (cm^{-1})

Energy (meV)

Fe_NRIXS

FT-IR

Raman

Intensity (a.u.)

Energy (cm⁻¹) → $Energy (cm^{-1})$

[NEt$_4$]$_2$[Fe$_2$S$_2$Cl$_4$].

Some unique advantages of NRIXS

1. Low frequency motions: ~ total mass
2. No selection rule except motion of atoms along x-ray propagation
3. Peak intensity ~ mode participation ~ actual displacement
4. No matrix effects or limitations
5. Element and isotope selective
6. No unpredictable cancellations in scattering terms

$$\phi_\alpha = \frac{1}{3}\frac{\bar{v}_R}{\bar{v}_\alpha} e^2_{j\alpha}(\bar{n}_\alpha + 1)f$$

Matt Smith, et al, Inorganic Chemistry, 2005, 44,5562

~ 0.1meV, all-vacuum high resolution monochromator

Fe partial phonon dos (1/atom)

Energy (meV)

Argonne NATIONAL LABORATORY

Thomas S. Toellner
toellner@anl.gov

77
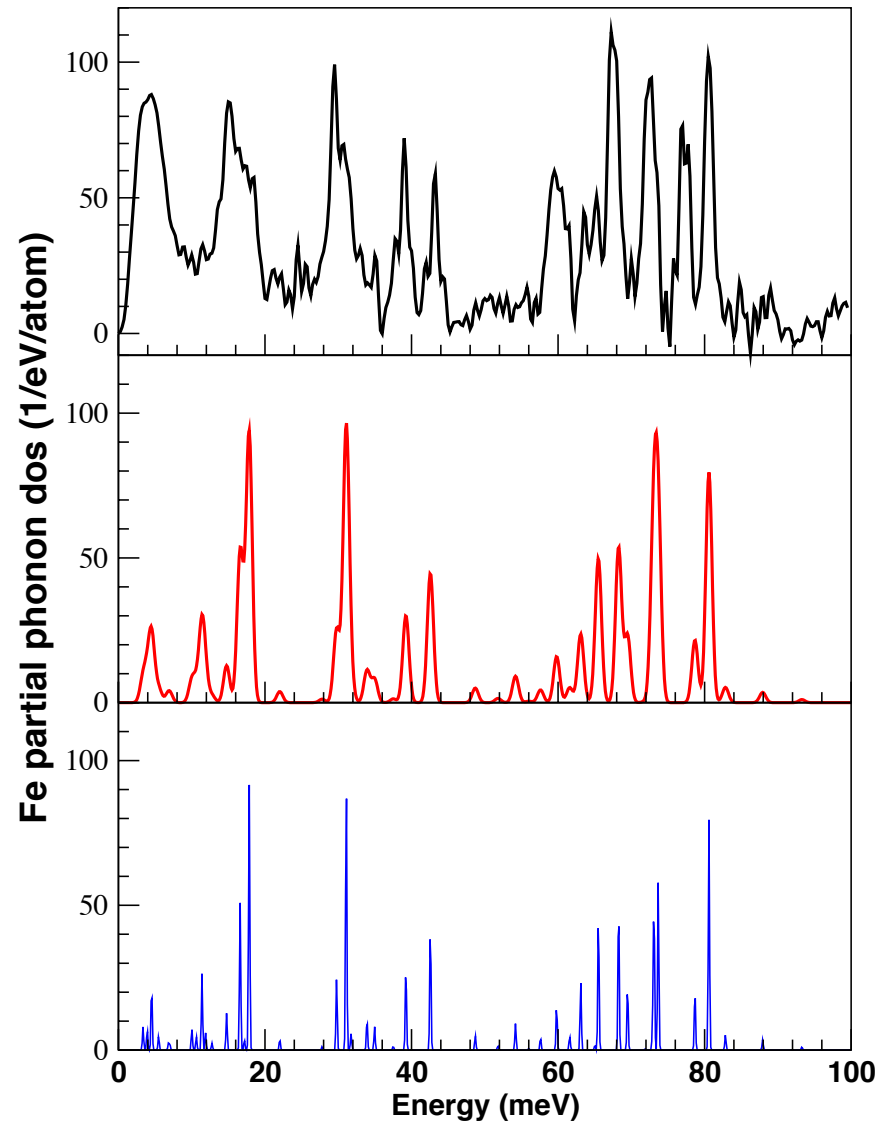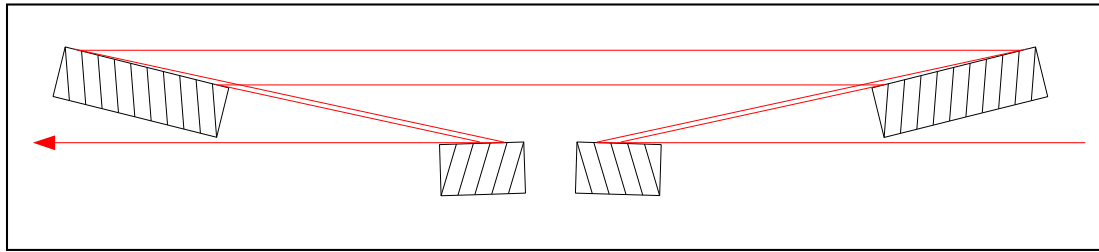
Protonation state of oxo-ligand in heme protein intermediates:

Synchrotron-Derived Vibrational Data Confirm Unprotonated Oxo Ligand in Myoglobin Compound II

Weiqiao Zeng,[†] Alexander Barabanschikov,[†] Yunbin Zhang,[†] Jiyong Zhao,[‡] Wolfgang Sturhahn,[‡] E. Ercan Alp,[‡] and J. Timothy Sage*,[†]
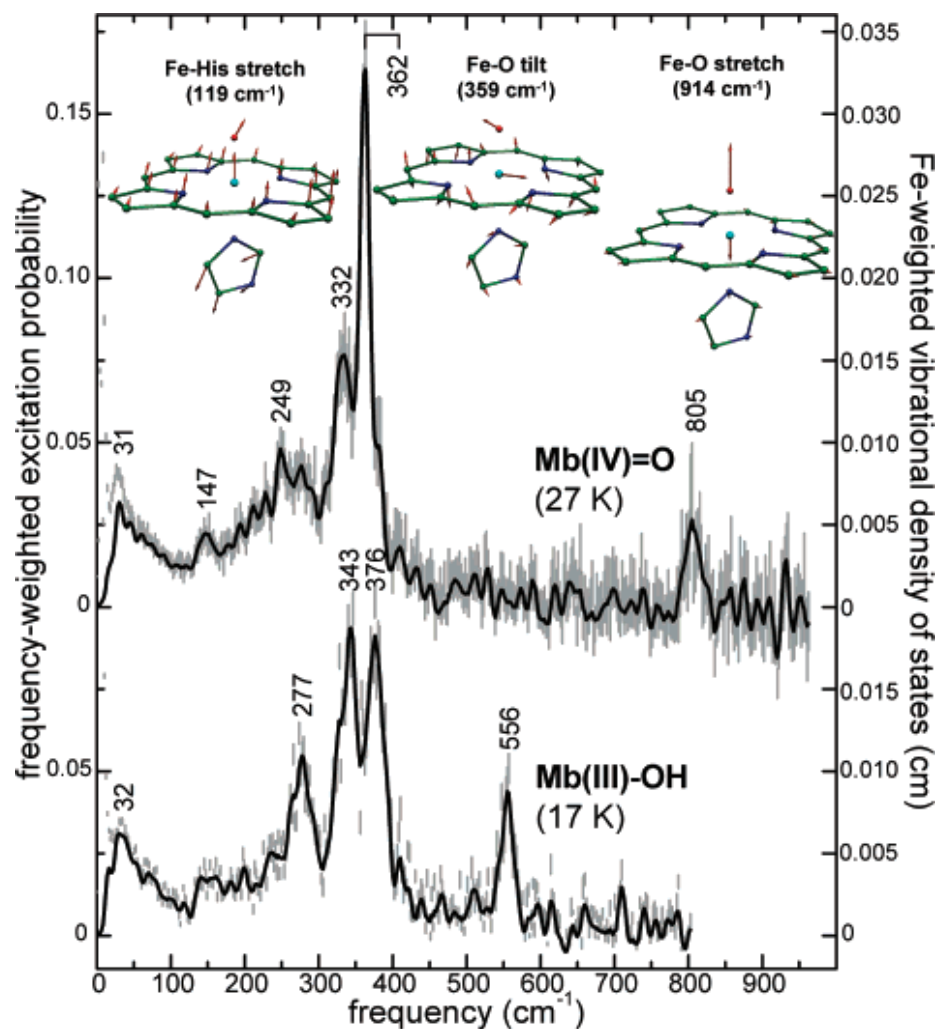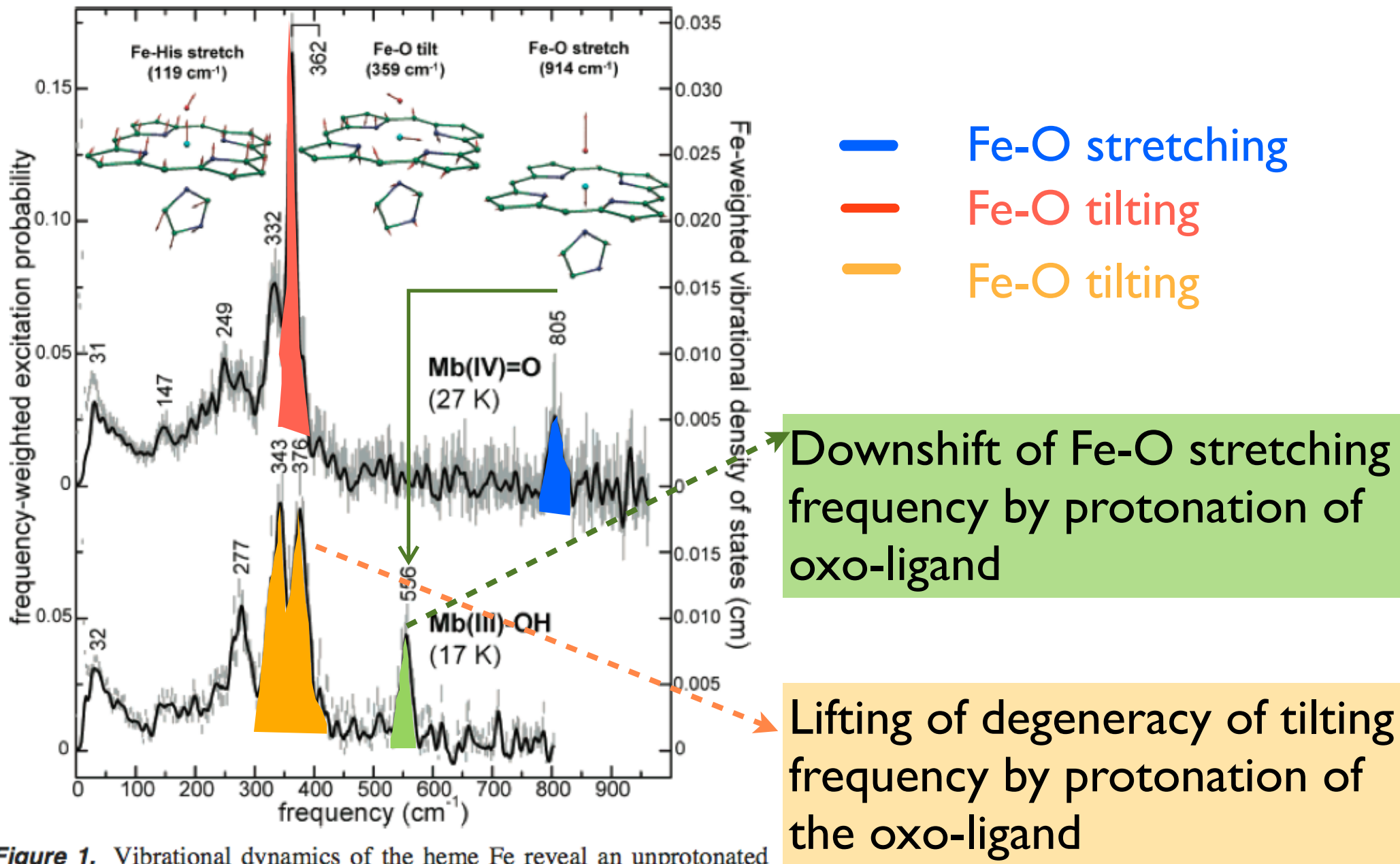
Figure 1. Vibrational dynamics of the heme Fe reveal an unprotonated oxo ligand in Mb(IV)=O, in contrast with the bound hydroxyl group in Mb(III)−OH. Protonation of the oxo ligand results in a downshift of the Fe−O stretching frequency from 805 cm^{-1} to 556 cm^{-1}, and splits the Fe−O tilting vibrations, which are degenerate near 362 cm^{-1} in Mb(IV)=O, but are separated by 33 cm^{-1} in the asymmetrically protonated heme Mb(III)−OH complex. Error bars represent the normalized experimental signal,

The 20 Mössbauer isotopes observed with synchrotron radiation (1985-2015)

Isotope	Energy (eV)	Half-life (ns)	ΔE (neV)	Tabulated E (eV)
^{181}Ta	6215.5	9800.	0.067	6238
^{169}Tm	8401.3	4.	114.0	8409.9
^{83}Kr	9403.5	147.	3.1	9400
^{187}Os	9776.8	2.16	211.	
^{57}Fe	14412.5	97.8	4.67	14413
^{151}Eu	21541.4	9.7	47.0	21532
^{149}Sm	22496.	7.1	64.1	22490
^{119}Sn	23879.4	17.8	25.7	23870
^{161}Dy	25651.4	28.2	16.2	25655
^{129}I	27770.	16.8	27.2	27800
^{40}K	29834.	4.25	107.0	29560
^{125}Te	35460	1.48	308.0	35491.9
^{121}Sb	37129.	4.53	100.0	37133.
^{129}Xe	39581.3	1.465	311.2	39578.
^{61}Ni	67419.	5.1	89.0	67400
^{73}Ge	68752	1.86	245.	68752
^{176}Hf	88349.	1.43	319.4	83000
^{176}Hf	88349.	1.43	319.4	83000
^{99}Ru	89571.	28.8	15.8	89651.8
^{67}Zn	93300.	9200.	0.049	

Thank you ....